

**Department of Environment Systems**

**Graduate School of Frontier Sciences**

**The University of Tokyo**

**2022**

**Master's Thesis**

**Supercritical Water Gasification of  
Simulated Gutter Oil**

「模擬地溝油の超臨界水ガス化に関する研究」

**Submitted July 20, 2022**

**Advisor: Associate Professor Teppei Nunoura**

**Co-advisor: Professor Tomochika Tokunaga**

**温 雅茹**

**Wen Yaru**

## ACKNOWLEDGMENTS

I would like to thank the below individuals for their roles in my development in completing this master's thesis.

First of all, thanks to my supervisor, Professor Teppei Nunoura, who patiently guided me to explore my topic in depth, was always available during the Covid-19 and at all inconvenient times to give me useful advice and was generous to me and to all members of the research laboratory. He is a role model for everyone to admire and is what a true researcher should be. I have had many mentors in my life, but he is the most knowledgeable and kind one.

Next, I would like to sincerely thank Dr. Osamu Sawai, an assistant professor in our lab, for his unstinting and righteous words as a generous tip, mainly a lot of constructive criticism to make me look at my research and experiments properly. Meanwhile, I would also like to thank my sub-supervisor, Prof. Tokunaga, for the valuable insights and advice, which help me improve my research discussions. Meanwhile, thanks to the Institute for Solid State Physics (ISSP) and the Microanalytical Laboratory, both of which generously allowed me to utilize the instruments for my study.

My acknowledgements also go to my lab colleagues. Especially Diane-san, who teaching me a lot during my research, it is very much appreciated. Many of the things she taught me have been applied to my current research, and I cannot finish my research without her. To my friends, Mr. Zhang Peng, Ms. Yang Dan, Mr. Dang Bowen with Ms. Dang Siyan, Ms. Jia Yanqiong with Ms. Cheng Yumeng, I wish you good luck to find the thing you love and enjoy your future journey.

Last but not least, please allow me to thank my family, Mr. Wen Yunhai and Ms. Ma Yunxia for their great support and understanding during my life. I wish my parents happy and healthy. They thought me to be a good, honest, and sincere person and I am glad I became such a person. As a result, I met so many kind friends who helped me a lot. As for Ms. YJ, thank you for accompanying me during my years, especially in Japan, I am glad to spend my life with you.

Thank you all!

Wen Yaru

## Table of Contents

<b>CHAPTER 1. INTRODUCTION.....</b>	<b>1</b>
1.1. Renewable energy sources.....	1
1.2. Gutter oil introduction.....	1
1.2.1. Value of gutter oil.....	2
1.2.2. Risks of gutter oil.....	3
1.3. Significance of GO biomass .....	4
1.4. Current technology for GO treatment.....	4
1.5. Hydrothermal technology .....	5
1.5.1. Characteristics.....	5
1.5.2. Supercritical water gasification.....	7
1.5.3. Biomass for SCWG.....	8
1.5.4. Catalysts for SCWG.....	8
1.6. Objectives .....	8
<b>CHAPTER 2. METHODOLOGY .....</b>	<b>9</b>
2.1. Preparation of simulated gutter oil.....	9
2.1.1. Choice of cooking method.....	9
2.1.2. Cooking and deterioration.....	10
2.2. Experiment device .....	13
2.2.1. Batch type reactor .....	13
2.2.2. Salt bath device .....	14
2.3. Feedstock .....	17
2.3.1. Initial element analysis of SGO .....	17
2.3.2. Catalysts.....	17
2.3.3. Deionized water .....	17
2.4. Experiment method.....	17
2.4.1. Conditions .....	17
2.4.2. Collections .....	19

2.5.	Analysis method.....	21
2.5.1.	Liquid Analysis .....	21
2.5.2.	Gas Analysis.....	22
2.5.3.	Catalyst Characterization.....	23
<b>CHAPTER 3. DECOMPOSITION OF SIMULATED GUTTER OIL .....</b>		<b>24</b>
3.1.	Overall Carbon Balance .....	24
3.2.	Gas Product Analysis .....	26
3.2.1.	Carbon and hydrogen gasification efficiency, gas yield .....	28
3.2.2.	Cold gas efficiency .....	37
3.3.	Liquid Phase Analysis.....	45
3.3.1.	TOC Analysis.....	45
3.3.2.	GC-MS Analysis .....	47
3.3.3.	Summary and Discussion.....	54
3.4.	Effect of catalyst .....	56
3.4.1.	Gas yield and efficiencies .....	56
3.4.2.	Overall carbon balance .....	58
3.4.3.	Summary and discussion.....	59
<b>CHAPTER 4. CHARACTERIZATION OF CATALYST .....</b>		<b>60</b>
4.1.	Initial catalysts characterization.....	60
4.2.	Catalyst characterization after SCWG.....	61
4.2.1.	SEM-EDX Analysis.....	62
4.2.2.	XRD Analysis .....	67
<b>CHAPTER 5. CONCLUSIONS AND RECOMMENDATIONS .....</b>		<b>68</b>
5.1.	Conclusions.....	68
5.2.	Recommendations.....	69
<b>REFERENCES.....</b>		<b>70</b>

# Chapter 1. INTRODUCTION

## 1.1. Renewable energy sources

Global energy consumption and energy-related carbon dioxide emissions increase as a result of population and economic growth[1], which has led to an increased demand for fossil fuel production and environment pollution. In addition, growing concerns over the environmental impact of fossil fuels and their inevitable depletion[2], and dramatic climate change have led to an unprecedented global focus on the development of renewable and environment-friendly energy sources. In order to meet the growing energy demands and greenhouse gas emission reduction targets, there is an urgent need to explore renewable energy sources and develop energy technologies that offer tremendous opportunities to replace conventional energy sources, mitigate greenhouse gas emissions, and reduce global warming.

As research has progressed, the increasing use of renewable energy has been identified as a pathway to a low carbon future. Renewable energy sources are those resources which can be used to produce energy again and again, e.g., solar energy, wind energy, biomass energy. Among the renewable energies, hydrogen has been identified as an energy source that can be widely used[3]. Hydrogen energy can be utilized as a clean energy source without carbon dioxide products emission to the environment which water is the outlet combustion products[4]. Also, as a fuel hydrogen has a gravimetric energy density which is about 2.5-3 times higher than the most commonly used fossil fuels today[5]. As a result, hydrogen fuel is accepted worldwide as a clean energy source that can be used on its own.

However, most H<sub>2</sub> is currently produced from nonrenewable sources such as oil, natural gas, and coal[6]. It is indicated that there are still disadvantages with these technologies, such as causing emissions of harmful compounds into the atmosphere and total energy consumption. Therefore, it is crucial to find alternative renewable sources.

Biomass can produce clean fuels and could be a vital, renewable energy source for the future. Thermochemical conversion processes such as pyrolysis and gasification of biomass have considerable potential for producing renewable hydrogen, which is beneficial to exploit biomass resources, to develop a highly efficient clean way for large-scale hydrogen production, and to lessen dependence on insecure fossil energy sources[7]. In conclusion, the search for a suitable biomass resource as a feedstock for hydrogen production is a promising subject to be explored.

## 1.2. Gutter oil introduction

Used cooking oil is mainly generated in restaurants and domestic areas. In the management of waste cooking oil[8], most developed countries adopt a government-led management model throughout the whole process, and government departments have strict legislation and severe punishment measures. In addition, a strict tracking

system is formed from the collection, transportation and processing of waste edible fats and oils, which helps to regulate the whole process, with the participation of all people, and educate the nationals to form the awareness of collecting waste oil and develop good habits. However, it is unfortunate that these excellent handling behaviors and management measures are difficult to be formed in developing countries. Until today, there are no collection facilities for used cooking oil in many countries, such as India and China. In the absence of collection facilities, used cooking oil from restaurants and domestic areas is discharged directly into the drainage system. In the drains, the oily part floats on top of the foul-smelling water phase. This oily phase is separated out by smugglers in mainland China. The waste oily material is then reprocessed, which is also known as gutter oil[9].

Gutter oil (GO) is a general term for waste cooking oil. It refers to the oil extracted from waste food or residue. It can be divided into three categories: one is greasy floating objects in the sewer or the oil that is processed and refined from swill, the other is inferior quality oil produced after processing of pork, pig offal, and pigskin, the third is the repeated fried oil. The picture of gutter oil is shown as Figure 1-1.



Figure 1-1 The picture of gutter oil[10]

### 1.2.1. Value of gutter oil

China's food culture depends heavily on cooking oil for daily use. In China, approximately 4.5 million tons of waste cooking oil is generated per year[11]. Given its food culture that heavily depends on oil for daily cooking, China generated as much 2.73 times as much GO as produced by European Union, U.S., and Canada combined[12](Figure1-2). An input-output based life cycle assessment (IO-LCA) model to quantify the amount of waste oil, comprising gutter oil, acid oil and rice

bran oil, from a production and consumption perspective [10]. The results show that in 2010 China produced 13.74 million tons of waste oil, about twice as much as during 1990, making China the world largest GO producer[10]. This shows the huge amount of gutter oil, therefore, if it could be converted to energy use, it would greatly reduce the pollution caused by fossil fuel combustion and meet the global energy demand.

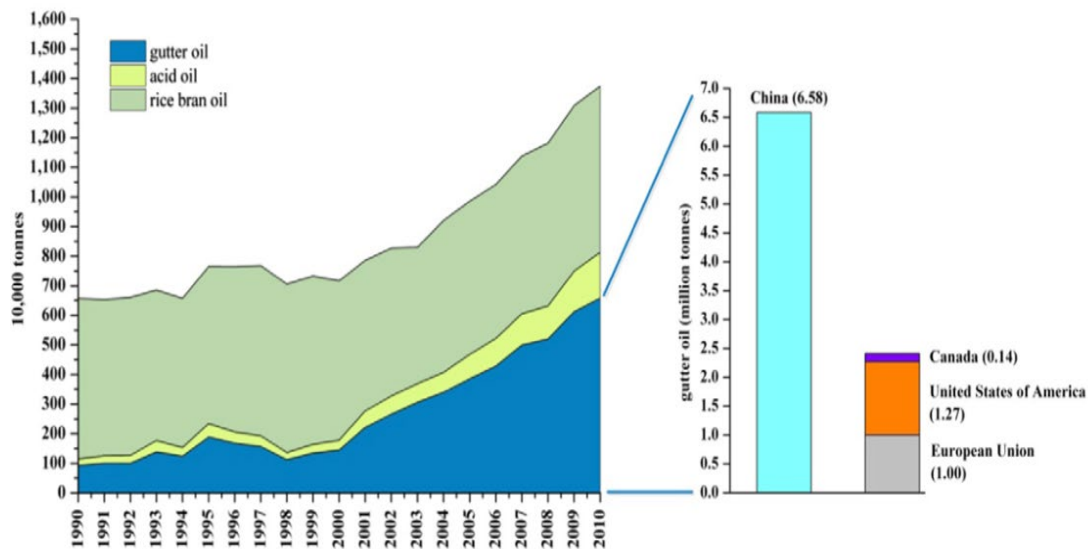


Figure 1-2 China's potential supply of waste oil in the period of 1990-2010, while that of the United States of America and Canada was calculated by their population.[12]

### 1.2.2. Risks of gutter oil

GO have several risks, the first being that it can cause food safety problems. It is well known that oil is subject to rancidity and oxidation when contaminated. In other words, it will lead to various diseases when people ingest it, for example, indigestion, diarrhea, severe abdominal pain, stomach cancer and bowel cancer[13]. However, many restaurants illegally collect GO from hotels and restaurants, process it through refining, remove the bad smell and flow into the edible oil market in order to profit from it. This refining process is the cause of GO toxins. After heavy heating, cooking oil undergoes chemical changes such as oxidation of unsaturated fatty acids, degradation of triglycerides, and formation of toxic chemical compounds[9]. In addition, GO is known to contain various toxic chemicals such as aflatoxins, polycyclic aromatic hydrocarbons, 4-hydroxy-trans-2-nonenal and other aldehydes[9]. Long-term consumption of GO can be a hazard to health, which is challenging the management of GO and its handling has attracted public attention.

The second risk is that if GO is not properly collected and disposed of, then when it is discharged into the sewer it can cause clogging or damage to the sewer due to acidification and corrosion of the pipes, which also is challenging the treatment of GO in many development countries.

### **1.3. Significance of GO biomass**

The rising price of crude oil and the resulting concerns about energy security have made it necessary for developing countries to search for inexpensive alternative energy sources to meet their growing energy needs. Along with people's living activities, a large amount of GO is generated, which can be considered as a sustainable renewable resource from a sustainability perspective. Therefore, it is recommended to utilize GO in biomass.

Biomass is the only energy type with diversified utilization among renewable energy sources, which can be converted into solid fuels (direct combustion), liquid fuels (bioethanol, biodiesel, and bio-airline coal, etc.) and gaseous fuels (biogas, carbon monoxide and hydrogen, etc.).

Although GO is harmful for health, it can be used as raw material for biomass energy. Throughout the world, there is substantial amounts of waste cooking oil and waste foods obtained annually by households and catering companies from cooking activities, the results of the study suggest that roughly one-third of food produced for human consumption is lost or wasted globally, which amounts to about 1.3 billion tons per year [14]. Using this biomass as a feedstock is a practical option because its processing and bioenergy conversion are achieved simultaneously. In other words, it is promising that recycling GO into biomass energy will meet global energy needs while addressing food safety concerns. Treating this biomass as a raw material is a workable option because its processing and bioenergy conversion are achieved simultaneously.

### **1.4. Current technology for GO treatment**

#### **1.4.1.1. GO for produce biodiesel (biofuel)**

Its known treatment method of GO is utilization for biofuel or conversion to second-generation biodiesel through transesterification and hydrodeoxygenation processes [15].

#### **1.4.1.2. GO for prepare mineral processing chemicals[16]**

Professor Wang Huajun and others from the Department of Environmental Engineering at the University of Science and Technology Beijing have developed a comprehensive utilization technology for the preparation of mineral processing chemicals from GO. This technology allows the production of fatty acids and sodium fatty acids for mineral processing from GO with little to no secondary contamination.

#### **1.4.1.3. GO production of ethanol, biogas new technology[17]**

This technology is to convert part of GO into raw material for biodiesel after sorting and barreling, another part continues to ferment into fuel ethanol and biogas, and the remaining waste residue is all converted into fertilizer. The fats and oils in the garbage are separated and refined into biodiesel, carbohydrates and proteins are converted into

fuel ethanol through an enzymatic and anaerobic fermentation process, ethanol fermentation residue and other organic components are fermented to produce biogas, and the biogas business liquid is processed into biofertilizer.

#### **1.4.1.4. GO transformed into aviation oil[18]**

The key step in the conversion of GO to aviation oil is hydrocracking, where the carbon bonds between molecules are broken under continuous hydrogen pressure to produce smaller hydrocarbons, the products of which are unsaturated hydrocarbons that are very close to the fuel and then undergo isomerization, i.e., changing the composition of the chemical itself, is performed to become the desired "renewable flight fuel".

#### **1.4.1.5. GO transformed into drilling lubricant[19]**

China National Petroleum Chuanqing Drilling Company has developed GO into drilling lubricant for the first time in China. Using GO as the basic raw material oil, it has successfully developed bio-oil lubricant for drilling fluid after purification, modification and compounding, which helps to protect the ground and reduce the cost. This is the result of scientific research for large-scale application in the field of oil drilling.

#### **1.4.1.6. Disadvantages for current technology**

These methods of processing GO have several unavoidable drawbacks. The efficiency of processes, such as transesterification and hydrodeoxygenation, is significantly affected high free fatty acid and water content[15].

In addition, despite the low commercial price of GO, the necessary pretreatment is unavoidable and incurs additional processing costs since GO cannot be used directly in production. Therefore, these reasons lead to low yields. In addition to this, not all the above treatment options are aimed at the energy demand towards a low carbon and environmental perspective, so there is a need to find new technologies for GO treatment.

### **1.5. Hydrothermal technology**

#### **1.5.1. Characteristics**

Hydrothermal technology is the technology under the hot water compress, which could be defined as an important thermo-chemical conversion process of reactants in a high-temperature (200–374 °C), high-pressure (4–22 MPa) reaction environment in a special closed reaction vessel[20], [21]. It is divided into subcritical water and supercritical water depending on temperature and pressure. The critical point of water is 374 °C and 22.1MPa. Water in a state above the critical point is called supercritical water, and water near the critical point is called subcritical water.

The three major reaction mechanisms occur during hydrothermal gasification of biomass namely: (1) depolymerization; (2) decomposition through cleavage,

dehydration, decarboxylation, and deamination; and (3) recombination of reactive fragments.[22]

Hydrothermal technology has many unique advantages in that the reaction medium is typically water or an aqueous solution. First of all, water, being a green and low-cost reaction medium, has a negligible impact on the environment. Secondly, water molecules can catalyze a reaction by directly participating in the transition state and reducing its energy[23]. It is known from previous studies that individual water molecules can participate in the basic reaction steps as catalysts, sample reactions where water acts as a source of acid or base catalysts, and as a catalyst for modifying and stabilizing the transition state. In addition, the raw materials involved in the experiments do not need to be dehydrated and dried, therefore, the energy consumption is reduced[23]. Lastly, a good sealing environment can avoid secondary contamination during the operation[24].

Figure 1-3 shows the phase diagram of water. The state of substance will change with the rising of reaction temperature and pressure.

Figure 1-4 shows that beyond the critical point of water, the dielectric constant of water decreases significantly. A higher dielectric constant implies that polar substances (inorganic compounds) are more soluble, while a lower dielectric constant implies that nonpolar substances (organic compounds) are more soluble. It is known from this that subcritical and supercritical water readily dissolves organic matter and precipitates inorganic matter, compared to water at ambient temperature and pressure.

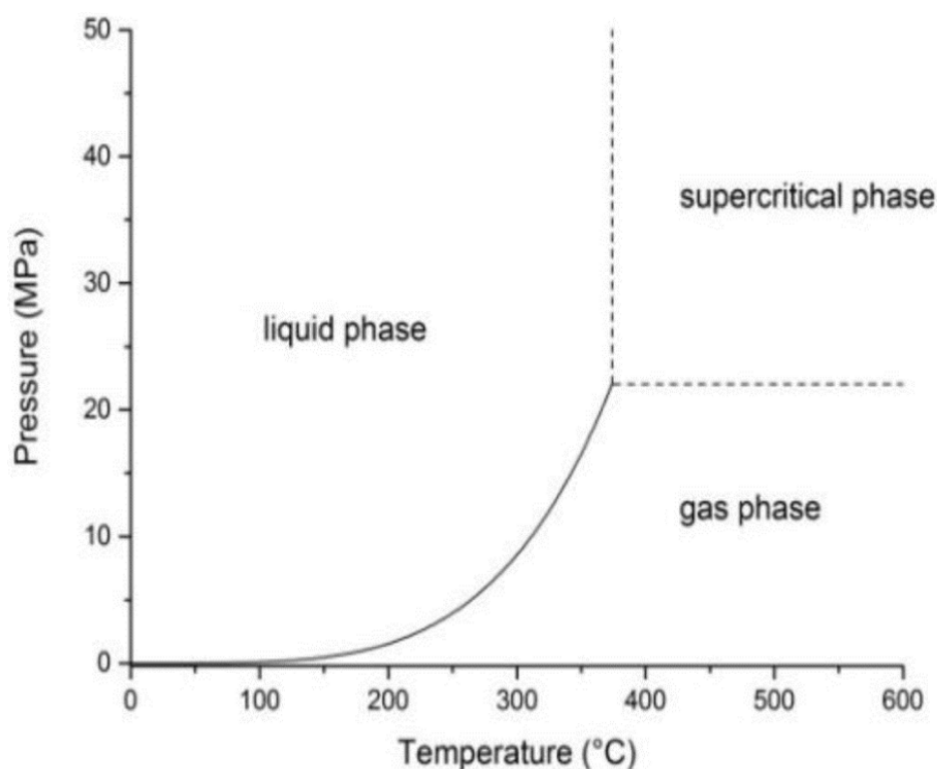


Figure 1-3 Phase diagram of water[25]

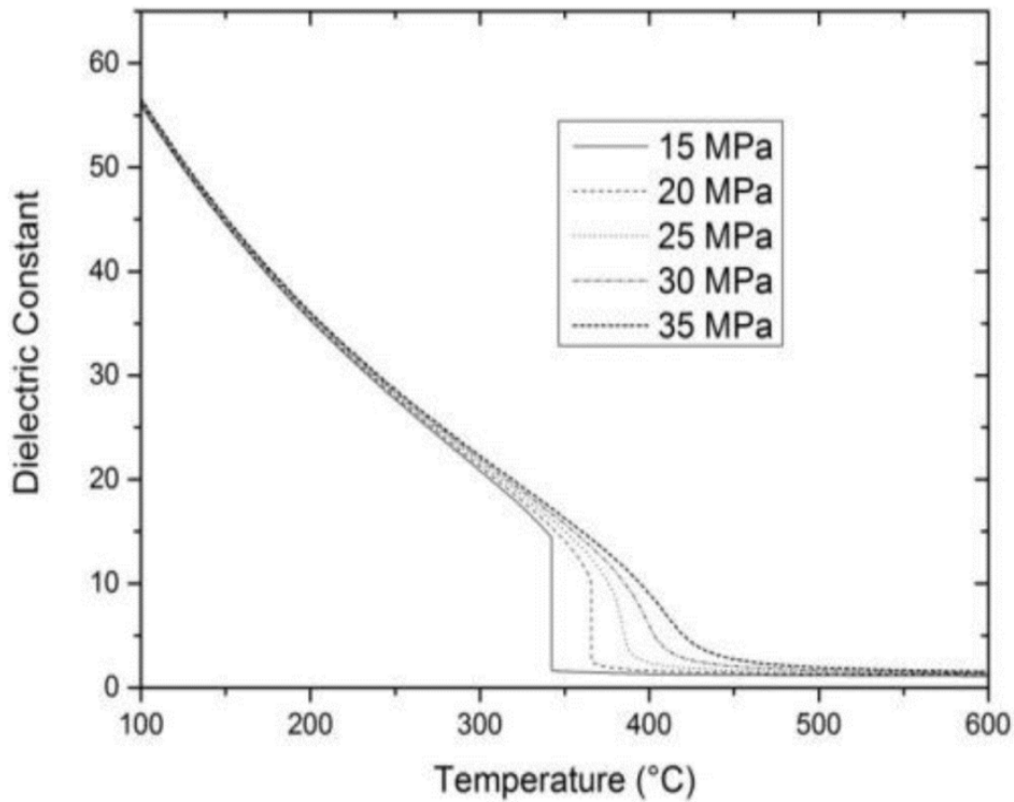
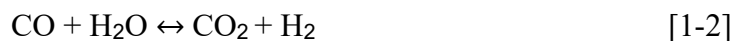


Figure 1–4 Dielectric constant of water at various temperature and pressure[25]

### 1.5.2. Supercritical water gasification

Supercritical water gasification (SCWG) is a hydrothermal process involving the reaction of biomass in hot compressed water above its critical point (374.1 °C, 22.1 MPa). The reasons for operating at high temperatures and pressures may be found in the unique properties of supercritical water, which is able to dissolve non-polar compounds and promote the production of H<sub>2</sub> and/or CH<sub>4</sub>, depending on the selected reaction conditions[26].

Under supercritical water conditions, organic compounds are readily dissolved and rapidly decomposed. SCWG is the process of final decomposition of organic compounds into gases. Therefore, the application of hydrothermal technology in organic waste treatment is being widely investigated. Three main reactions[27] were identified in the SCWG process, including steam reforming, water-gas transfer, and CO and CO<sub>2</sub> methanation reactions, represented by Equations 1-1 to 1-3, respectively.



### **1.5.3. Biomass for SCWG**

Recently, the application of supercritical water (SCW) for biomass gasification has received a lot of attention. The study of an innovative method of converting biomass with high moisture content into viable syngas has been acknowledged by research communities and researchers worldwide. Supercritical water gasification (SCWG) is considered as an aqueous phase reforming process to produce hydrogen enriched syngas from biomass and other organic wastes [28]. Meanwhile, with the hydrolysis of residual fat, oils, and grease from grease traps, diesel-like hydrocarbon fuel[29], [30] is supposed to be produced. Therefore, the recyclability of GO in SCWG to produce hydrogen and diesel-like hydrocarbon is considered a sustainable way to minimize waste dumping while meeting the growing energy needs.

### **1.5.4. Catalysts for SCWG**

SCWG can be performed in the presence of catalyst to reduce the high temperature requirement, improve the selectivity towards H<sub>2</sub> and lessen the chances of tar and char formation during gasification[31]. Hydrothermal technology is safer and saves more energy if the catalyst can achieve the same results as higher temperatures at lower temperatures.

Existing studies[32]have shown that H<sub>2</sub> production increases and the water-gas conversion reaction is enhanced by the addition of catalyst compared to the absence of catalyst. In addition to this, the use of Raney nickel, known as a hydrogenation catalyst, facilitates the formation of CH<sub>4</sub>, thus, the effect of the nickel catalyst on the hydrothermal reaction will also be considered in this study.

## **1.6. Objectives**

The main objective of this study is to investigate the decomposition of simulated gutter oil in supercritical water gasification.

Specifically, it aims to three parts.

1. Identify the primary products (such as hydrogen and diesel-like hydrocarbons) produced in supercritical water conditions.
2. Investigate the effects of reaction parameters (such as temperature and residence time on the product yield and distribution).
3. Investigate the effect of catalyst addition.

## Chapter 2. METHODOLOGY

### 2.1. Preparation of simulated gutter oil

The experimental conditions applied in this study were appropriately chosen to represent SCWG of gutter oil. To keep the consistency of feedstock, it is necessary to prepare simulated gutter oil (SGO), instead of obtaining directly from the restaurant. In this study, three common cooking oils were selected for this experiment, namely lard, soybean oil, and peanut oil, all of which were purchased from Japan. The picture of cooking oil as shown in Figure 2-1.



Figure 2-1 Lard, soybean oil, and peanut oil

#### 2.1.1. Choice of cooking method

The chemical structure of the oil is triglyceride, which is a glycerol molecule connected with three fatty acids. The main difference between different cooking oils is the composition of these fatty acids. Fatty acids can be divided into three categories: saturated fatty acids, monounsaturated fatty acids and polyunsaturated fatty acids.

Different cooking oils should be cooked in different ways:

(1) Saturated fat is very stable and does not deteriorate easily during heating and storage; therefore, for cooking oils that require high temperatures, especially for long-term high-temperature heating (repeated deep frying), oils with high saturated fatty acid content should be used, such as lard.

(2) The main component of soybean oil is unsaturated fatty acid. It contains double bonds, which are prone to oxidation. In addition, the higher the temperature, the faster the oxidation rate. Oxidation will produce some harmful ingredients and unpleasant odors. So, it is suitable for low-temperature cooking.

(3) The main component of peanut oil is monounsaturated fatty acid. The proportions of various fatty acids are relatively balanced. It produces a lower concentration of oil fume and produces relatively less harmful substances under high temperature conditions, so it is more suitable for cooking.

### 2.1.2. Cooking and deterioration

Three cooking methods and dishes were chosen according to the characteristics of different cooking oils and typical local ingredients. The purpose was to simulate the authentic cooking process and to ensure the success of the simulated gutter oil as much as possible. The first dish is deep-fried chicken wings cooked in lard, as shown in Figure 2-2. Second dish, sliced lotus roots stir-fried in soybean oil, as shown in Figure 2-3. Last one, Mapo tofu cooked in peanut oil, as shown in Figure 2-4. The seasonings used in the dishes are, salt and pepper, bean paste, dried pepper and pepper. The purpose is to season and enhance the flavor, so that the SGO can be closer to real life. All cooking processes were performed in the laboratory kitchen.



Figure 2-2 Deep-fried chicken wings cooked in lard.



Figure 2-3 Sliced lotus roots stir-fried in soybean oil.



Figure 2-4 Mapo tofu cooked in peanut oil.

After cooking, the remaining dishes were then combined in a bucket for deterioration. In order to ensure the universality of the experiment, an oleic acid test that most restaurants or convenience stores would utilize was used, namely AV-check[33]. Acid value (AV) is an index of refining and alteration of fats and oils. The number of milligrams of potassium hydroxide required to neutralize free fatty acids present in 1 gram of oils is defined as the acid value. Crude oils (unrefined oils) generally have a high acid value (about 7 to 20) because the hydrolases contained in these raw materials have strong power. However, when making edible oil, all cooking oils must be deoxidized and refined to an acid value of 0.5 or less. In other words, the acid value is an index showing the degree of refining of oils. The picture and instruction are shown in Figure 2-4. After several weeks of acidity and denaturation for waste cooking oil and mixing dishes, SGO with a poor grade was created which is shown in Figure 2-6.



Figure 2-5 Test paper for Acid value (AV) check of oil of Hazard Analysis Critical Control Point system[34]



Figure 2-6 The picture of SGO and AV-check paper

## 2.2. Experiment device

### 2.2.1. Batch type reactor

This study, a type of batch reactor was used in the experiment to study the treatment results of the hydrothermal method. A schematic diagram of the reactor is shown in Figure 2-7.

In this experiment, a stainless steel (SUS316) batch reactor with a content area of 7.3 ml was used and the upper experimental pressure limit was 35 MPa. A gas recovery reactor was designed to collect gases generated from the synthesis reactor. The reactor section is a 10 cm tube with a diameter of 1/2 inch and a thickness of 1.65 mm. One side of the tube is fitted with a 1/2-inch cap. On the other side, a 1/2-inch to 1/8-inch reduced union is connected. A 20 cm 1/8-inch tube is then connected to the 1/8-inch T-piece; to the left of the T-piece a pressure transducer (Keyence Type AP-V80) and a sampling valve are connected, which is used to collect gas samples after hydrothermal reactions. An SD16A21-05 indicator (manufactured by SHIMADEN CO< LTD) was used as a temperature monitor.

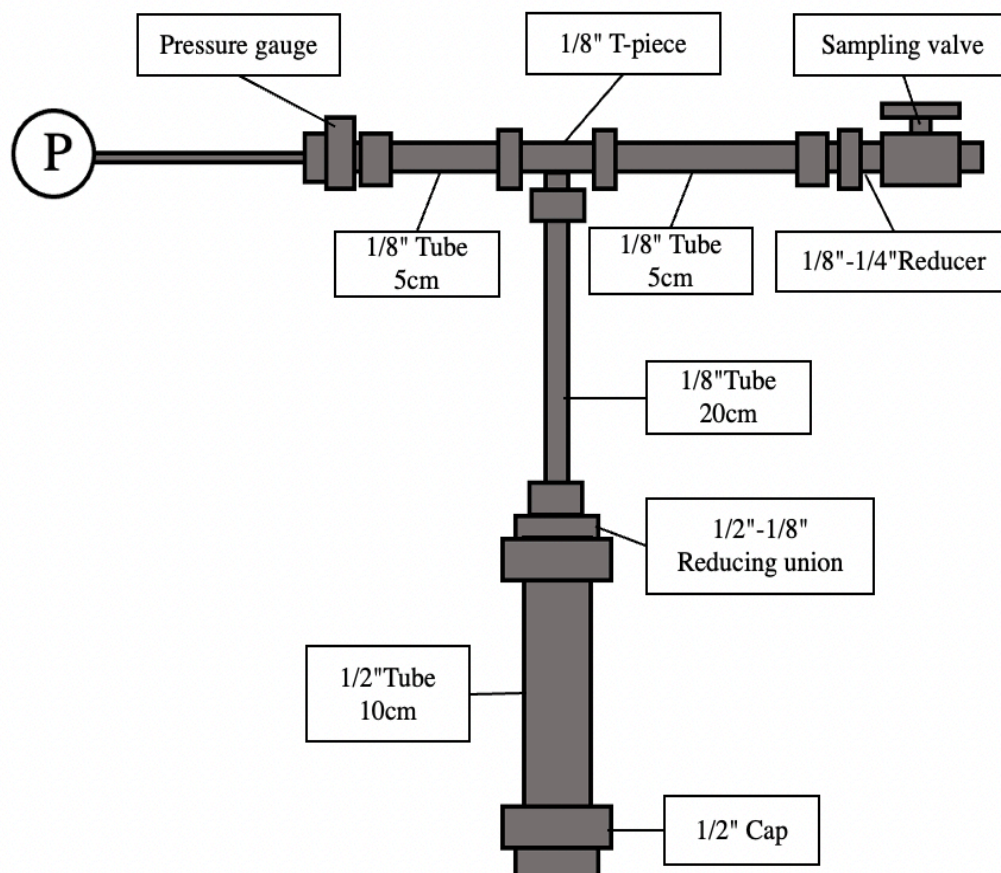


Figure 2-7 The schematic diagram of batch reactor

### 2.2.2. Salt bath device

In the hydrothermal reaction in this study, a salt bath system is used to heat the reactor. The salt bath contains a mixture of  $\text{KNO}_3$ ,  $\text{NaNO}_2$  and  $\text{NaNO}_3$  with a mass ratio of 6:5:1. The temperature of the salt bath is controlled by thermocouples and a T-35 type sheath thermocouple (produced by SAKAGUCHI E.H VOC CORP) is fed into the molten salt by an air pump to ensure a uniform temperature in the salt bath. The salt bath equipment is shown in Fig. 2-8.

Heating the sample in the reactor until it reaches the set temperature takes few minutes, so the heating time of the salt bath must be known. Therefore, before the hydrothermal experiments were conducted, a series of blank experiments were done to plot the change curve by monitoring the pressure and temperature changes inside the reactor.

Figure 2-9 show that the temperature in the reactor can reach a temperature relatively close to the set temperature after about 3 minutes. Therefore, for an experiment with a residence time of 30 minutes, the reactor should be placed in a salt bath for 33 minutes. Figures 2-10 and 2-11 show the pressure curves under different SGO concentration (2wt% and 20wt%), and the pressure target is 25MPa.



Figure 2-8 Salt bath device

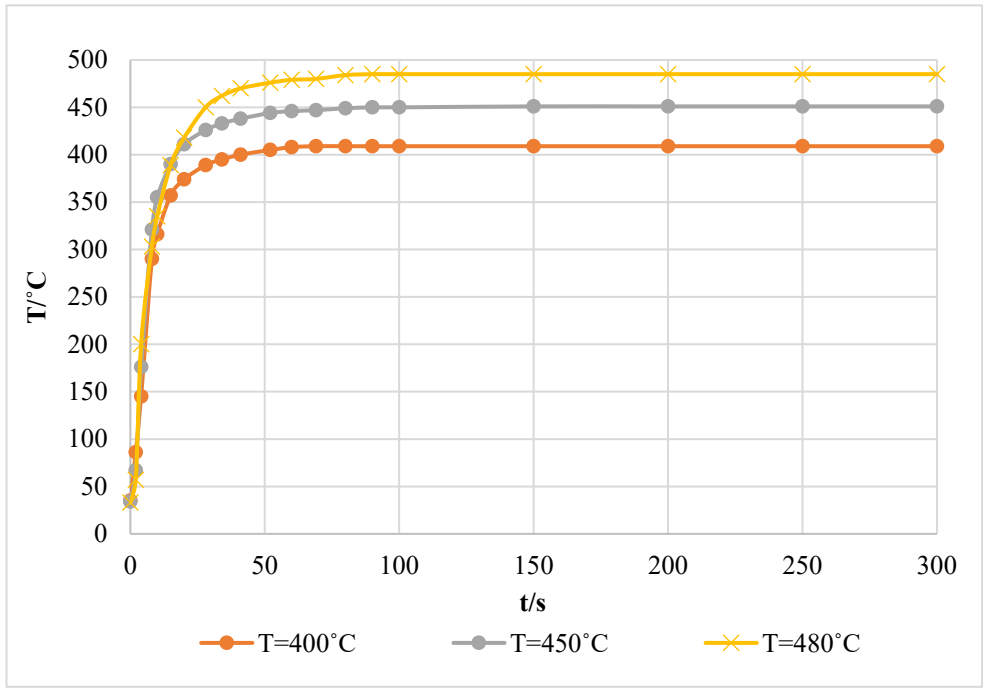


Figure 2-9 Temperature curve

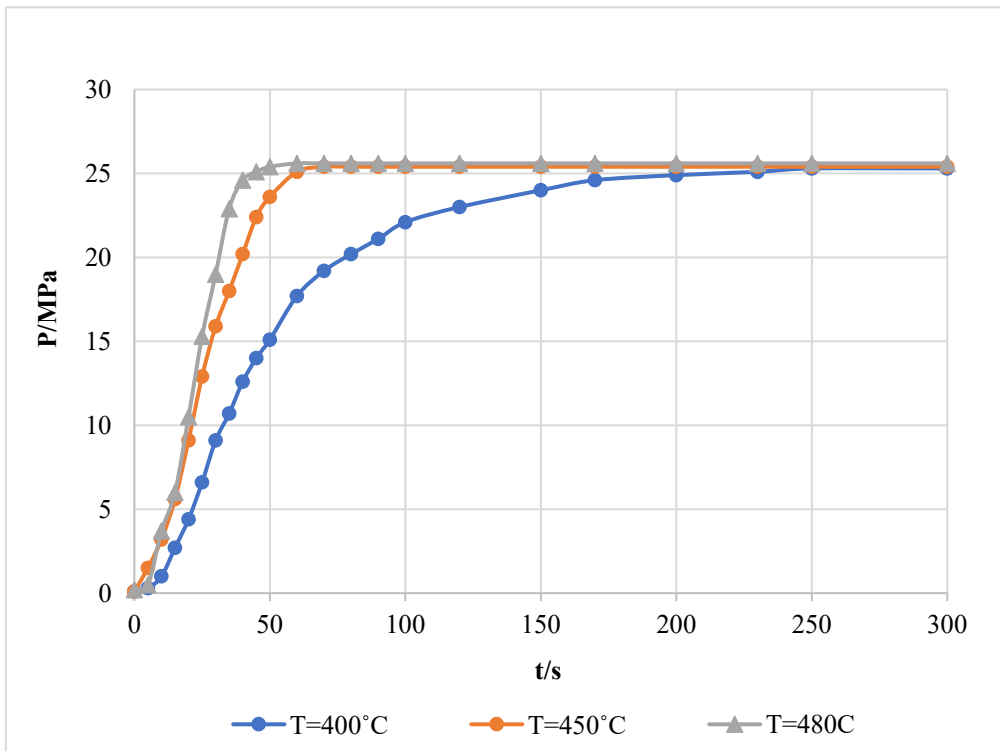


Figure 2-10 Pressure curve of 2wt% SGO

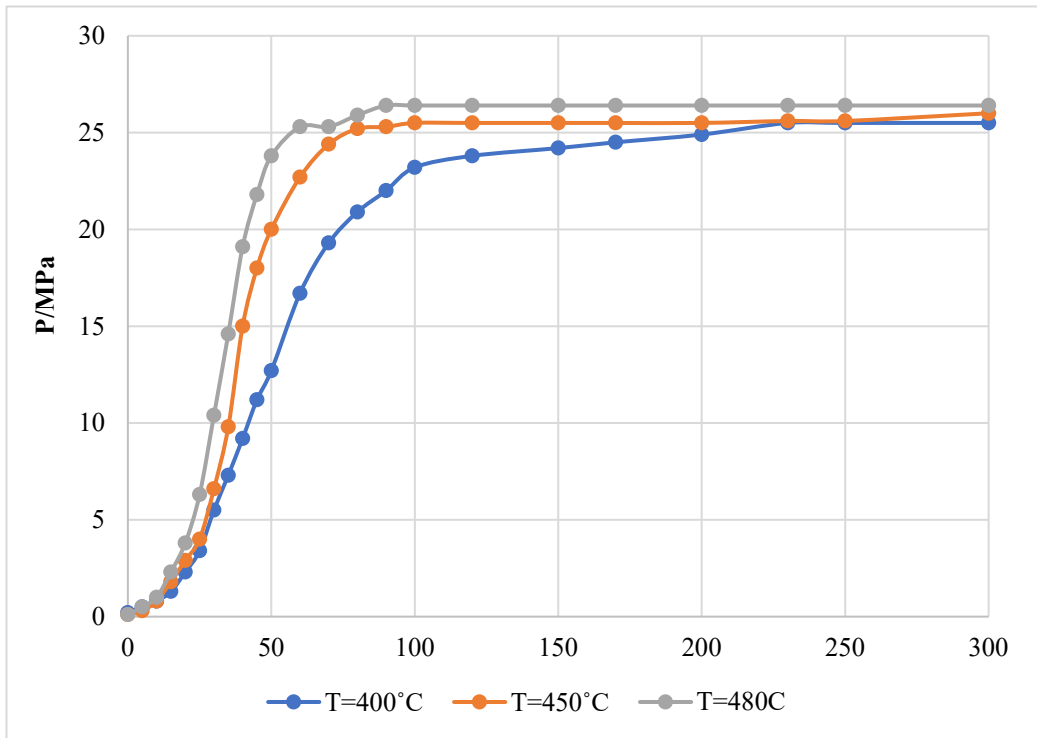


Figure 2-11 Pressure curve of 20wt% SGO

## **2.3. Feedstock**

### **2.3.1. Initial element analysis of SGO**

SGO was chosen as the biomass in this study. It is mainly composed of C (76.97%), H (11.72%), N (0.22%) and O (11.09%) as determined by CHN analysis. The analysis was conducted with the CHN coder in the Microanalytical Laboratory, Department of Chemistry, School of Science, The University of Tokyo.

### **2.3.2. Catalysts**

The catalyst used in the study was composed of Ni (67.2%), Al (31.9%), and Mo (0.9%) with an average surface area of 58.23 m<sup>2</sup> g<sup>-1</sup> and was purchased from Nikko Rica, Japan.

### **2.3.3. Deionized water**

Deionized water was used throughout the experiments which was prepared in our laboratory using Milli-Q A10 (Millipore), which is regularly cleaned and replaced to ensure cleanliness.

## **2.4. Experiment method**

### **2.4.1. Conditions**

In the experimental condition for SCWG, the same type of catalyst was used, the residence time was set to 15 min, 30 min, and the reaction temperatures were chosen to be 400°C, 450°C, and 480°C. According to the literatures[35], [36], different pressures contribute little to the variation of the gasification results, therefore, a constant pressure of 25 MPa was used in SCWG experiments.

In addition to this, the oil concentration was varied in order to determine the appropriate biomass for the SCWG experiments of SGO. A total of two biomass concentrations were tested in the experiment: 2 and 20 oil weight %. The gasification products in the gas and liquid phases were also analyzed to determine the possible decomposition pathways of SGO at high and low concentrations. In summary, the operating parameters evaluated in this study were biomass concentration, catalyst, reaction temperature and residence time. Table 2-1 shows the experimental conditions of the hydrothermal reaction for the treatment of SGO.

Table 2-1 Experimental condition

No	Temperature /°C	Concentration of SGO/wt%	Residence time/min	Target Pressure/MPa	Catalyst /g
1	400	2	15	25	0
2	450				
3	480				
4	400	20			
5	450				
6	480				
7	400	2	30		
8	450				
9	480				
10	400	20			
11	450				
12	480				
13	400	2	15		0.5
14	450				
15	480				
16	400	20			
17	450				
18	480				

## **2.4.2. Collections**

### **2.4.2.1. Collection of gas samples.**

After the hydrothermal reaction, wait for the batch reactor to cool down. Gas sample is collected and analyzed first. Thus, a gas sampling system is used as shown in Figure 2-12.

Collecting procedure is as follows.

- (1) Dock the reactor (valve 1) to the gas sampling system (valve2 side).
- (2) Keep valve1 closed.
- (3) Open valve 2 and 3.
- (4) Close valve 4.
- (5) Turn on the vacuum pump.
- (6) Wait until the whole system is evacuated.
- (7) Shut valve 3.
- (8) Turn off the vacuum pump.
- (9) Open valve 4 immediately.
- (10) Open valve 1 and wait until the gas flows into the sampling system.

Then, the gas samples will be analyzed according to the following procedure.

- (1) Take 1mL gas by syringe.
- (2) Analyze that part of gas sample by GC-TCD.
- (3) Get analysis result and calculate.

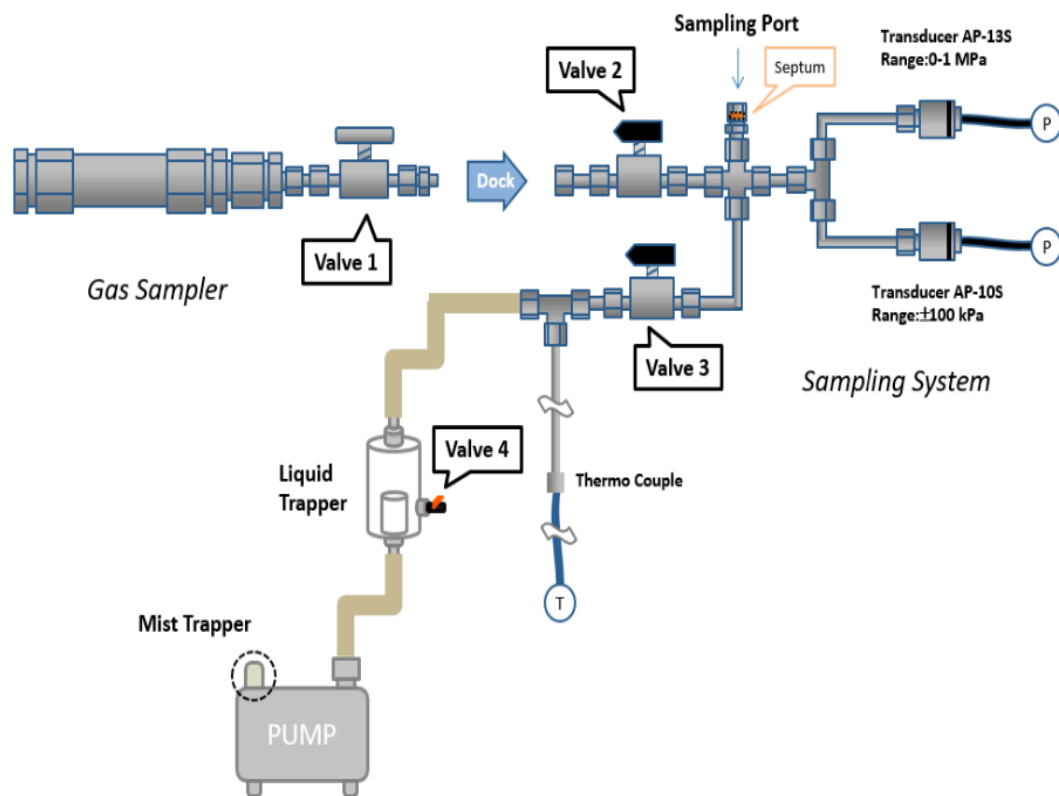


Figure 2–12 Gas sampling system.

The amount of total gas in the reactor could be calculated by the formula below:

$$n = \frac{(V_1 + V_2 + V_c - V_w) \times (P_2 + P_a) - V_2 \times (P_1 + P_a)}{(273 + T) \times R} \quad [ 2-1 ]$$

$n$ : amount of total gas in the reactor (mol)

$V_1$ : volume of reactor (7.3 mL)

$V_2$ : volume of sampling system (2 mL)

$V_c$ : volume changed when valve closed and opened (0.65 mL)

$V_w$ : volume of water input

$P_1$ : pressure of sampling system before opening valve (Pa)

$P_2$ : pressure of sampling system after opening valve (Pa)

$P_a$ : atmosphere pressure (Pa)

$T$ : room temperature (°C)

$R$ : gas constant (8.314 kg·m<sup>2</sup>/s<sup>2</sup>·K·mol)

#### 2.4.2.2. Collection of liquid samples.

After collecting the gas samples, open the batch reactor and separate the solid and liquid phases. However, since there is no solid product in this experiment, only the liquid product is considered for collection. After that, transfer the liquid phase to a volumetric flask and store the liquid sample for later analysis.

### 2.5. Analysis method

#### 2.5.1. Liquid Analysis

The liquid products obtained were analyzed using Total Organic Carbon (TOC), Gas Chromatography – Mass Spectrometer (GC-MS). Each analysis procedure is covered in more detail in the next section.

##### 2.5.1.1. TOC analysis

To determine the carbon content contained in a sample, the TOC 5000-A (SHIMADZU) Total Organic Carbon analyzer was used. The measurable analytes are Total Carbon (TC), Inorganic Carbon (IC) and Total Organic Carbon (TOC). TOC values were used to account for the overall carbon content required for carbon balance. The method operates via a combustion/non-dispersive infrared gas analysis method, with a combustion temperature of 680 °C. The carrier gas is air, with an inflow rate of 150 mL/min. Calibration curves for TC and IC were prepared using standard solutions prior to analysis. The preparation procedure for each standard solution is described below.

- (1) TC standard solution: 1000 ppm  
2.125 g of potassium hydrogen phthalate ( $C_8H_5KO_4$ ) dissolved in 1000 mL  $H_2O$ .
- (2) IC standard solution: 1000 ppm  
3.50g sodium hydrogen carbonate ( $NaHCO_3$ ) + 4.41g sodium carbonate ( $Na_2CO_3$ ) dissolved in 1000 mL  $H_2O$ .
- (1) Calibration curves were prepared by diluting stock solutions. Stock solutions were stored in a cooling system for future use. Sample prepared and analysed according to the following procedure.
- (2) Samples were diluted with deionized water. The decomposed sample is miscible with water and the detection limits for TC and IC are well within the 0-50 ppm calibration curve.
- (3) TOC values were calculated using Equation 2-2. Once the TOC value is obtained, multiply it by the dilution factor to obtain the actual TOC in the sample.

$$TOC \text{ (ppm)} = TC - IC \quad [ 2-2 ]$$

- (4) Then the carbon present in the liquid phase could be calculated using the equation:

$$\text{C in liquid (\%)} = \frac{\text{mol C in effluent}}{\text{mol C in SGO}} \times 100 \quad [ 2-3 ]$$

#### 2.5.1.2. GC-MS analysis

The aim of this analysis is to identify chemical compounds present in the liquid phase and SGO GC-MS analysis was performed on a Shimadzu GC-2010 equipped with a mass selective detector MS QP-2010. Helium was used as carrier gas. The electron ionisation energy was 70 eV, the ion source temperature was 200 °C and the interface temperature was 280 °C. The column was 5% phenyl polydimethylsiloxane (DB-5MS 30 m x 0.32 mm i.d. and 0.25 µm film thickness, J&W Scientific). Data acquisition was performed using Mass Lab software with a mass range of 30 - 300 m/z and a scan rate of 1 scan/s. Compounds were identified by comparing their mass spectra with data from the National Institute of Standards and Technology (NIST, USA).

#### 2.5.2. Gas Analysis

##### 2.5.2.1. GC-TCD

Gas Chromatography –Thermal Conductivity Detector (GC-TCD) is used to analyze H<sub>2</sub>, O<sub>2</sub>, N<sub>2</sub>, CO, CH<sub>4</sub> and CO<sub>2</sub> in gas sample. The instrument is GC-2014 Gas Chromatography produced by SHIMADZU Corporation. Calibration curves were made using 300, 500 and 1000 µL of standard gas which contains 5.59% H<sub>2</sub>, 14.20% CO, 18.39% CO<sub>2</sub>, 4.44% CH<sub>4</sub> and the rest is N<sub>2</sub> balance. During analysis, the baseline may become unstable. In this case, the glass wool inside the injector can be replaced. Gas analysis was carried out using the following procedure.

- (1) Measure 300, 500 and 1000 µL of gas from an aluminium bag containing standard gas using a gas-tight microsyringe to produce a calibration curve for each gas.
- (2) 1000 µL of SCWG gas sample was taken from the gas sampling device using a syringe. The same procedure was used for analysis. Gas compositions and ratios were calculated.

##### 2.5.2.2. GC-FID

Gas Chromatography-Flame Ionization Detector (GC-FID) is used to analyze C<sub>2</sub>H<sub>4</sub>, C<sub>2</sub>H<sub>6</sub>, C<sub>3</sub>H<sub>6</sub>, C<sub>3</sub>H<sub>8</sub>, C<sub>4</sub>H<sub>8</sub> and C<sub>4</sub>H<sub>10</sub> in gas sample. Calibration curves were made using 30, 50, 100 µL of standard gas which contains 1.00% C<sub>2</sub>H<sub>4</sub>, 1.02% C<sub>2</sub>H<sub>6</sub>, 1.02% C<sub>3</sub>H<sub>6</sub>, 1.01% C<sub>3</sub>H<sub>8</sub>, 1.00% C<sub>4</sub>H<sub>8</sub> and 1.01% C<sub>4</sub>H<sub>10</sub>.

Gas analysis procedure as below:

- (1) To make a calibration curve for each gas; a measured gas volume of 30, 50, 100 µL

was taken from an aluminum bag containing the standard gas using a gas syringe.

- (2) Using syringe, 100  $\mu\text{L}$  of SCWG gas sample was taken from the gas sampling system. The same procedure was used for the analysis. Gas composition and ratios were calculated.

### **2.5.3. Catalyst Characterization**

#### **2.5.3.1. SEM-EDX**

Quantitative analysis of the catalyst surface was carried out using a scanning electron microscope JSM 5600 (JEOL) equipped with energy-dispersive X-rays at the electron microscopy laboratory of the Institute of Solid-State Physics, University of Tokyo. Samples were attached to double-sided adhesive carbon tape and mounted on a silver sample holder. By moving the holder and adjusting the focus, an ideal image of the sample was found and stored in the computer.

#### **2.5.3.2. XRD**

X-ray diffractometers (XRD) are used to analyse the metal oxidation results of catalyst samples after SCWG. The equipment is located in the X-ray analysis laboratory of the Institute for Solid State Physics at the University of Tokyo. The voltage and current used for analysis are 40 keV and 30.0 mA, respectively. The analysis range is 10-90 degrees, and the analysis speed is 4 degrees/min.

The sample analysis method as the procedure below:

- (1) Take catalyst samples from liquid phase, save it immediately.
- (2) Crush samples into powder by mortar before XRD analysis.
- (3) Put the sample on the glass plate and make sure it as the correct place.
- (4) Analyze the sample by XRD.
- (5) Analyze the data of the peaks.

## Chapter 3. DECOMPOSITION OF SIMULATED GUTTER OIL

Chapter 3 presents the results of the SCWG experiments using the experimental methods and analytical techniques in Chapter 2. In the first section, the results of converting the SGO to a gaseous product are discussed. This assesses the effect of biomass concentration using two different SGO concentrations, high and low, with the aim of determining the optimal oil concentration during SCWG as well as exploring the feasibility of SGO processing at high concentrations. This discussion is essential for understanding the reactivity of SGO in SCW and its conversion to gaseous product formation. Part 2 presents the decomposition products identified in the liquid phase. The liquid phase analysis indicates the carbon conversion and the products produced in the SGO of SCWG process. The overall carbon mass balance derived from the analytical results is presented in the third part. The fourth part presents the effect of catalyst on the hydrothermal experiments with the aim of comparing the process performance and efficiency and the trend of gaseous product formation at catalysts addition.

### 3.1. Overall Carbon Balance

To determine the proportion of product distribution, the overall carbon balance is plotted. Considering that only the carbon concentrations in the water-phase and gas phases were directly analyzed, the carbon concentration in another phase was named “oil” which was calculated by the Equation 3-1.

$$C(\text{oil}) = 100\% - C(\text{water}) - C(\text{gas}) \quad [3-1]$$

Figure 3-1 and Figure 3-2 present the carbon balance of SCWG for 2wt% and 20wt% SGO, respectively. The experimental group with 2 wt% SGO had a higher proportion of gas products compared to the experimental group with 20 wt% SGO. This indicates that the system is capable of converting low concentration biomass into gas products, but high concentration biomass needs to be at high temperature to have a better percentage of gas products. Also, the experimental group with longer residence time obtained a higher percentage of gas, which indicates that the system can gasify biomass to gas products over time. However, at high concentrations at low temperatures, the oil ratio was high, as in No. 4.

In addition, in the experiments with higher oil concentrations, a black oil-like substance was observed to flow out of the system and on top of the liquid product, and therefore that could represent the oil ratio in the carbon balance. Take some examples, the pictures of liquid products are shown in Figure 3-3, and the comparison pictures of low concentration is shown in Figure 3-4.

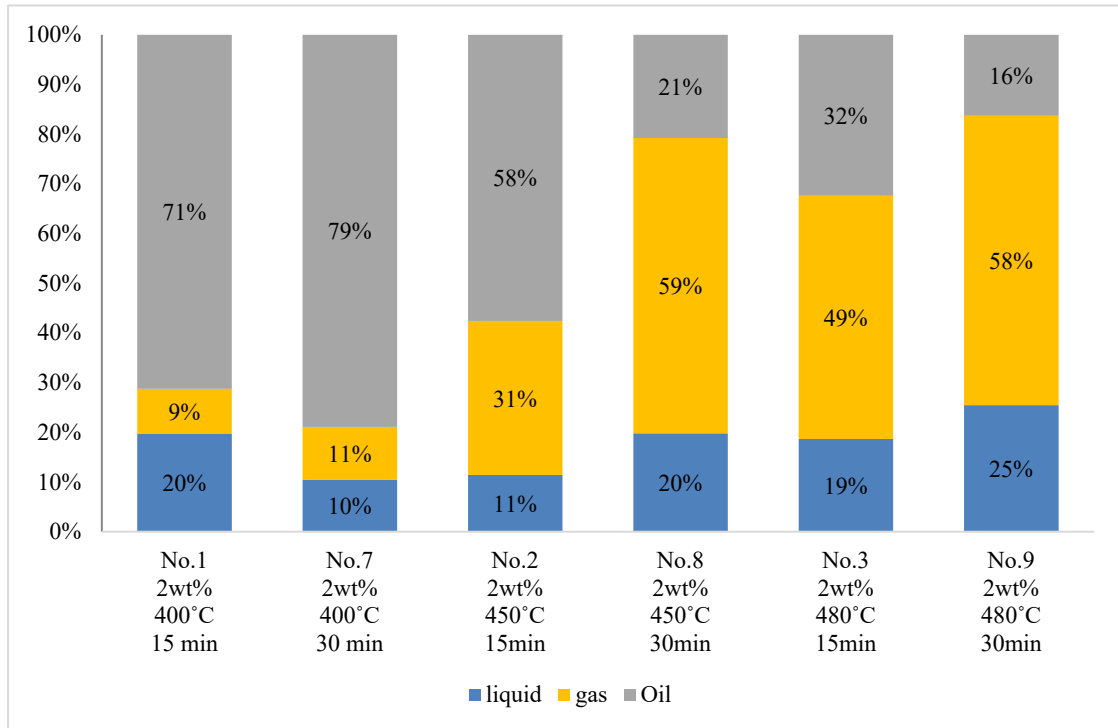


Figure 3-1 Carbon balance for SCWG of 2wt% SGO.

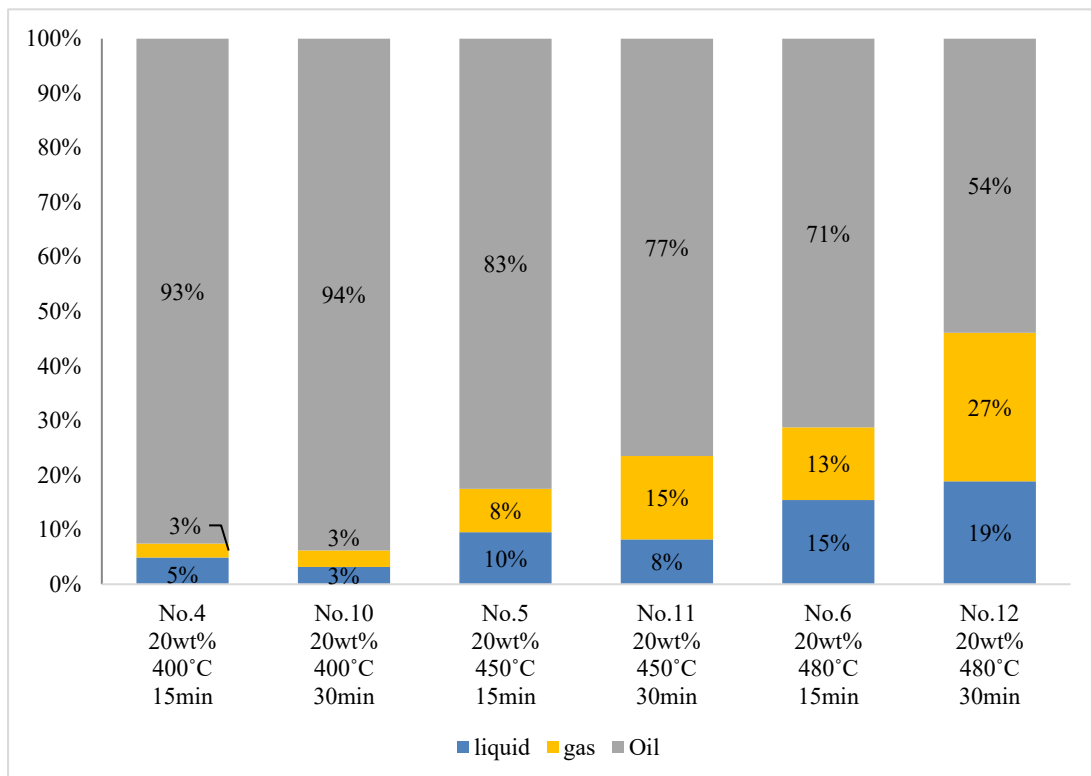


Figure 3-2 Carbon balance for SCWG of 20wt% SGO.

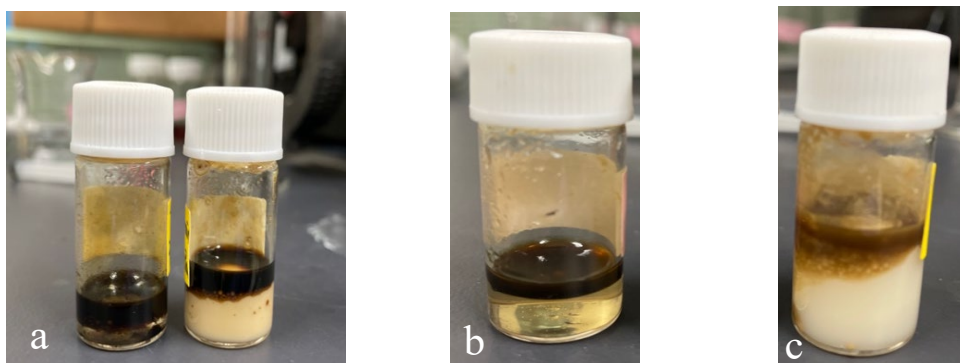


Figure 3-3 Liquid samples pictures, a: 480°C, 20wt%, 15min (left), 30min (right)  
 b: 450°C, 20wt%, 15min, c: 400°C, 20wt%, 30min.



Figure 3-4 Liquid samples pictures, 480°C, 2wt%, 15min (left), 30min (right)

### 3.2. Gas Product Analysis

To investigate the extent of SGO conversion into gaseous product, gas products were analyzed using GC-TCD and GC-FID. Analytical results of gas samples after hydrothermal reactions include gas yield, cold gas efficiency (CoGE), and hydrogen gasification efficiency (HGE), carbon gasification efficiency (CGE).

The number of multiple gases is calculated based on the amount of gas samples collected by the syringe at room temperature. The total results are shown in Table 3-1 to Table 3-3.

By comparing the tables, it is clear that the best experimental group is the catalytic SCWG at 480°C with a SGO concentration of 2 wt%. All data are the highest, with HGE close to 90%, which means that a high conversion of hydrogen is achieved, and, with CoGE over 50%, which represents an ideal energy conversion, it is undoubtedly the best of all experimental groups.

Table 3-1 Gas analysis results for SCWG at 400°C

Condition	400°C					
	2wt%		20wt%		2wt%	20wt%
	15min	30min	15min	30min	15min, 0.5g catalysts	
Gas yield [mol/kg]	2.58	2.70	0.730	0.940	7.90	2.96
HGE [%]	10.2%	11.5%	2.54%	3.25%	30.0%	11.9%
CGE [%]	9.09%	10.7%	2.55%	3.04%	24.9%	8.76%
CoGE [%]	5.47%	5.89%	0.800%	1.84%	13.7%	5.01%

Table 3-2 Gas analysis results for SCWG at 450°C

Condition	450°C					
	2wt%		20wt%		2wt%	20wt%
	15min	30min	15min	30min	15min, 0.5g catalysts	
Gas yield [mol/kg]	7.86	14.9	2.12	4.90	14.9	8.62
HGE [%]	36.8%	66.1%	8.80%	17.3%	56.5%	33.9%
CGE [%]	31.0%	59.4%	7.95%	15.3%	44.2%	26.0%
CoGE [%]	11.4%	20.7%	3.26%	8.70%	23.0%	21.3%

Table 3-3 Gas analysis results for SCWG at 480°C

Condition	480°C					
	2wt%		20wt%		2wt%	20wt%
	15min	30min	15min	30min	15min, 0.5g catalysts	
Gas yield [mol/kg]	14.9	18.1	4.07	9.18	23.2	21.1
HGE [%]	54.4%	68.4%	15.7%	33.1%	87.6%	83.5%
CGE [%]	48.9%	58.2%	13.3%	26.9%	66.1%	61.6%
CoGE [%]	15.7%	22.3%	7.89%	12.4%	50.2%	53.0%

### 3.2.1. Carbon and hydrogen gasification efficiency, gas yield

To evaluate the conversion of SGO in hydrothermal reactions, gas yield, hydrogen gasification efficiency and carbon gasification efficiency indices were used as defined in Equation 3-2 to Equation 3-4. Meanwhile, the results of the SCWG experimental gas products were divided into three parts according to temperature, residence time and biomass concentration, as shown in Figures 3-5 to 3-20.

$$\text{Gas yield [mol/kg]} = \frac{\text{mole of gas production[mol]}}{\text{amount of biomass [kg]}} \quad [3-2]$$

Carbon gasification efficiency (CGE) [%]

$$= \frac{n\text{CO}_2 + n\text{CO} + n\text{CH}_4 + 2n\text{C}_2\text{H}_4 + 2n\text{C}_2\text{H}_6 + 3n\text{C}_3\text{H}_6 + 3n\text{C}_3\text{H}_8 + 4n\text{C}_4\text{H}_8 + 4n\text{C}_4\text{H}_{10}}{n(\text{carbon atoms in SGO})} \quad [3-3]$$

Hydrogen gasification efficiency (HGE) [%]

$$= \frac{2n\text{H}_2 + 4n\text{CH}_4 + 4n\text{C}_2\text{H}_4 + 6n\text{C}_2\text{H}_6 + 6n\text{C}_3\text{H}_6 + 8n\text{C}_3\text{H}_8 + 8n\text{C}_4\text{H}_8 + 10n\text{C}_4\text{H}_{10}}{n(\text{hydrogen atoms in SGO})} \quad [3-4]$$

### 3.2.1.1. Temperature dependence

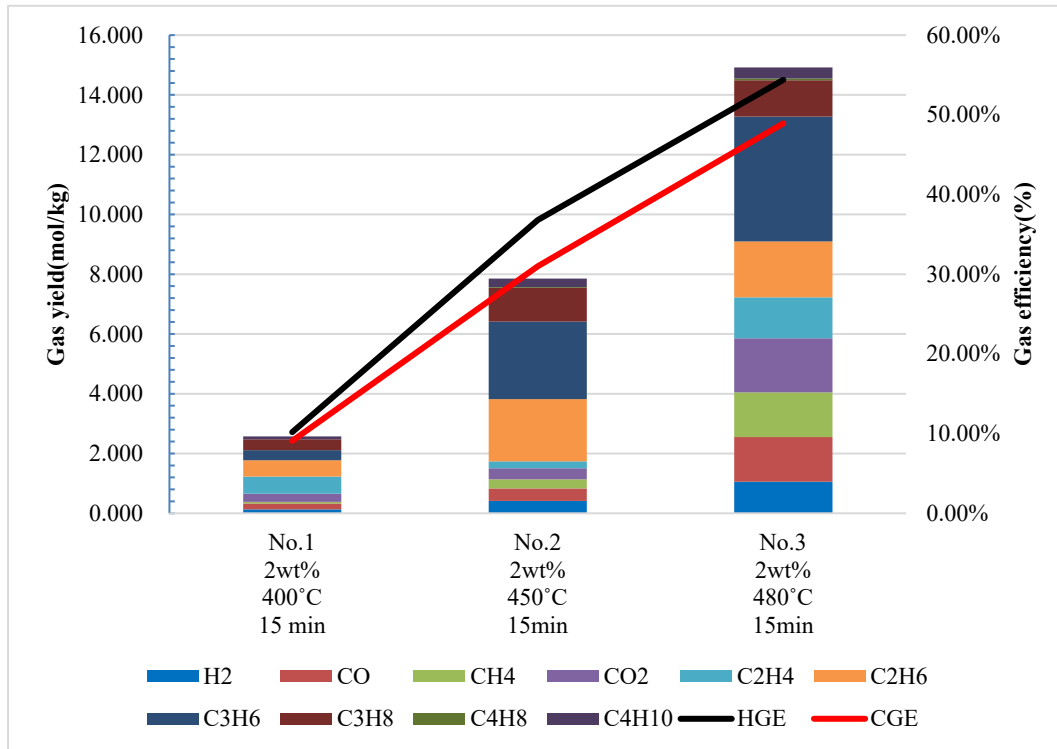


Figure 3-5 Gas yield and efficiencies of SCWG at 25 MPa and 15min residence time with 2wt% SGO.

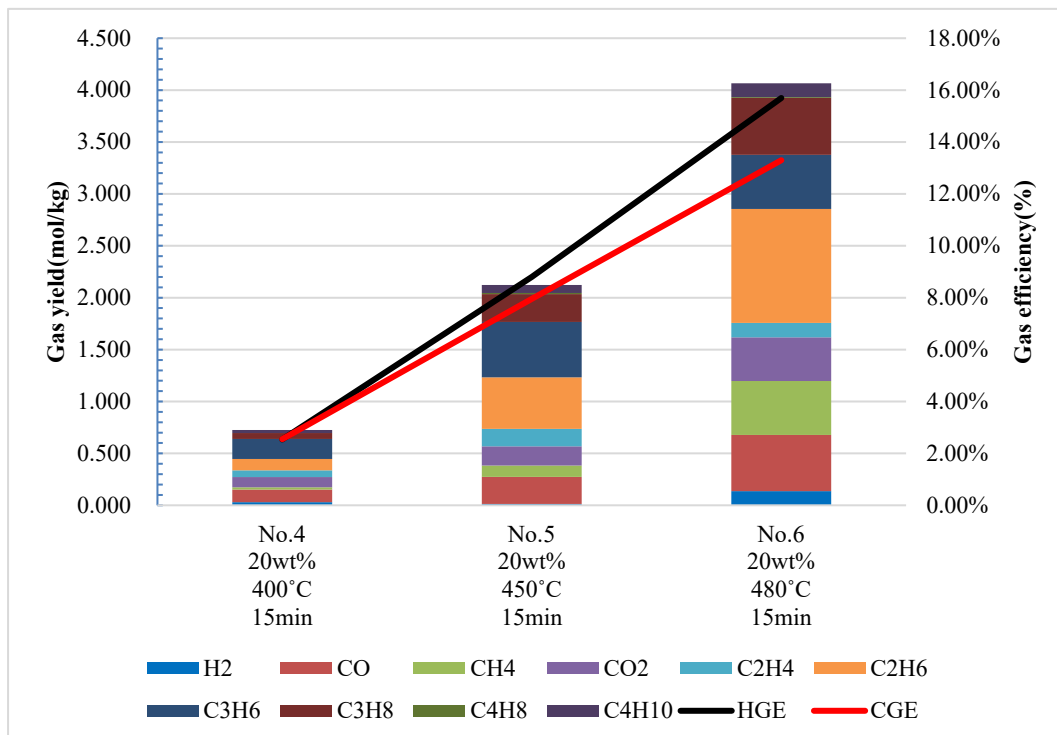


Figure 3-6 Gas yield and efficiencies of SCWG at 25 MPa and 15min residence time with 20wt% SGO.

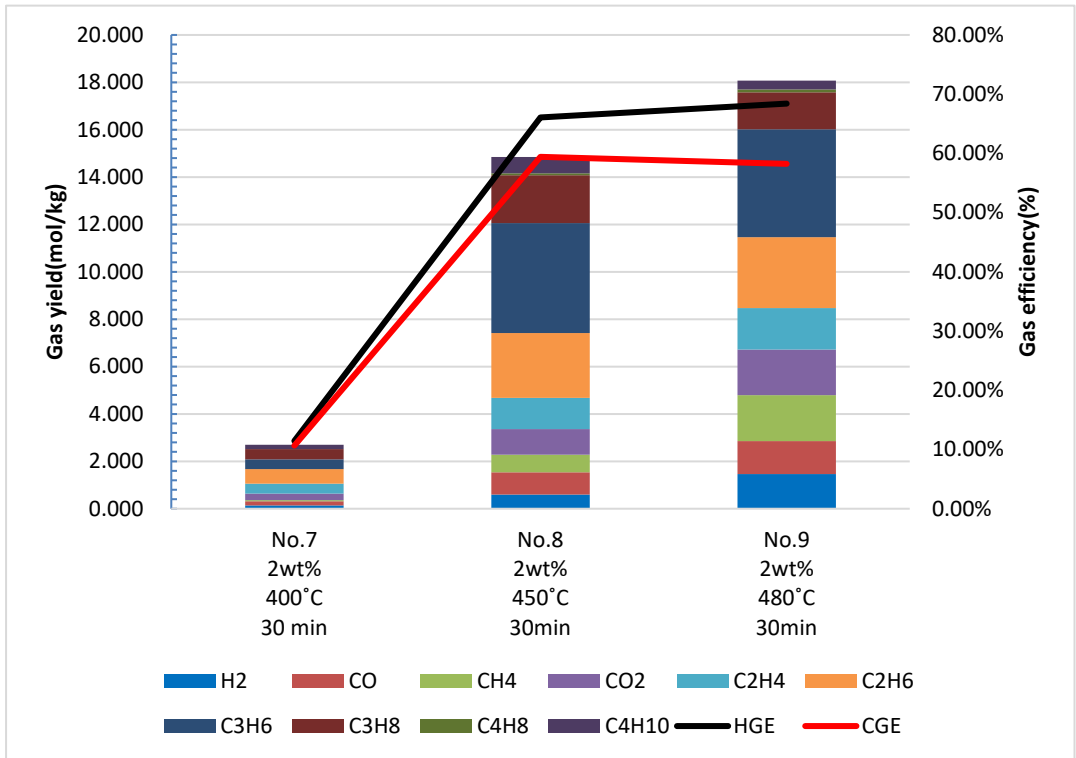


Figure 3-7 Gas yield and efficiencies of SCWG at 25 MPa and 30min residence time with 2wt% SGO.

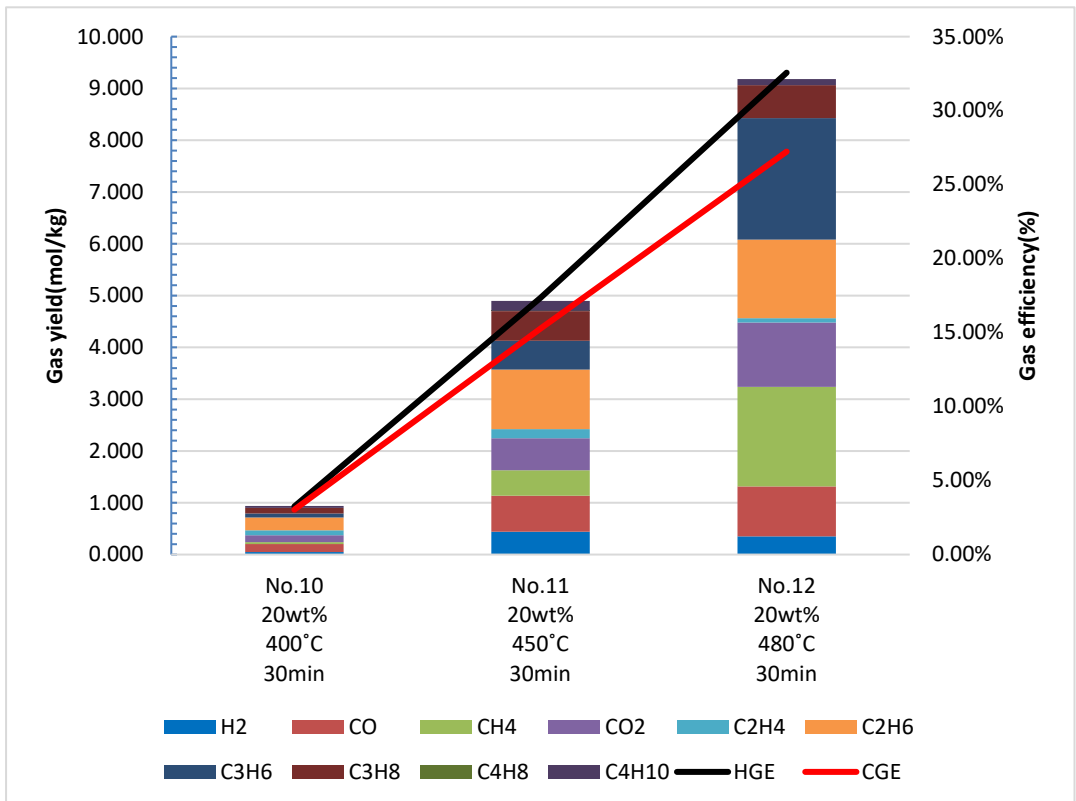


Figure 3-8 Gas yield and efficiencies of SCWG at 25 MPa and 30min residence time with 20wt% SGO.

### 3.2.1.2. Concentration dependence

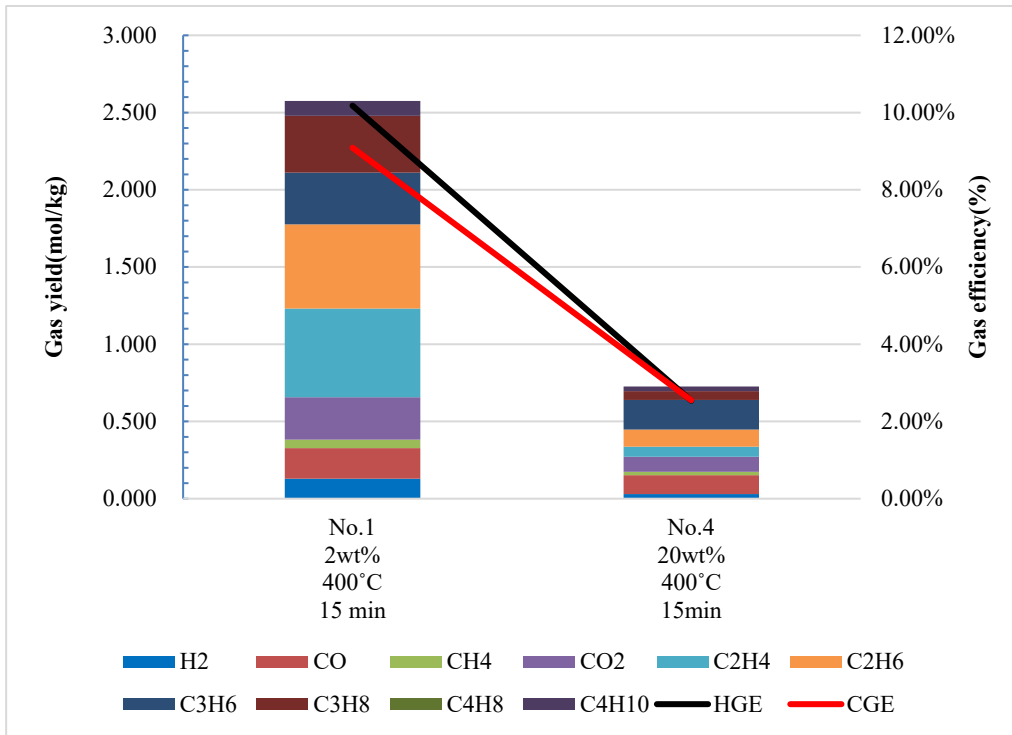


Figure 3-9 Gas yield and efficiencies of SCWG at 400°C, 25 MPa and 15min residence time.

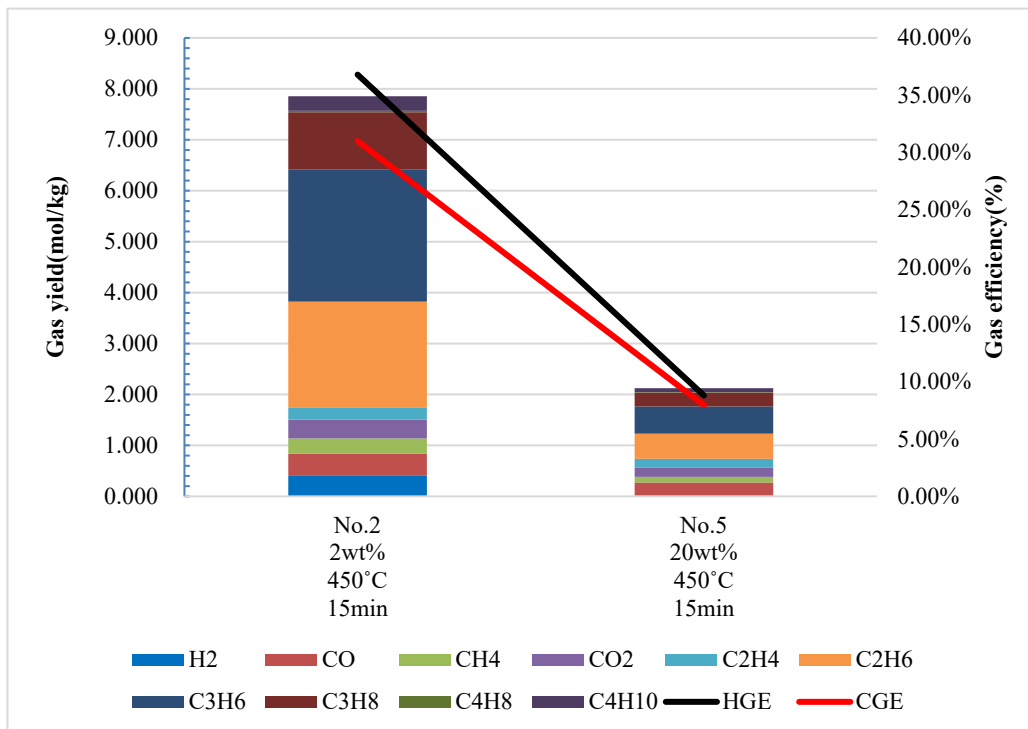


Figure 3-10 Gas yield and efficiencies of SCWG at 450°C, 25 MPa and 15min residence time.

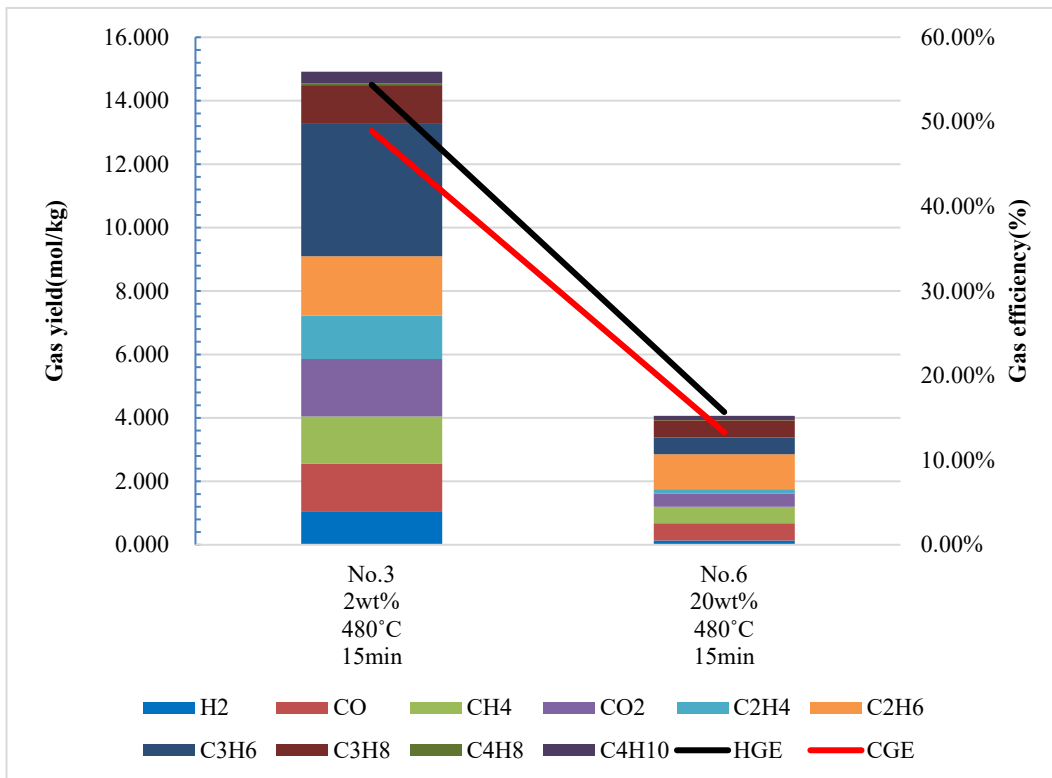


Figure 3-11 Gas yield and efficiencies of SCWG at 480°C, 25 MPa and 15min residence time.

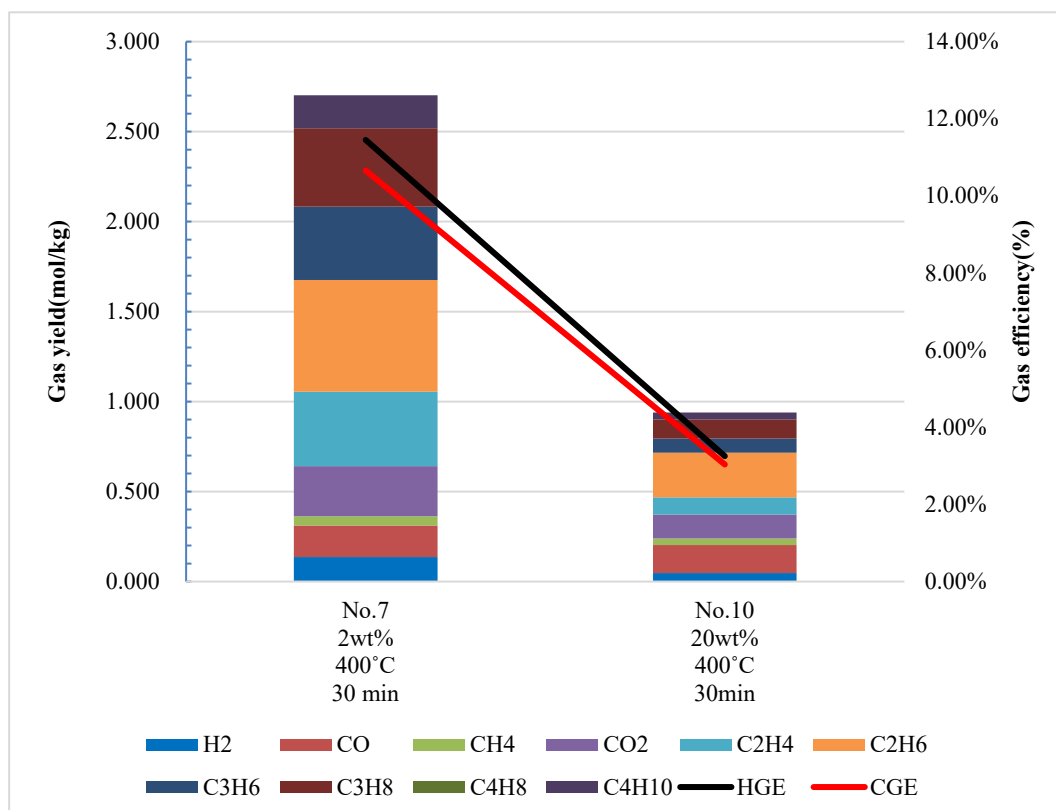


Figure 3-12 Gas yield and efficiencies of SCWG at 400°C, 25 MPa and 30min residence time.

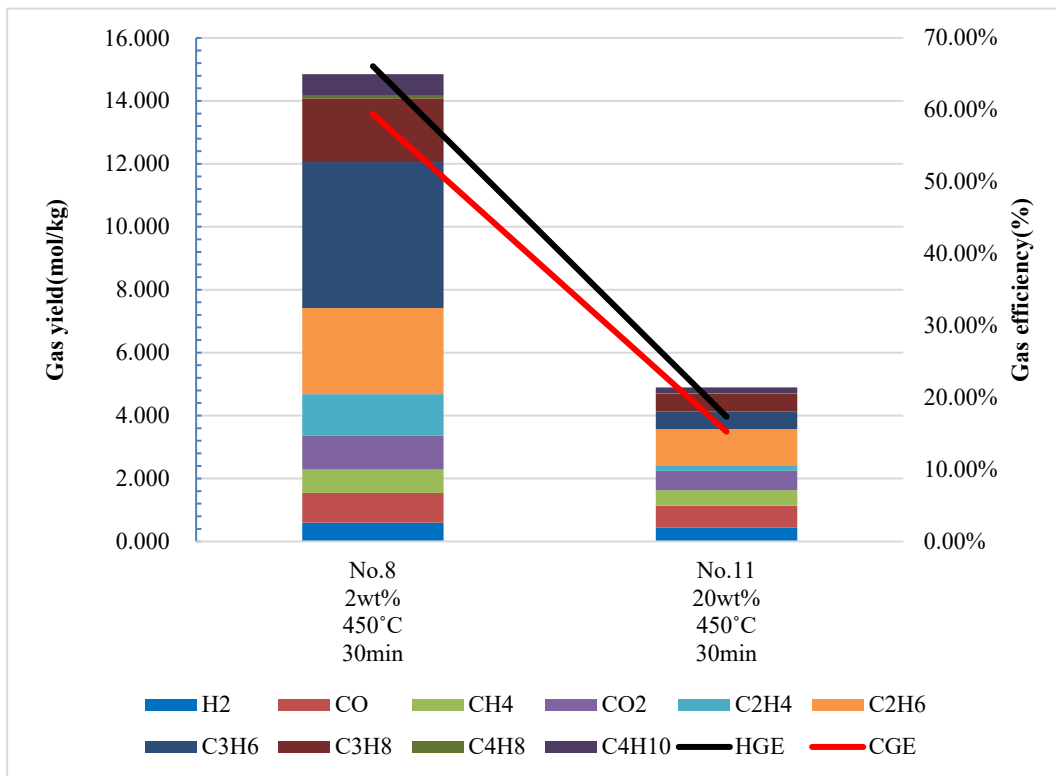


Figure 3-13 Gas yield and efficiencies of SCWG at 450°C, 25 MPa and 30min residence time.

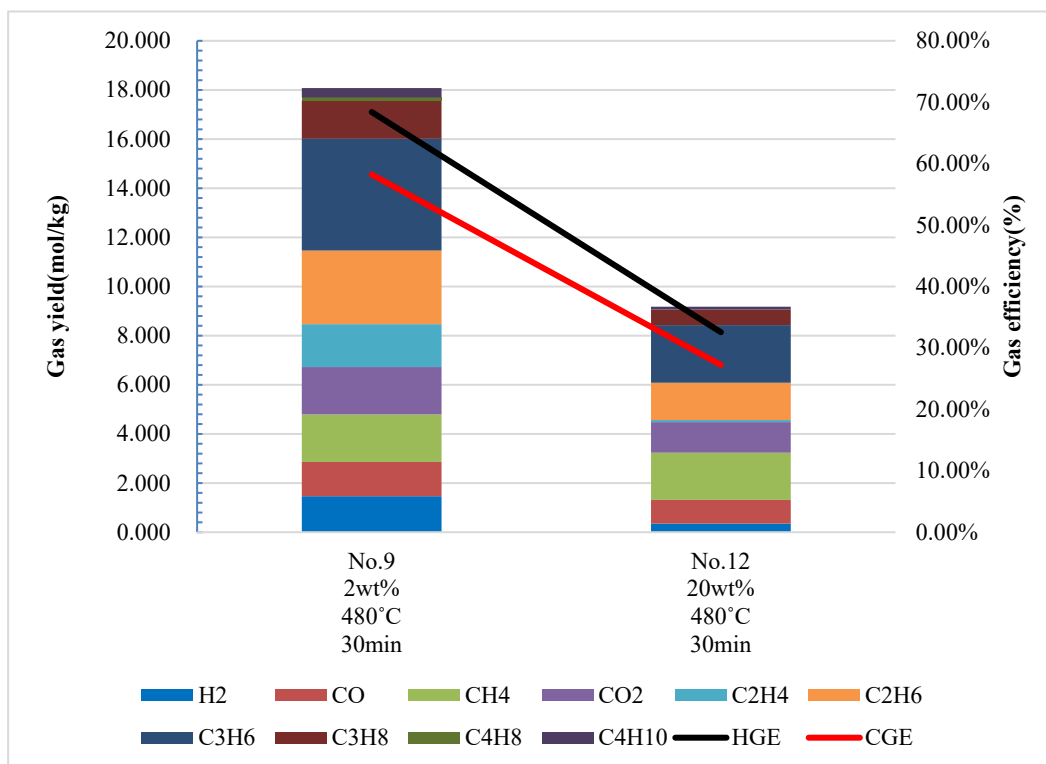


Figure 3-14 Gas yield and efficiencies of SCWG at 480°C, 25 MPa and 30min residence time.

### 3.2.1.3. Residence time dependence

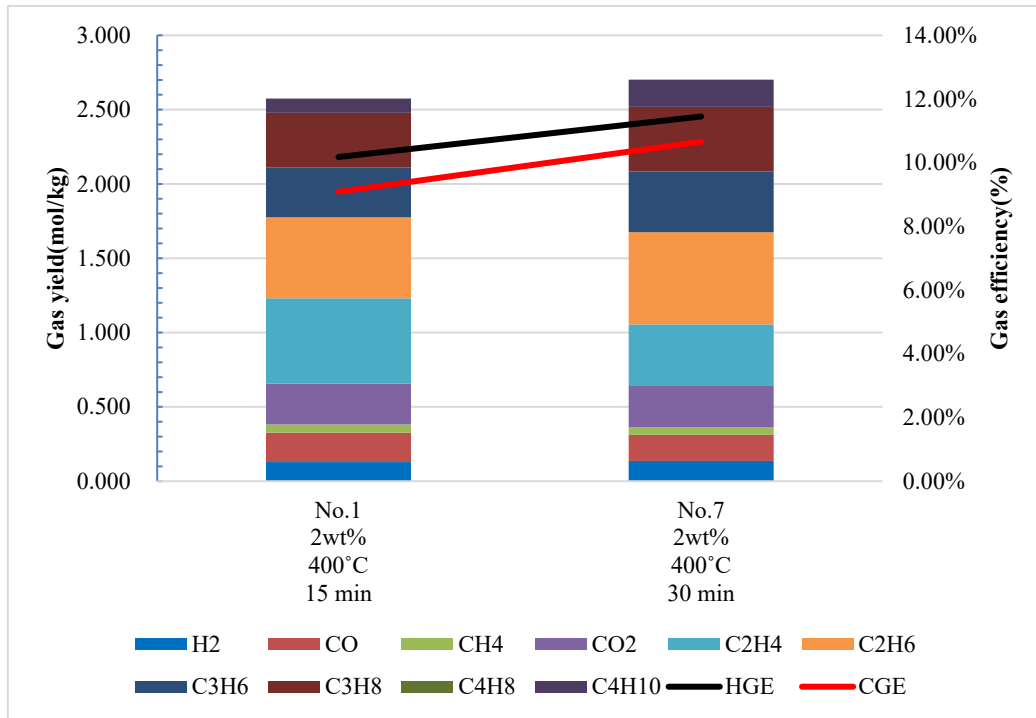


Figure 3-15 Gas yield and efficiencies of SCWG at 400°C, 25 MPa and with 2wt% SGO.

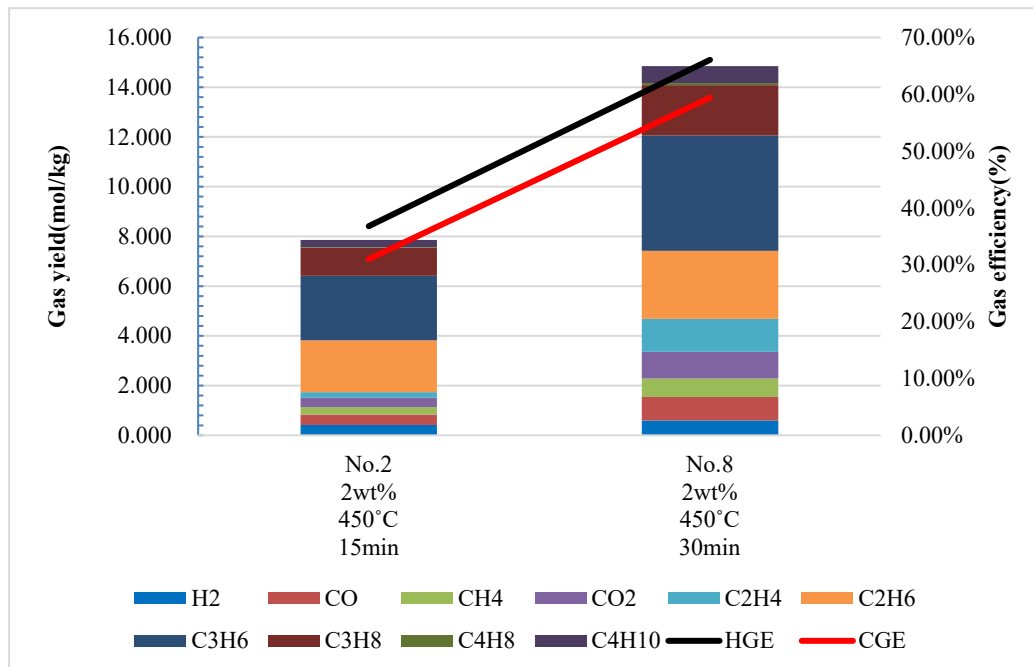


Figure 3-16 Gas yield and efficiencies of SCWG at 450°C, 25 MPa and with 2wt% SGO.

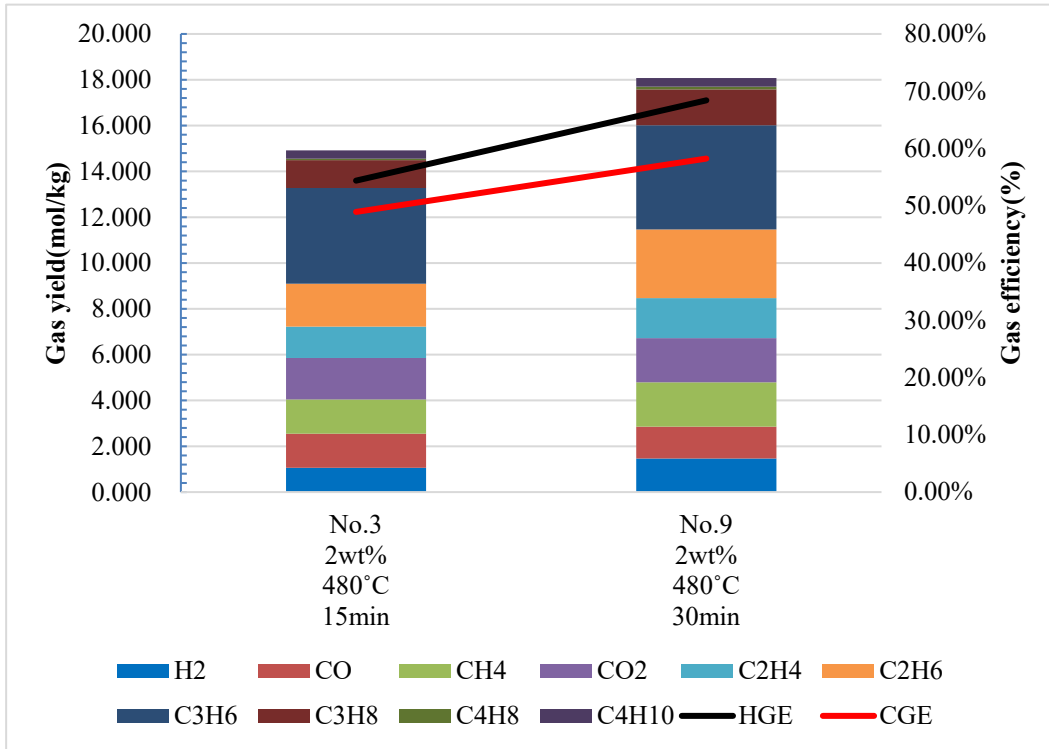


Figure 3-17 Gas yield and efficiencies of SCWG at 480°C, 25 MPa and with 2wt% SGO.

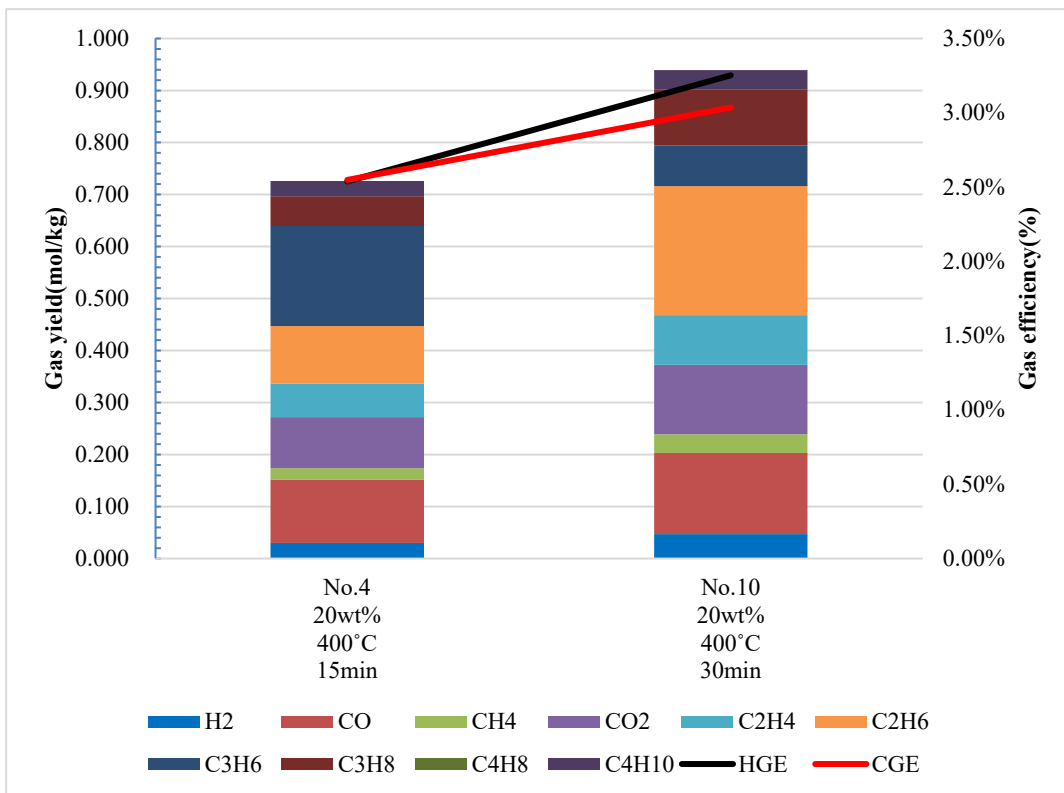


Figure 3-18 Gas yield and efficiencies of SCWG at 400°C, 25 MPa and with 20wt% SGO.

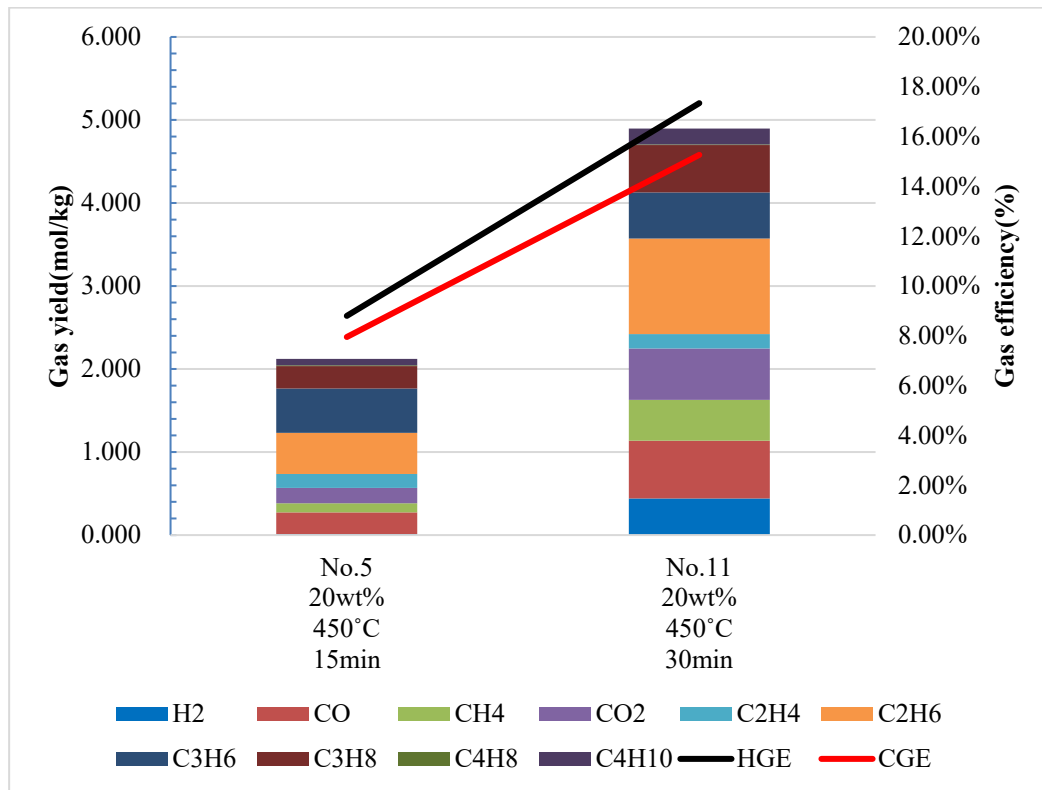


Figure 3-19 Gas yield and efficiencies of SCWG at 450°C, 25 MPa and with 20wt% SGO.

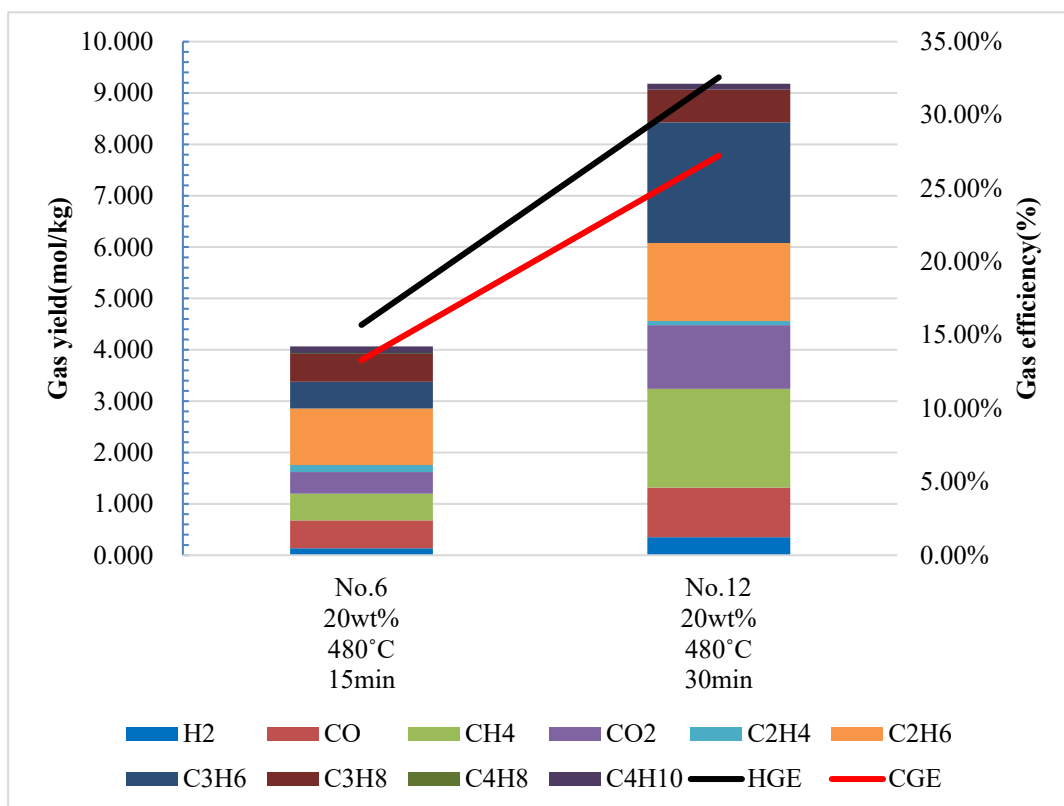


Figure 3-20 Gas yield and efficiencies of SCWG at 480°C, 25 MPa and with 20wt% SGO.

#### 3.2.1.4. Summary and discussion

From Figure 3-5 to Figure 3-8, it shows that the gas yield and efficiencies increase as the reaction temperature increases. It indicates that the system is able to gasify biomass well at high temperature but comparing No.8 and No.9, at the same low biomass concentration conditions the difference in gas efficiencies is not significant with little difference in high temperatures. Moreover, at high concentration conditions, the difference in gas efficiency with little difference in temperature is also significant. This implies that temperature is the key influencing factor for SGO gasification at high SGO concentrations.

From Figure 3-9 to Figure 3-14, it is noteworthy that the gas yield and efficiencies decreases as the SGO concentration increases. As observed, the No.9 SCWG experiments showed better performance in the tested conditions. Moreover, its high average gas yield indicates that the system is able to gasify SGO very well at lower concentrations.

From Figure 3-15 to Figure 3-20, it is shown that the gas yield and efficiency increase as the residence time increases. As comparison, the system is able to gasify biomass well at longer residence time. Besides that, the results show that at low temperature, the difference of gas production is not significant. The huge difference only shown at the high temperature and high concentration. Therefore, it concluded that the residence time also is one key factor for gasification of SGO.

#### 3.2.2. Cold gas efficiency

Cold gas efficiency (CoGE) indicates the energy conversion efficiency from biomass feedstock to syngas. It is an important parameter to be quantified, the amount of energy that can be transferred to the desired gaseous product. This amount can be calculated as the gas yield ( $Y_{gas}$ ) times the ratio between the higher heating value (HHV) of the product gas and that of the starting biomass.[37], [38]

The results of CoGE for SCWG experiments are shown in Figure 3-21 to Figure 3-29.

$$\text{CoGE [\%]} = \frac{\text{HHV of gas ( MJ/m}^3 \text{)}}{\text{HHV of feedstock ( MJ/kg)}} \times Y_{\text{gas}} [\text{m}^3/\text{kg}] \times 100\% \quad [ 3-5 ]$$

##### 3.2.2.1. HHV of SGO

The elemental composition of the utilized biomasses was measured using an elemental analyzer, is shown in Table 3-4. The higher heating value (HHV) of the feedstock estimated using the following Dulong's relation.[39]

$$\text{HHV} = 33.95C + 144.2(H - O/8) + 9.4S \text{ [MJ/kg]} \quad [ 3-6 ]$$

where C, H, O, and S represent the elemental composition of carbon, hydrogen, oxygen, and sulphur respectively.

Table 3-4 HHV and component analysis of the SGO.

Samples	Carbon (%)	Hydrogen (%)	Nitrogen (%)	Oxygen (%)	HHV (MJ/kg)
SGO	76.97	11.72	0.22	11.09	41.03

### 3.2.2.2. HHV of gas products

The higher heating value (HHV) of the gas product was calculated to indicate the calorific value of the gas product. The HHV of the syngas was computed from its composition and the HHVs of the single gaseous species. HHV of a gaseous fuel mixture can be calculated as Equation 3-7 [40], referring to the heating value of fuel gas constituents which are shown in Table 3-5.

In these experiments, since in the gas products only H<sub>2</sub>, CO, CH<sub>4</sub>, C<sub>2</sub>H<sub>4</sub>, C<sub>2</sub>H<sub>6</sub>, C<sub>3</sub>H<sub>8</sub>, C<sub>4</sub>H<sub>10</sub> are combustible, the HHV of syngas is the calorific value of these seven gases, which can be calculated by multiplying the gas composition and the HHV of each gas species, as in the Equation 3-8.

$$HV = \sum r_i HV_i \quad [3-7]$$

where  $r_i$  is the mole fraction of a constituent  $i$  of fuel gas, and  $HV_i$  is HHV of the constituent.

$$\begin{aligned} \text{HHV [MJ/m}^3\text{]} = & 12.78\omega_{\text{H}_2} + 12.64\omega_{\text{CO}} + 39.87\omega_{\text{CH}_4} + 63.5\omega_{\text{C}_2\text{H}_4} \\ & + 70.45\omega_{\text{C}_2\text{H}_6} + 63.5\omega_{\text{C}_3\text{H}_8} + 70.45\omega_{\text{C}_4\text{H}_{10}} \end{aligned} \quad [3-8]$$

where  $\omega$  is the mole fraction of gas species in the gas product.

Table 3-5 Heating Value of Fuel Gas Constituents[40]

Gas	Chemical Formula	LHV (MJ/m <sup>3</sup> )	HHV (MJ/m <sup>3</sup> )
Hydrogen	H <sub>2</sub>	10.81	12.78
Carbon monoxide	CO	12.64	12.64
Methane	CH <sub>4</sub>	35.93	39.87
Acetylene	C <sub>2</sub> H <sub>2</sub>	56.9	58.9
Ethylene	C <sub>2</sub> H <sub>4</sub>	59.55	63.5
Ethane	C <sub>2</sub> H <sub>6</sub>	64.5	70.45
Propane	C <sub>3</sub> H <sub>8</sub>	93	101
Butane	C <sub>4</sub> H <sub>10</sub>	123.8	134
Hydrogen sulfide	H <sub>2</sub> S	28.14	30.3

*Note:* HHV and LHV, higher and lower heating values of a fuel constituent.

Table 3-6 HHV, gas yield and CoGE for SCWG at 400°C

Condition	400°C					
	2wt%		20wt%		2wt%	20wt%
	15min	30min	15min	30min	15min, 0.5g catalysts	
HHV [MJ/m <sup>3</sup> ]	50.9	53.5	33.6	46.3	44.0	43.6
Gas yield [m <sup>3</sup> /kg]	0.0440	0.0450	0.0100	0.0160	0.128	0.0470
CoGE [%]	5.47%	5.89%	0.80%	1.84%	13.7%	5.01%

Table 3-7 HHV, gas yield and CoGE for SCWG at 450°C

Condition	450°C					
	2wt%		20wt%		2wt%	20wt%
	15min	30min	15min	30min	15min, 0.5g catalysts	
HHV [MJ/m <sup>3</sup> ]	42.9	41.9	42.8	42.8	46.9	53.8
Gas yield [m <sup>3</sup> /kg]	0.109	0.203	0.0310	0.0830	0.263	0.163
CoGE [%]	11.4%	20.7%	3.26%	8.70%	23.0%	21.3%

Table 3-8 HHV, gas yield and CoGE for SCWG at 480°C

Condition	480°C					
	2wt%		20wt%		2wt%	20wt%
	15min	30min	15min	30min	15min, 0.5g catalysts	
HHV [MJ/m <sup>3</sup> ]	32.4	35.6	46.4	38.0	49.3	54.1
Gas yield [m <sup>3</sup> /kg]	0.199	0.257	0.0700	0.133	0.418	0.402
CoGE [%]	15.7%	22.3%	7.89%	12.4%	50.2%	53.0%

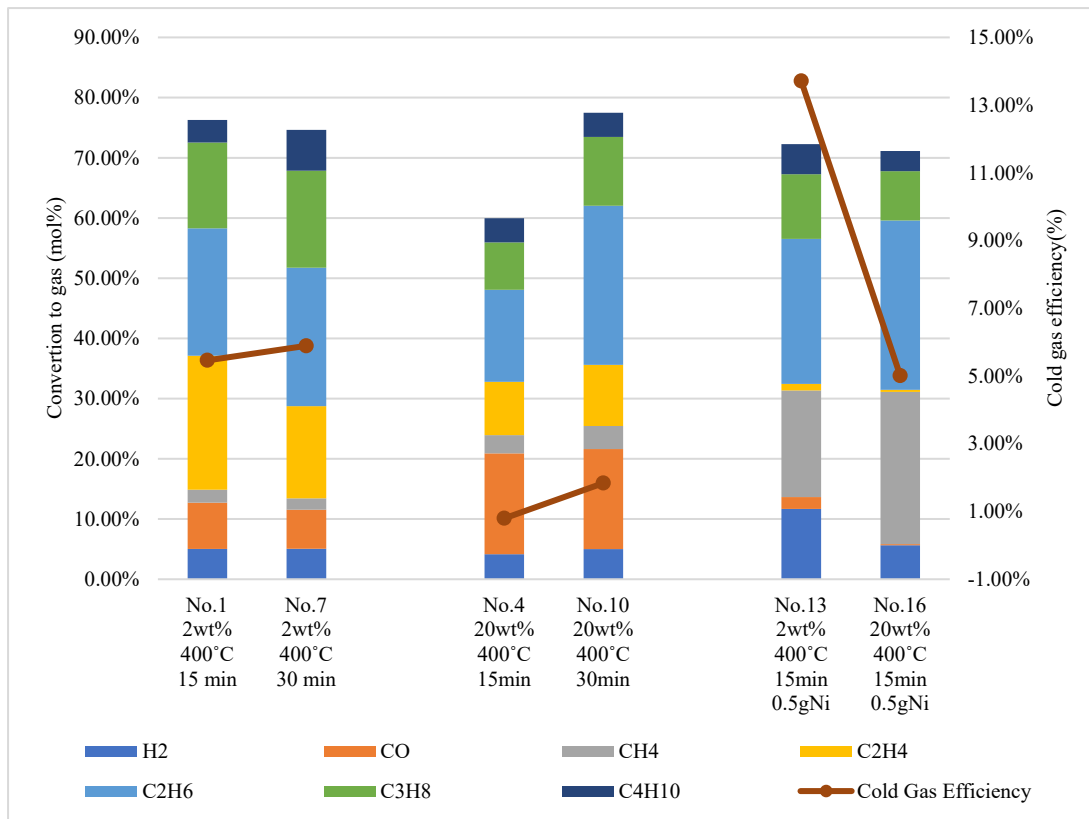


Figure 3-21 Cold gas efficiency of SCWG at 400°C.

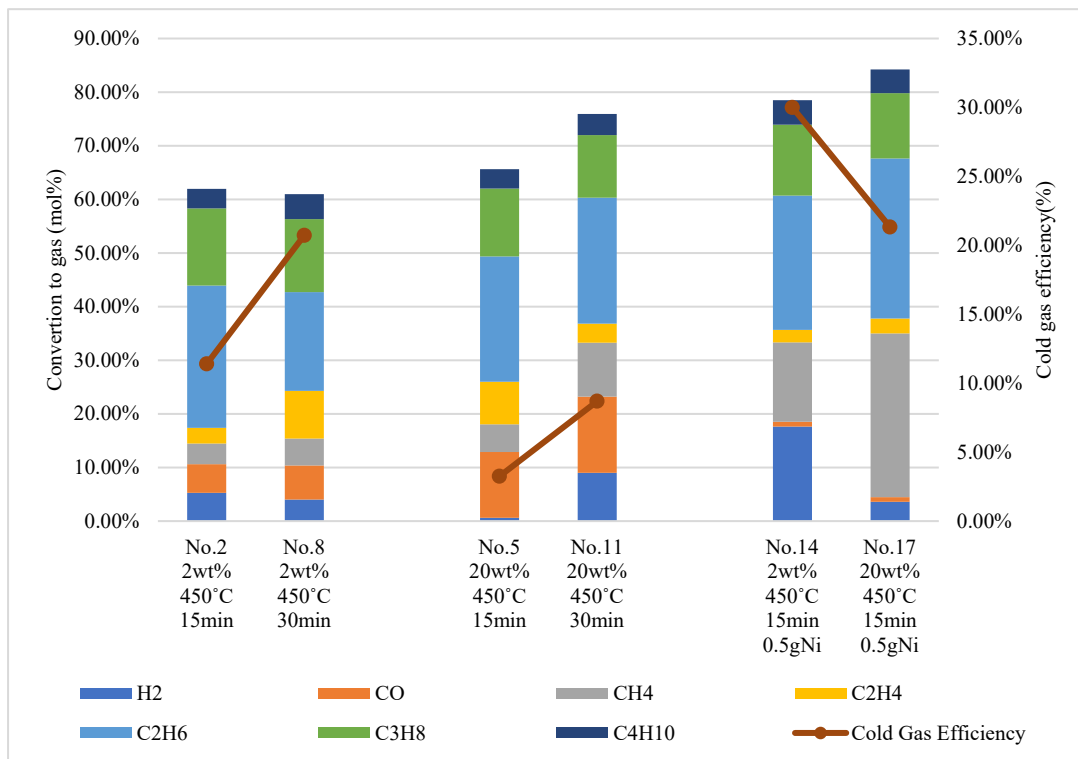


Figure 3-22 Cold gas efficiency of SCWG at 450°C.

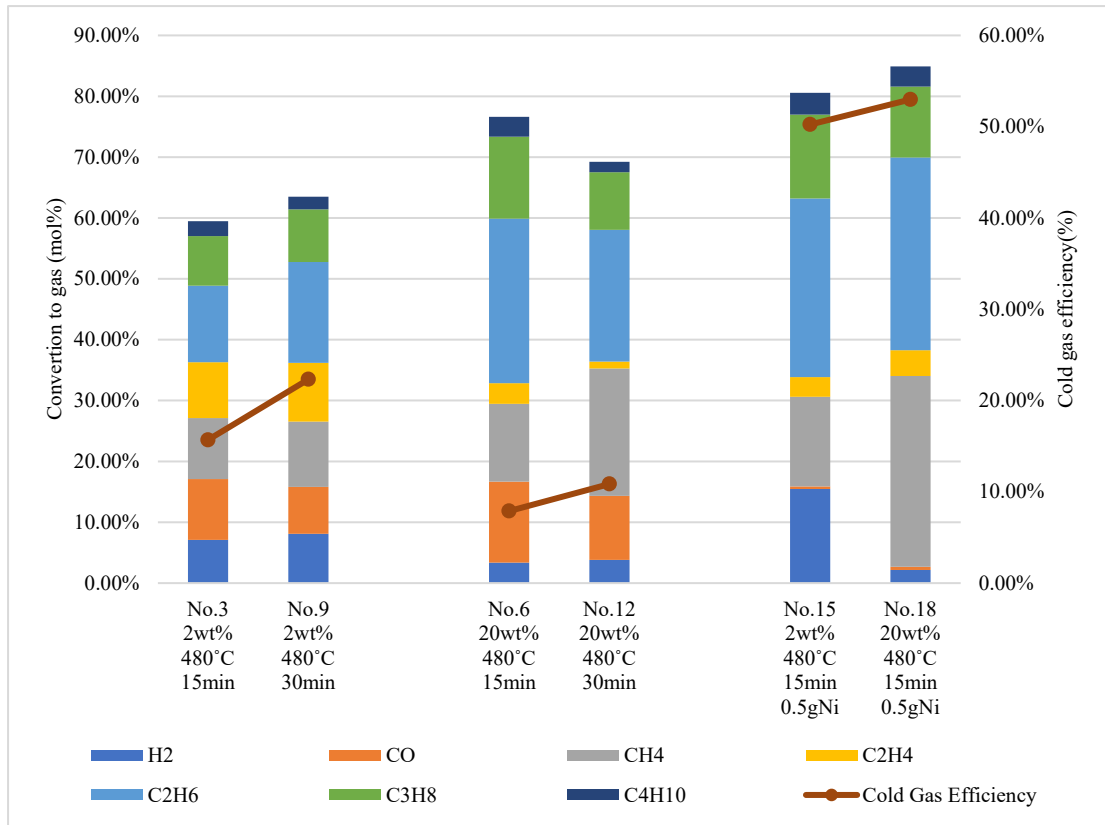


Figure 3-23 Cold gas efficiency of SCWG at 480°C.

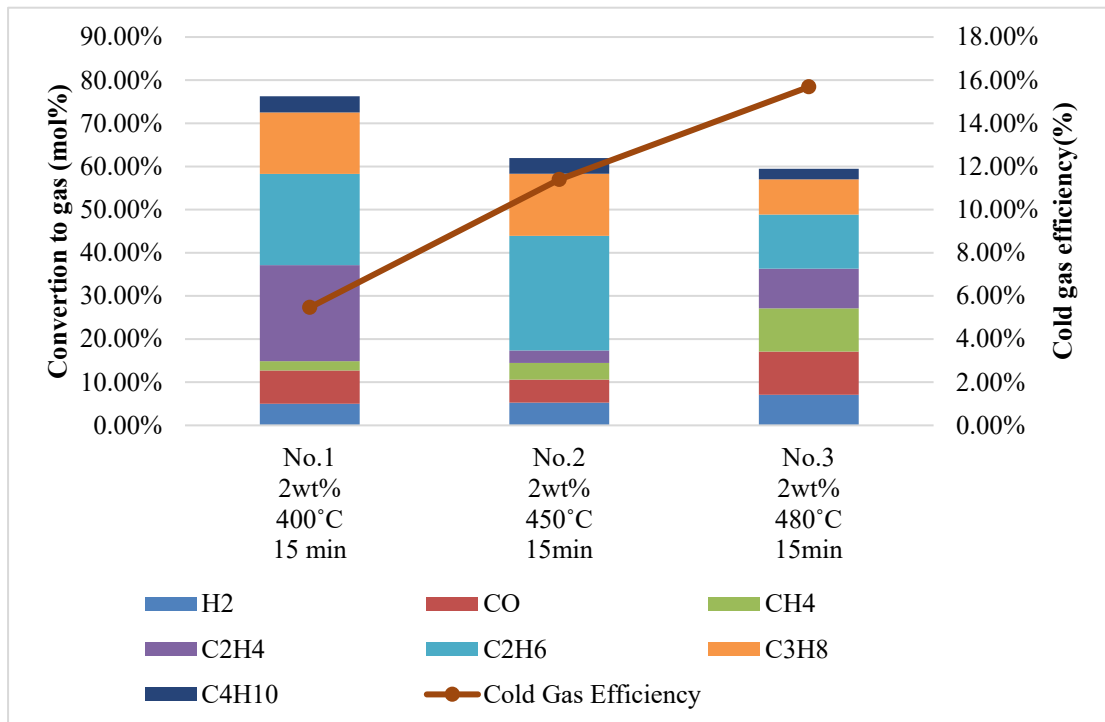


Figure 3-24 Cold gas efficiency of SCWG at 400°C, 25 MPa, 15min residence time and with 2wt% SGO.

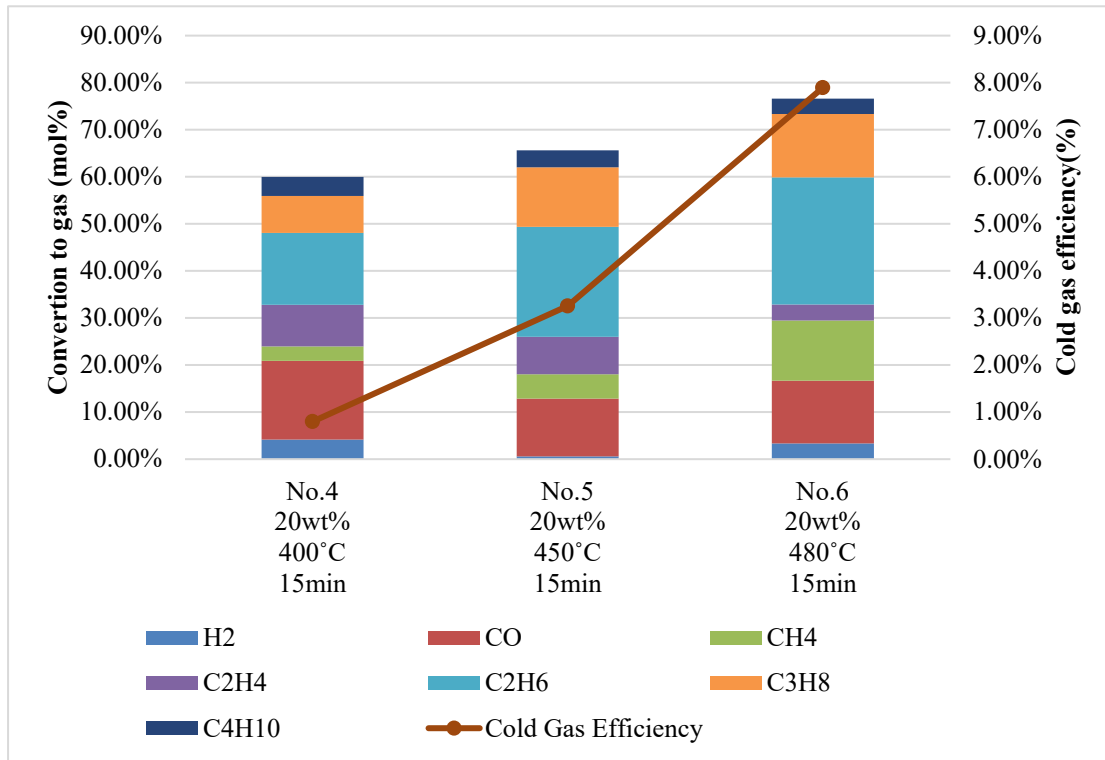


Figure 3-25 Cold gas efficiency of SCWG at 400°C, 25 MPa, 15min residence time and with 20wt% SGO.

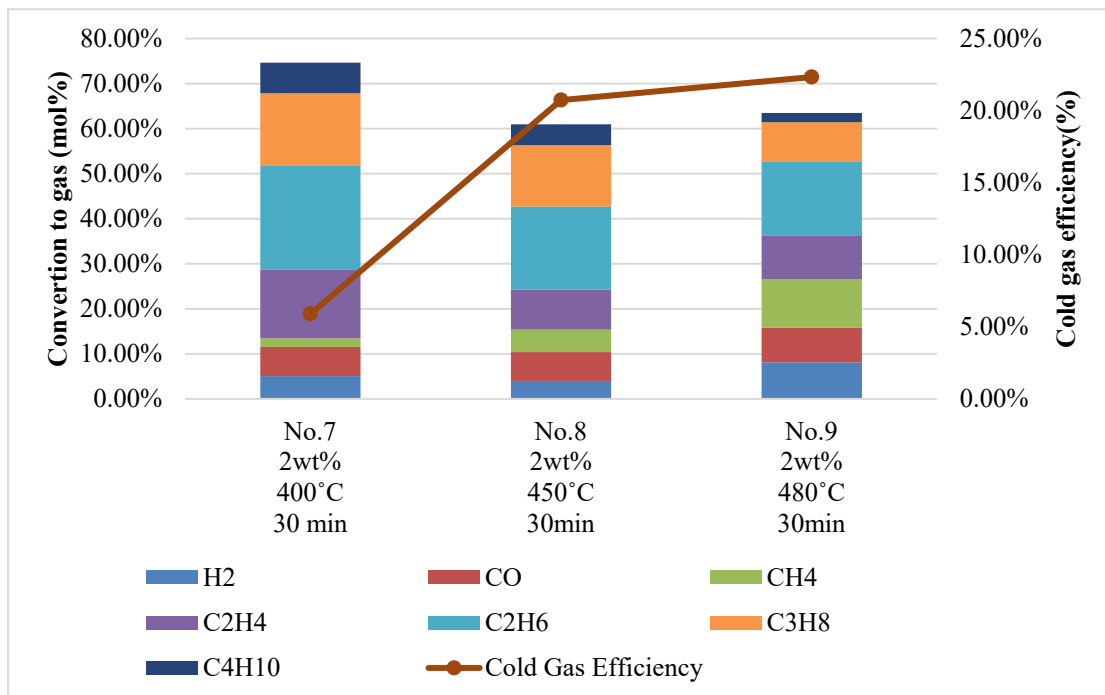


Figure 3-26 Cold gas efficiency of SCWG at 400°C, 25 MPa, 30min residence time and with 2wt% SGO.

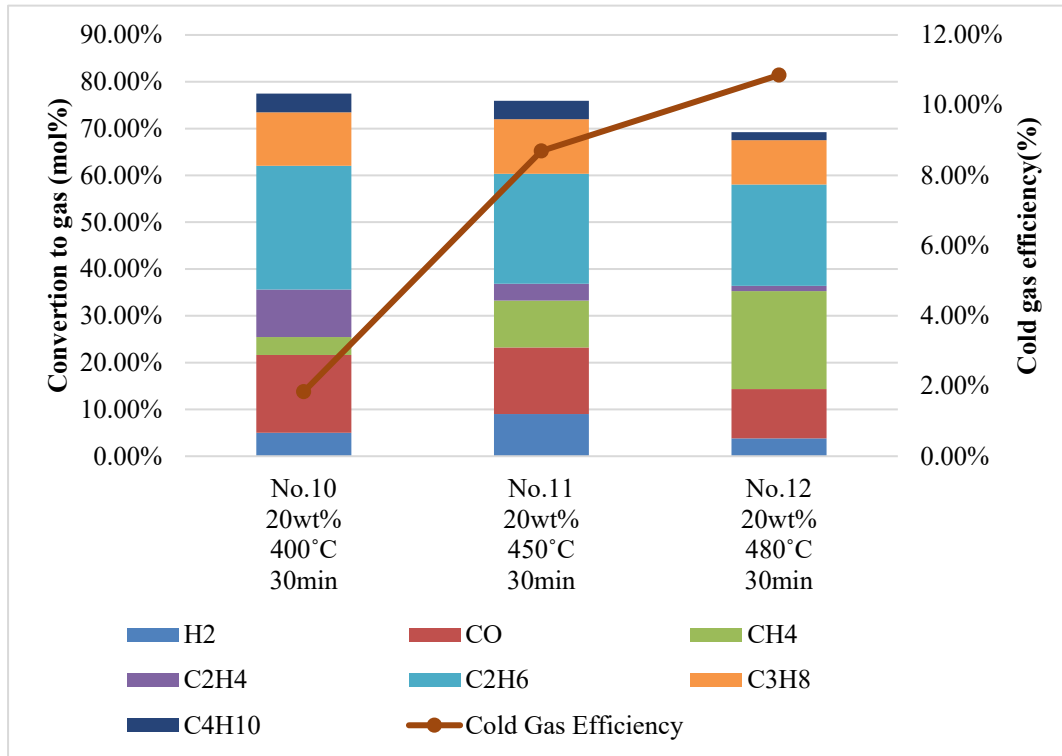


Figure 3-27 Cold gas efficiency of SCWG at 400°C, 25 MPa, 30min residence time and with 20wt% SGO.

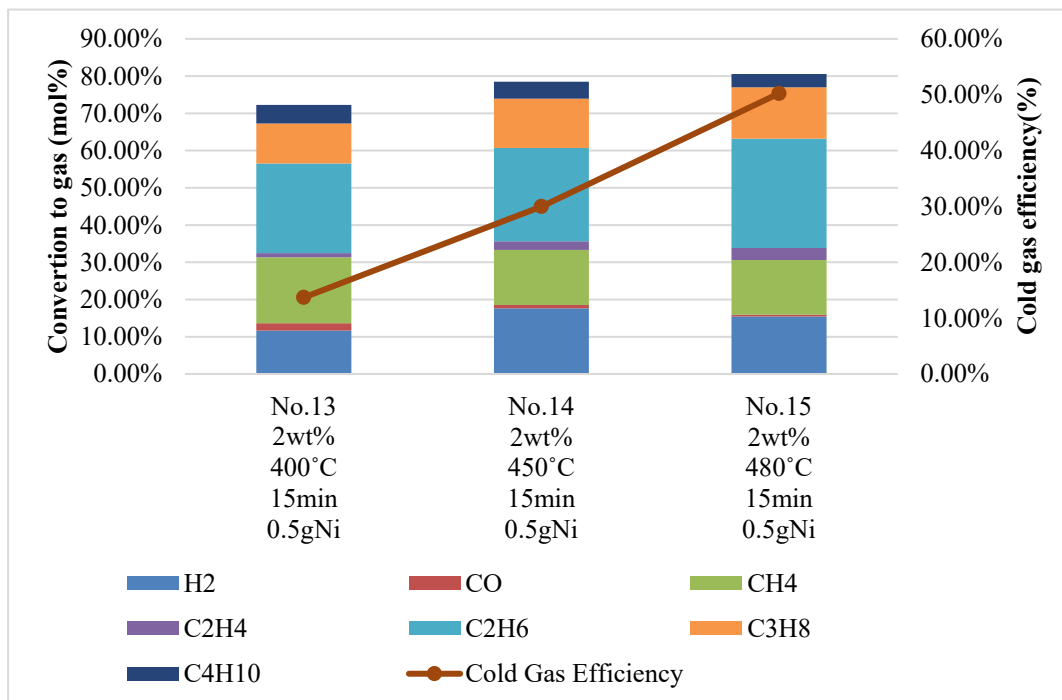


Figure 3-28 Cold gas efficiency of SCWG at 400°C, 25 MPa, 15min residence time, with 2wt% SGO and 0.5g catalysts.

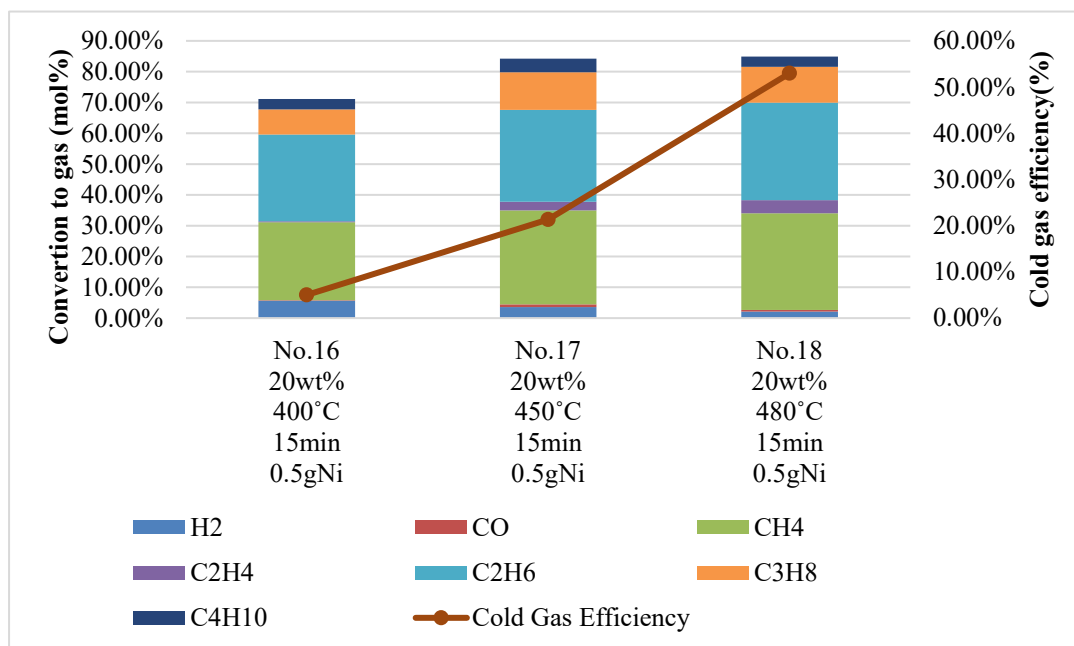


Figure 3-29 Cold gas efficiency of SCWG at 400°C, 25 MPa, 15min residence time, with 20wt% SGO and 0.5g catalysts.

### 3.2.2.3. Summary and discussion

From Figure 3-21 to Figure 3-29, it shown that the best SCWG experimental group is No.18 with the highest CoGE of 52.98%, meanwhile, the lowest samples are No.4 with the lowest CoGE of 0.8%. As time shifts from 15 to 30 minutes, CoGE increases with increasing residence time, however, conversely, CoGE decreases as the concentration of SGO changes from 2wt% to 20wt%, but this observation only occurs at 400°C and 450°C; when the temperature reaches 480°C, CoGE increases with increasing concentration. In addition, with the addition of catalysts, the content of hydrogen (H<sub>2</sub>) component, methane (CH<sub>4</sub>) and ethane (C<sub>2</sub>H<sub>6</sub>) component increased, meanwhile, CoGE is large than non-catalytic experiments. Observing the change of gas composition of No.13 with 16, No.14 with No.17, No.15 with No.18, it clear that the carbon monoxide (CO) content decreases and the amount of methane (CH<sub>4</sub>) more than doubles. From these gas changes, it can be assumed that the CO and CO<sub>2</sub> methanation reactions are well achieved during the gasification process, but unfortunately the hydrogen (H<sub>2</sub>) content decreases by as much as half.

To explore the effect of temperature on CoGE, Figure 3-24 to Figure 3-29 is plotted. It can be observed that as the temperature increases, so the CoGE of the test groups are increasing, which means that the temperature is positively affected. Observing the tables and combining it with the figures, it can be assumed that the factor affecting CoGE is not the overall percentage content of the gas product, but the individual gas composition and gas yield (m<sup>3</sup>/kg). Since the HHV of each different gas in the sample is different, for example, the HHV of C<sub>2</sub>-C<sub>4</sub> is larger, so the CoGE of the sample with a high molar percentage of C<sub>2</sub>-C<sub>4</sub> gas is also larger, such as No.18.

### 3.3. Liquid Phase Analysis

#### 3.3.1. TOC Analysis

The total organic carbon (TOC) in the liquid phase after the hydrothermal reaction was analyzed by a TOC analyzer.

Figure 3-30 to Figure 3-33 shows the results of the TOC at 400°C, 450°C, and 480°C, respectively. The TOC should come from the dissolved organic compounds. Therefore, any reduction of TOC in the liquid phase means that the organic compounds in the SGO sample are being transferred to the gas phase. For example, No. 15 in the Figure 3-33 has the least amount of TOC of all reactions, which means that most of the carbon is being converted to the gas product, which in combination with the gas yield supports this speculation. TOC can be observed not only for the dissolution of the sample in the liquid phase, but also for the calculation of the conversion of carbon in the solid gas liquid product, the results of which will be shown in subsequent sections.

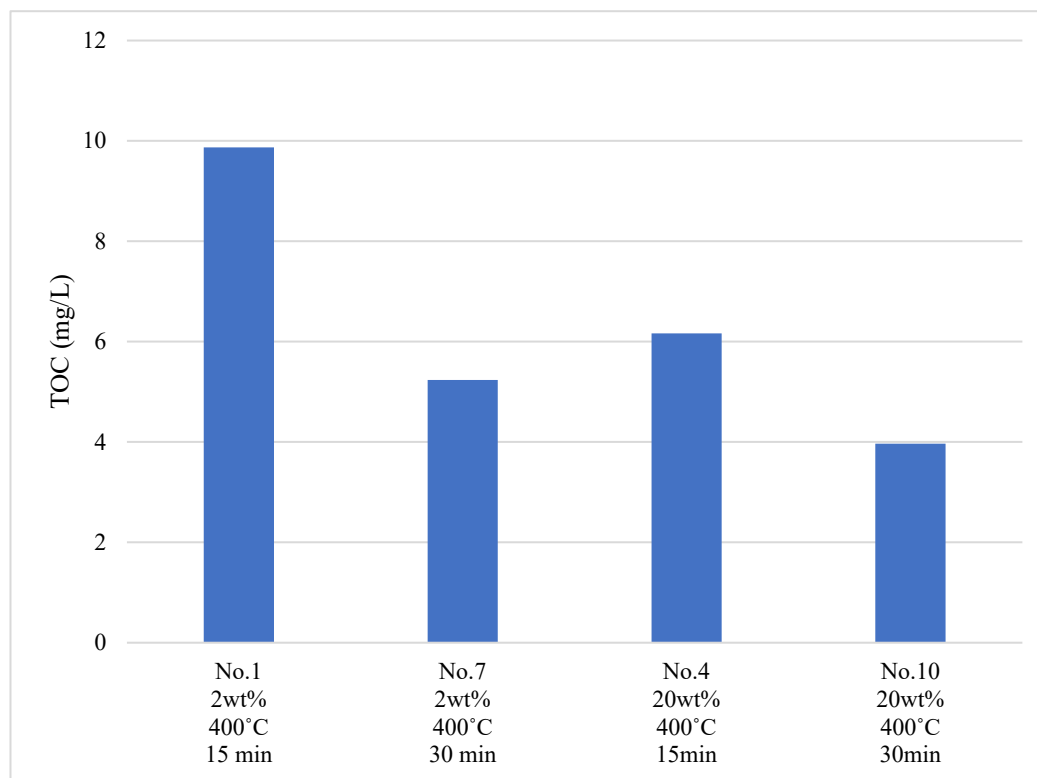


Figure 3-30 TOC analysis result of liquid phase of SCWG at 400°C.

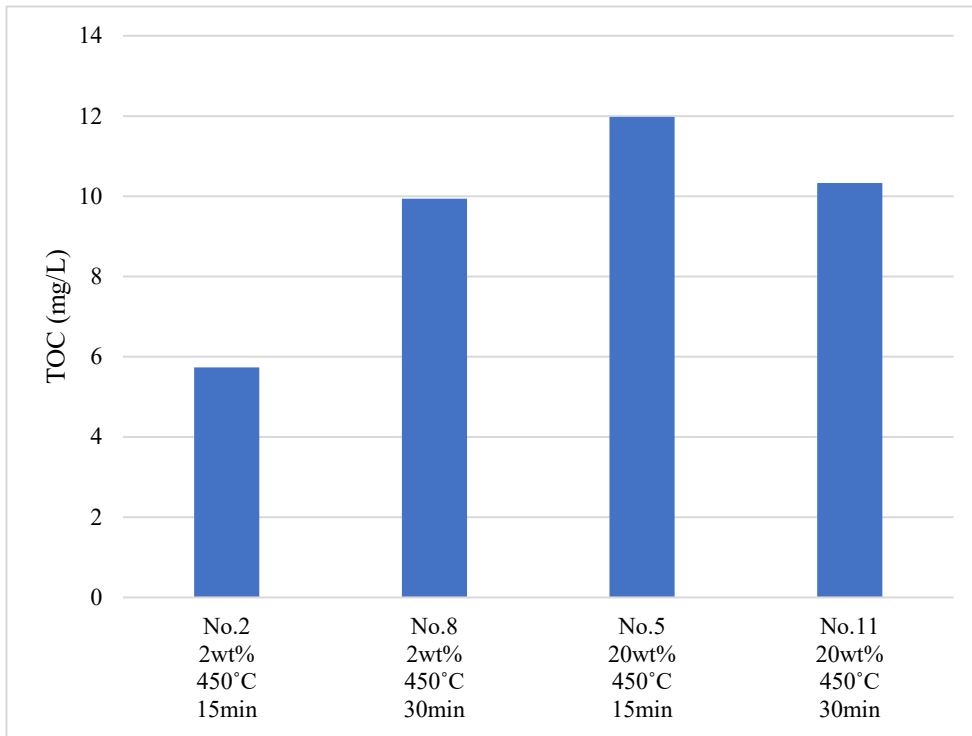


Figure 3-31 TOC analysis result of liquid phase of SCWG at 450°C.

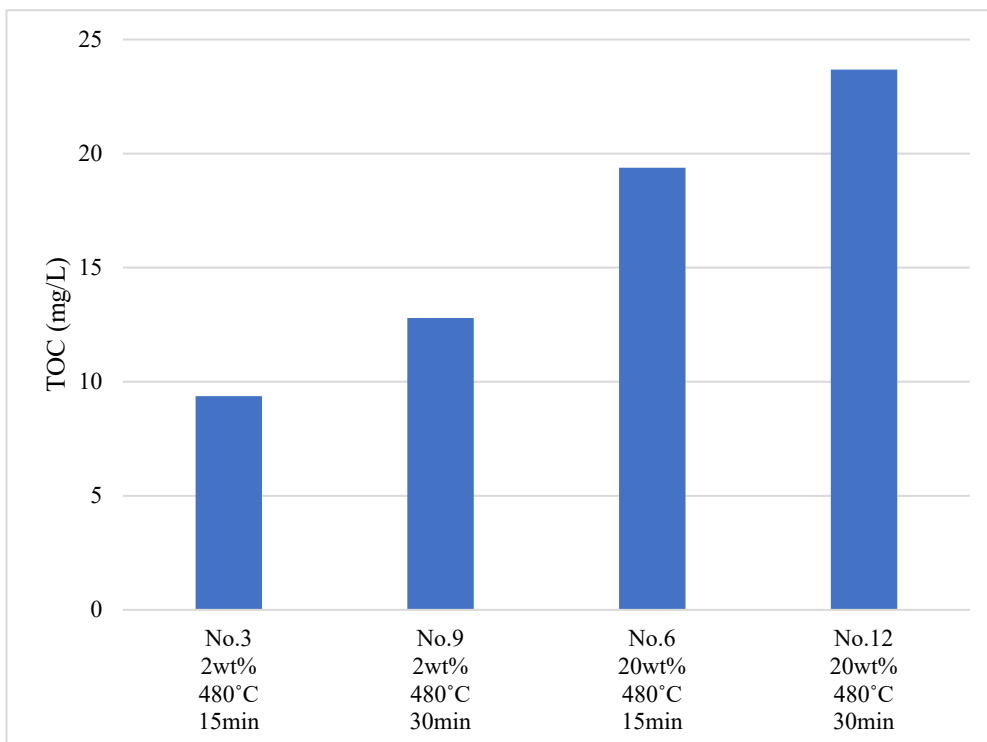


Figure 3-32 TOC analysis result of liquid phase of SCWG at 480°C.

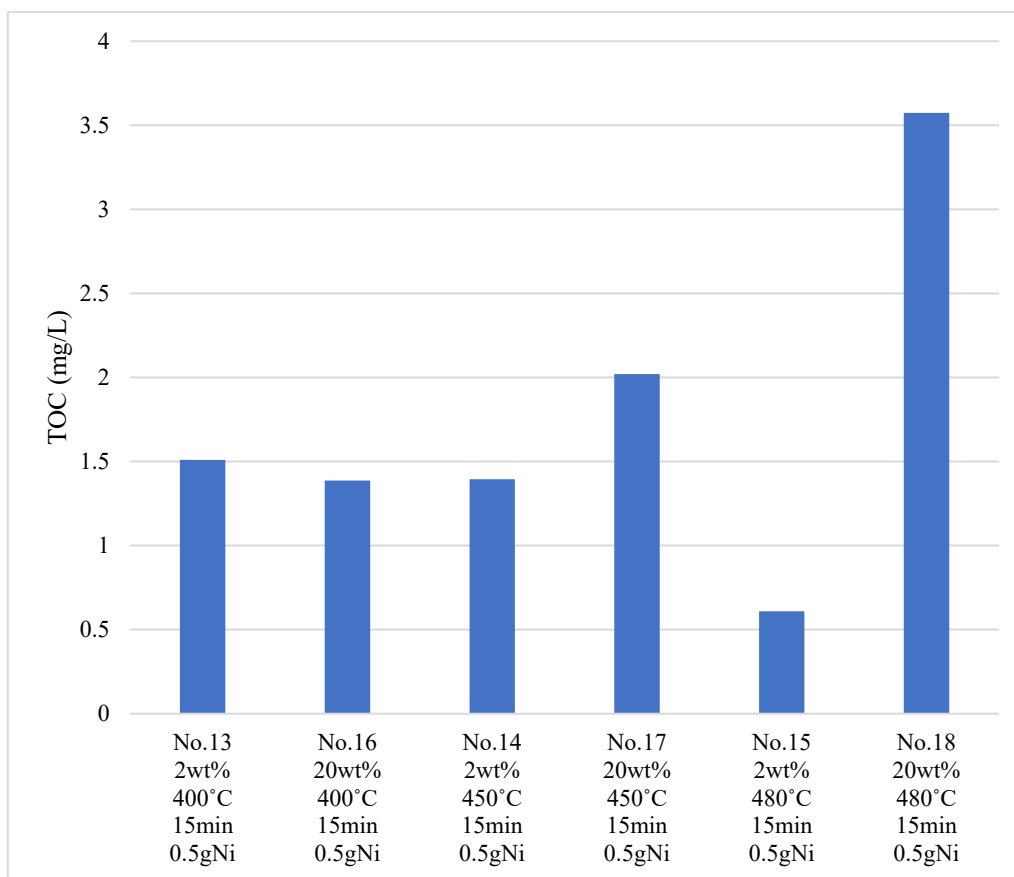


Figure 3-33 TOC analysis result of liquid phase of SCWG with 0.5g catalysts.

### 3.3.2. GC-MS Analysis

Liquid samples were dissolved in hexane or acetonitrile. In this GC-MS analysis experiment, 20 oil wt% samples were used to study at the high biomass concentration for the differences in the composition of the liquid products under different reaction conditions. The liquid product samples No.5, No.6, No.10, No.11, No.12 and No.16 were analyzed.

Figure 3-34 shows the GC/MS chromatogram of pure SGO. Table 3-9 tabulates the detected peaks. In addition to the fatty acids commonly found in cooking oil substances, simulated SGO also contains some chemical components with a benzene ring structure that can cause harm to humans when consumed.

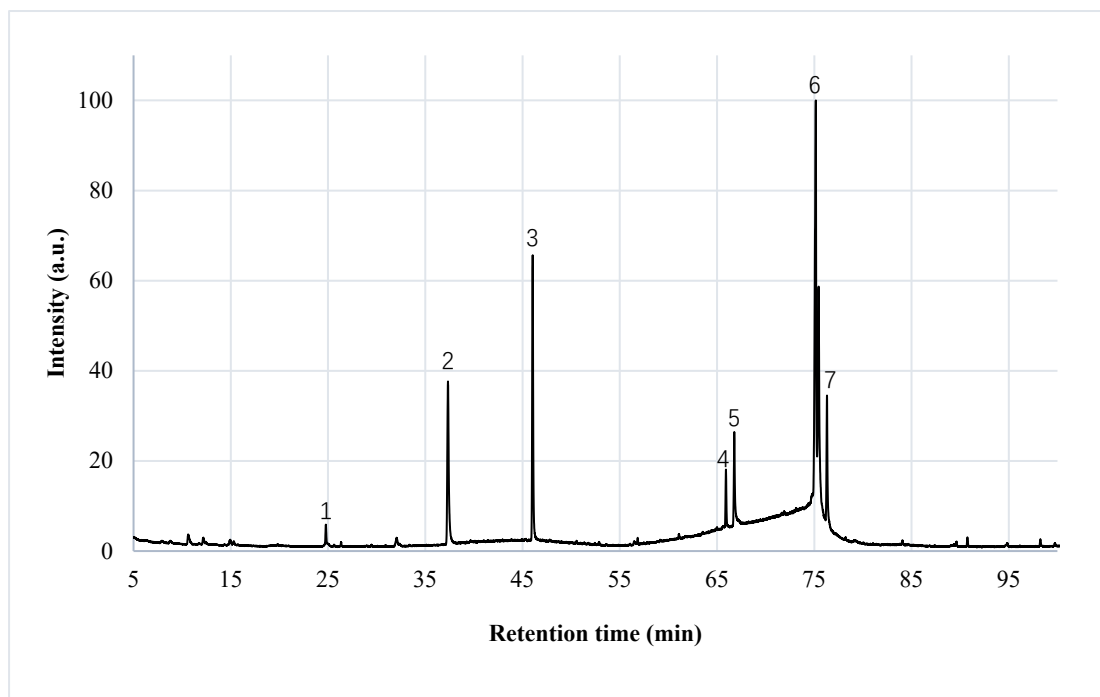


Figure 3-34 Pure SGO dissolved in hexane.

Table 3-9 The compounds present in SGO.

Peak	Compound	Common names	Formula
1	Linalyl anthranilate	Anthranilic acid	C <sub>17</sub> H <sub>23</sub> NO <sub>2</sub>
2	Dimethyl phthalate	-	C <sub>10</sub> H <sub>10</sub> O <sub>4</sub>
3	Diethyl Phthalate	-	C <sub>12</sub> H <sub>14</sub> O <sub>4</sub>
4	1,2-Benzenedicarboxylic acid	Phthalic acid	C <sub>22</sub> H <sub>34</sub> O <sub>4</sub>
5	n-Hexadecanoic Acid	Palmitic acid	C <sub>16</sub> H <sub>32</sub> O <sub>2</sub>
6	Oleic acid	Oleic acid	C <sub>18</sub> H <sub>34</sub> O <sub>2</sub>
7	Octadecanoic acid	Stearic acid	C <sub>18</sub> H <sub>36</sub> O <sub>2</sub>

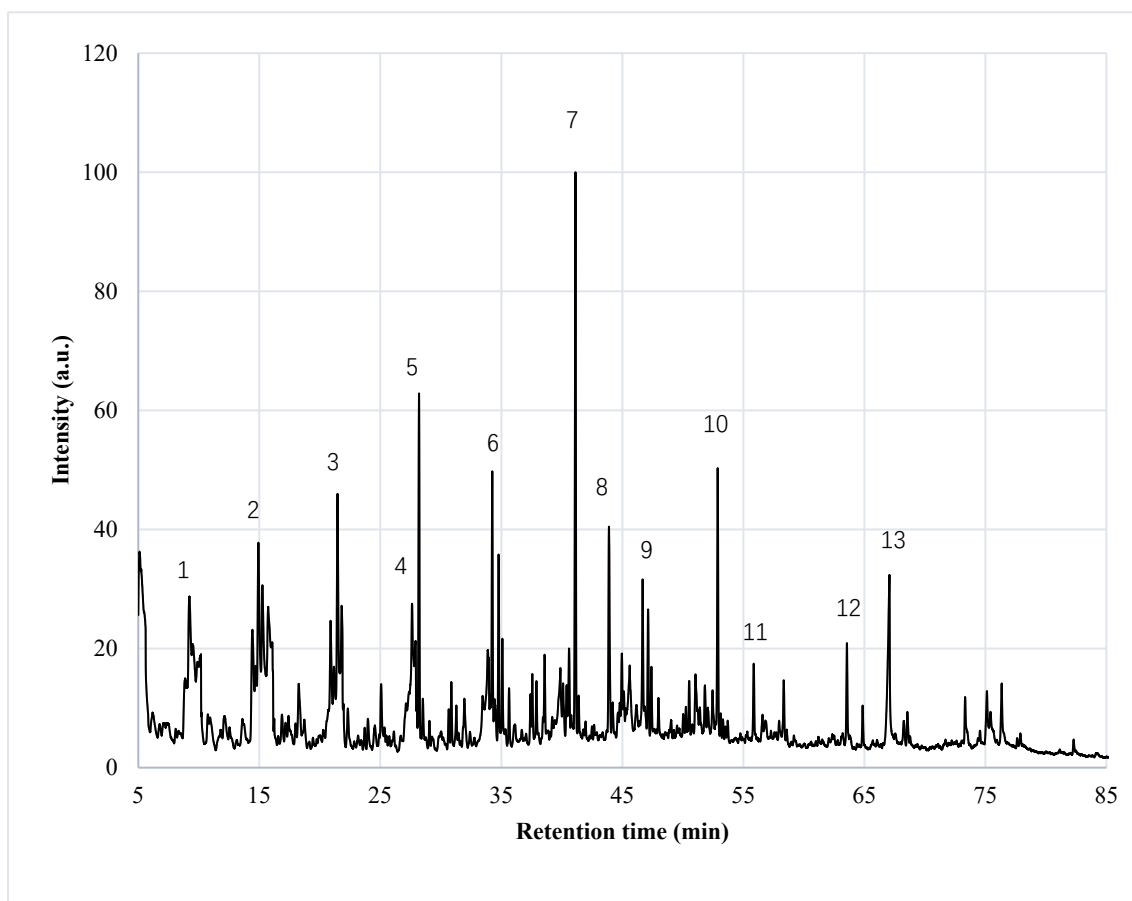


Figure 3-35 GC-MS for No.5(450°C, 20wt%, 15min) liquid sample.

Table 3-10 The compounds present in No.5 liquid sample.

Peak	Compound	Common names	Formula
1	Decane	-	C10H22
2	Undecane	-	C11H24
3	Dodecane	-	C12H26
4	Nonanoic acid	Pelargonic Acid	C9H18O <sub>2</sub>
5	Tridecane	-	C13H28
6	Octadecene	-	C18H26
7	Pentadecane	-	C15H32
8	n-Nonylcyclohexane	-	C15H30
9	9-Nonadecene	-	C19H38
10	Heptadecane	-	C17H36
11	Cyclohexane, undecyl-	-	C17H34
12	Tetratriacontane	-	C34H70
13	n-Hexadecanoic acid	Palmitic acid	C16H32O <sub>2</sub>

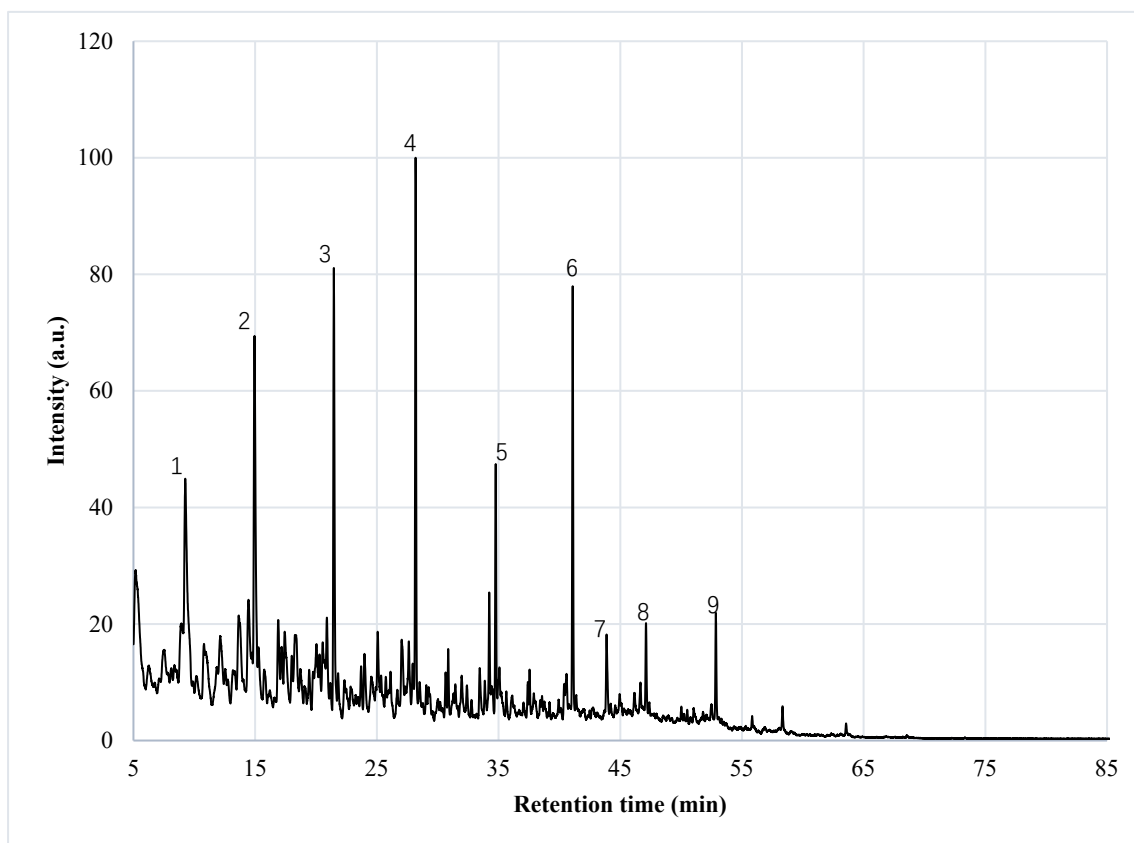


Figure 3-36 GC-MS for No.6(480°C, 20wt%, 15min) liquid sample.

Table 3-11 The compounds present in No.6 liquid sample.

Peak	Compound	Common names	Formula
1	Decane	-	C10H22
2	Undecane	-	C11H24
3	Dodecane	-	C12H26
4	Tridecane	-	C13H28
5	Octadecene	-	C18H26
6	Pentadecane	-	C15H32
7	n-Nonylcyclohexane	-	C15H30
8	9-Nonadecene	-	C19H38
9	Heptadecane	-	C17H36

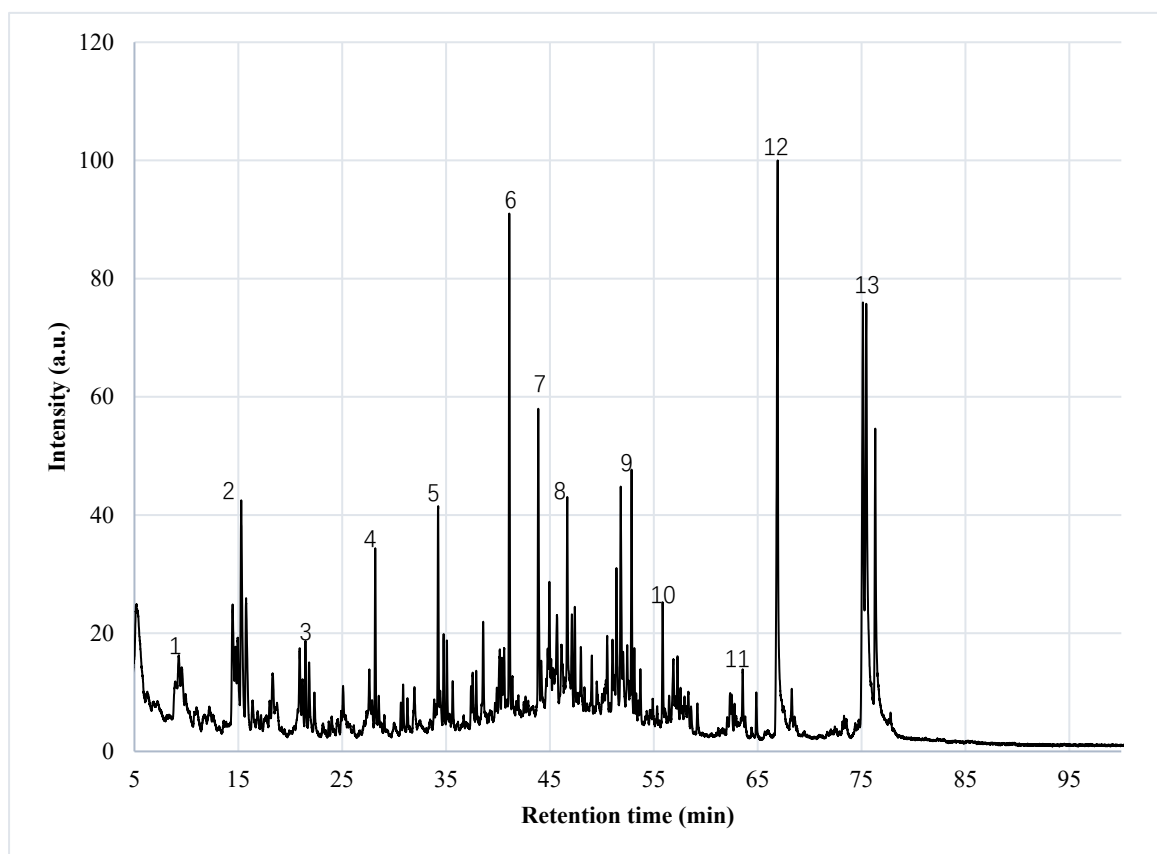


Figure 3-37 GC-MS for No.10(400°C, 20wt%, 30min) liquid sample.

Table 3-12 The compounds present in No.10 liquid sample.

Peak	Compound	Common names	Formula
1	Decane	-	C <sub>10</sub> H <sub>22</sub>
2	Undecane	-	C <sub>11</sub> H <sub>24</sub>
3	Dodecane	-	C <sub>12</sub> H <sub>26</sub>
4	Tridecane	-	C <sub>13</sub> H <sub>28</sub>
5	Octadecene	-	C <sub>18</sub> H <sub>26</sub>
6	Pentadecane	-	C <sub>15</sub> H <sub>32</sub>
7	n-Nonylcyclohexane	-	C <sub>15</sub> H <sub>30</sub>
8	9-Nonadecene	-	C <sub>19</sub> H <sub>38</sub>
9	Heptadecane	-	C <sub>17</sub> H <sub>36</sub>
10	Cyclohexane,undecyl-	-	C <sub>17</sub> H <sub>34</sub>
11	Tetratriacontane	-	C <sub>34</sub> H <sub>70</sub>
12	n-Hexadecanoic acid	Palmitic acid	C <sub>16</sub> H <sub>32</sub> O <sub>2</sub>
13	Octadecanoic acid	Stearic acid	C <sub>18</sub> H <sub>36</sub> O <sub>2</sub>

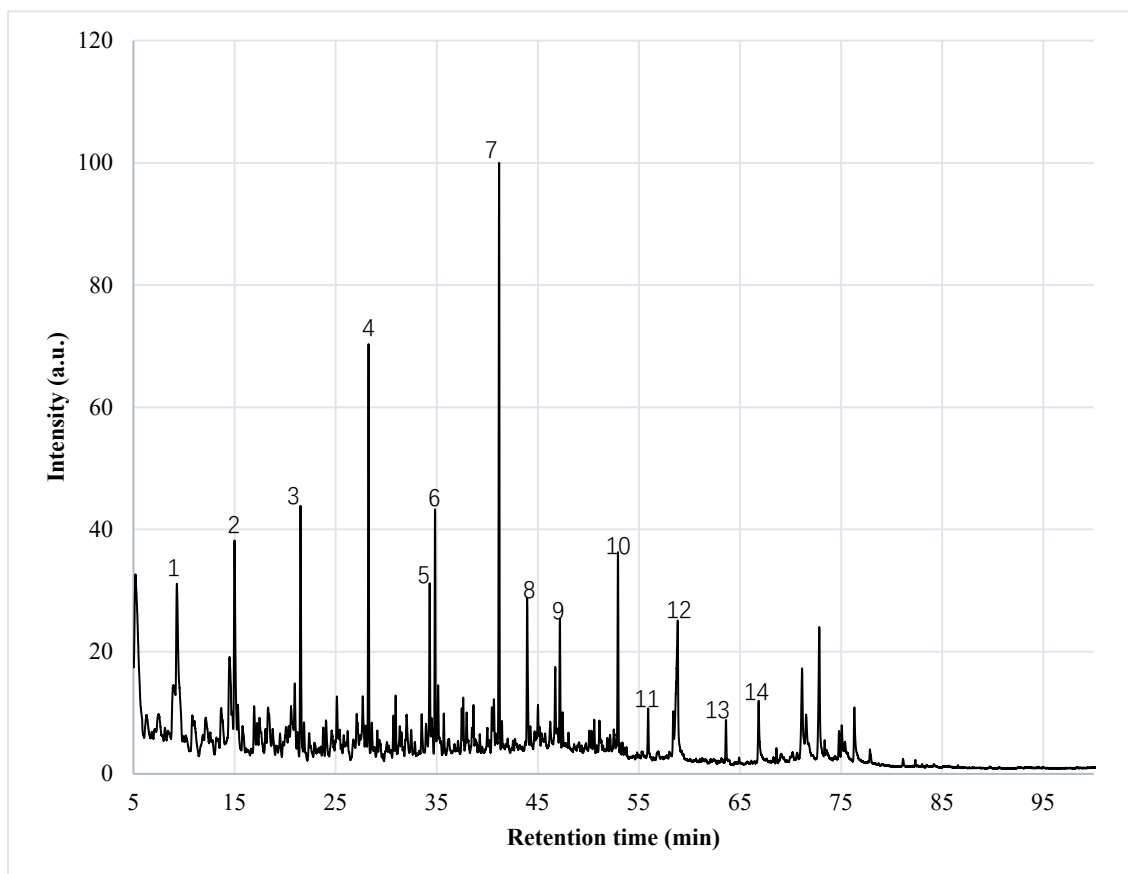


Figure 3-38 GC-MS for No.11(450°C, 20wt%, 30min) liquid sample.

Table 3-13 The compounds present in No.11 liquid sample.

Peak	Compound	Common names	Formula
1	Decane	-	C10H22
2	Undecane	-	C11H24
3	Dodecane	-	C12H26
4	Tridecane	-	C13H28
5	Octadecene	-	C18H26
6	Nonadecane	-	C19H40
7	Pentadecane	-	C15H32
8	n-Nonylcyclohexane	-	C15H30
9	9-Nonadecene	-	C19H38
10	Heptadecane	-	C17H36
11	Cyclohexane, undecyl-	-	C17H34
12	n-Pentadecylcyclohexane		C21H42
13	Tetratriacontane	-	C34H70
14	n-Hexadecanoic acid	Palmitic acid	C16H32O2

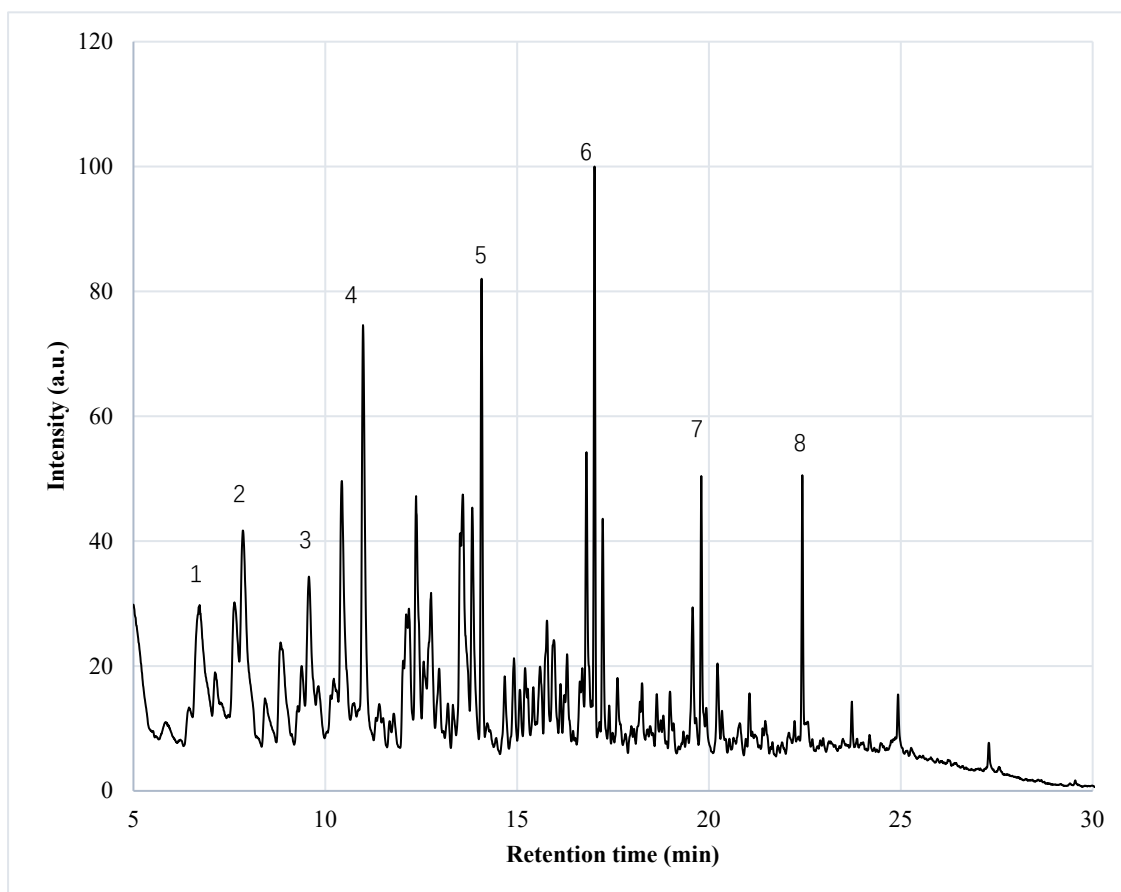


Figure 3-39 GC-MS for No.12(480°C, 20wt%, 30min) liquid sample.

Table 3-14 The compounds present in No.5 liquid sample.

Peak	Compound	Common names	Formula
1	Benzene, 1-ethyl-3-methyl-	3-Ethyltoluene	C <sub>9</sub> H <sub>12</sub>
2	Decane	-	C <sub>10</sub> H <sub>22</sub>
3	1-Phenyl-1-butene	-	C <sub>10</sub> H <sub>12</sub>
4	Undecane	-	C <sub>11</sub> H <sub>24</sub>
5	Dodecane	-	C <sub>12</sub> H <sub>26</sub>
6	Tridecane	-	C <sub>13</sub> H <sub>28</sub>
7	Tetradecane	-	C <sub>14</sub> H <sub>30</sub>
8	Pentadecane	-	C <sub>15</sub> H <sub>32</sub>

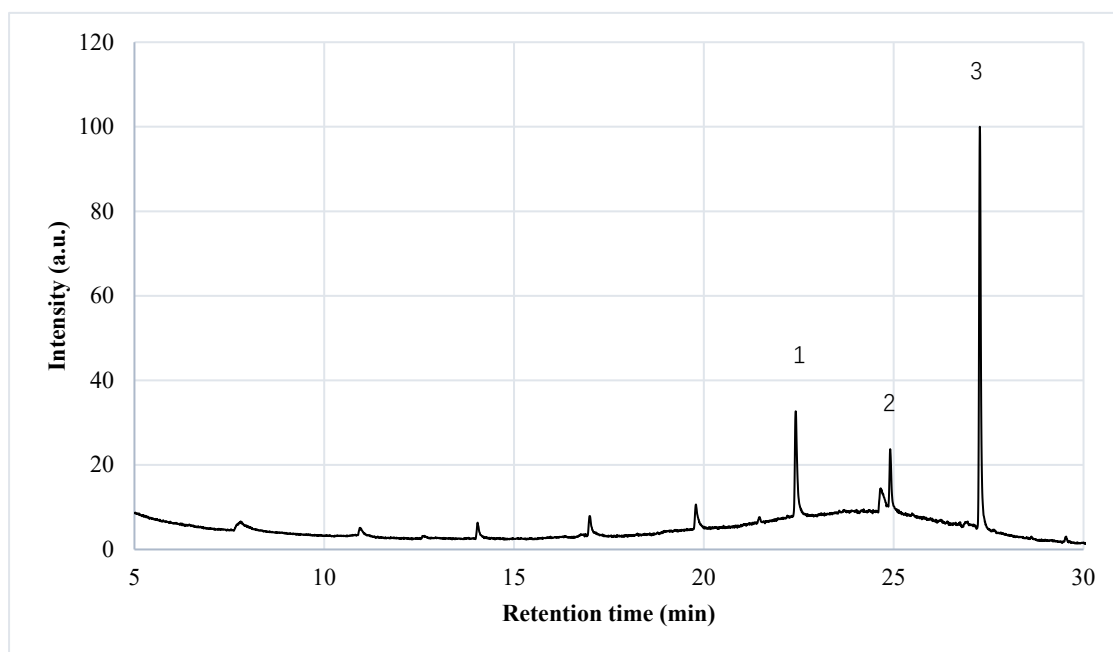


Figure 3-40 GC-MS for No.16(400°C, 20wt%, 15min, 0.5g catalysts) liquid sample.

Table 3-15 The compounds present in No.16 liquid sample.

Peak	Compound	Common names	Formula
1	Pentadecane	-	C15H32
2	10-Methylnonadecane	-	C20H42
3	Heptadecane	-	C17H36

### 3.3.3. Summary and Discussion

Comparing Figure 3-35(No.5) and Figure 3-36 (No.6), it can be found that at 20wt% oil concentration, medium-chain fatty acids (C: 6-12) and long-chain fatty acids (C >12) were still detected at 450°C, but as the temperature increased, the fatty acids decomposed at 480°C and the presence of alkanes and alcohols were detected. This suggests that the fatty acid may have undergone a decarbonization process and turned into aliphatic compounds. Since most aliphatic compounds are flammable, these hydrocarbons can also be used as fuels.

About Figure 3-37 (No.10) and Figure 3-38 (No.11), Tables 3-12 and 3-13 show that at the reaction temperature of 400°C, fatty acids were still detected in the liquid product, in addition to alkanes and cycloalcohols, presumably due to the substitution of hydrogen atoms by hydroxyl groups in the alicyclic hydrocarbons.

Comparing Figure 3-36 (No.6) and Figure 3-38 (No.11), it can be seen that as the reaction time increased from 15 to 30 minutes, no fatty acids were present in the No.11 sample, but the same was observed for the formation of many cycloalkanes. Similarly, it can be seen that fatty acid decomposition at 480°C high temperature is accompanied by the appearance of a large number of alkanes, and aromatics.

As for Figure 3-40 (No.16), Table 3-15 shows that with the addition of catalyst, the oil component in the liquid product was decomposed, and although alkanes were also formed, the variety of products was drastically reduced, and it can be presumed that more carbon and hydrogen atoms were converted into the water- phase product.

GC-MS analysis of SGO confirms the presence of functional groups characteristic of hydrocarbons (alkenes, alkanes, ring-containing alkenes, and ring-containing alkanes, cycloalkenes, cycloalkanes, and aromatics). The hydrocarbons identified in SGO by GC-MS present carbon chain length ranging from C9 to C34, indicating the presence of heavy gasoline compounds (C5-C10), kerosene-like fraction (C11-C12), light diesel-like fraction (C13-C17), and heavy diesel-like fraction (C18-C25), as defined in the literature[41]. The appearance of these functional groups proves the presence of diesel-like hydrocarbon in the liquid products after SCWG, which is valuable for further research.

### 3.4. Effect of catalyst

To determine the effect of catalyst on the SCWG process, experimental groups No.13 to No.18 were added. Two different reaction times, and three different reaction temperature experiments were conducted with 0.5 g catalyst amount to investigate the difference in gas yield and efficiencies.

#### 3.4.1. Gas yield and efficiencies

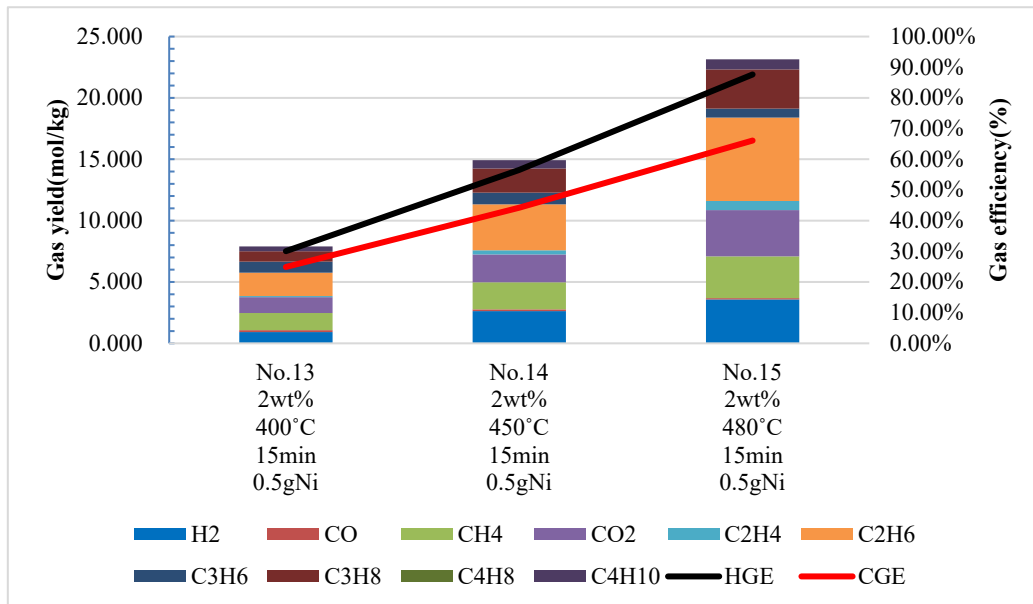


Figure 3-41 Gas yield and efficiency of SCWG at 2wt% gutter oil, 25 MPa and 15min residence time with 0.5g Ni catalysts.

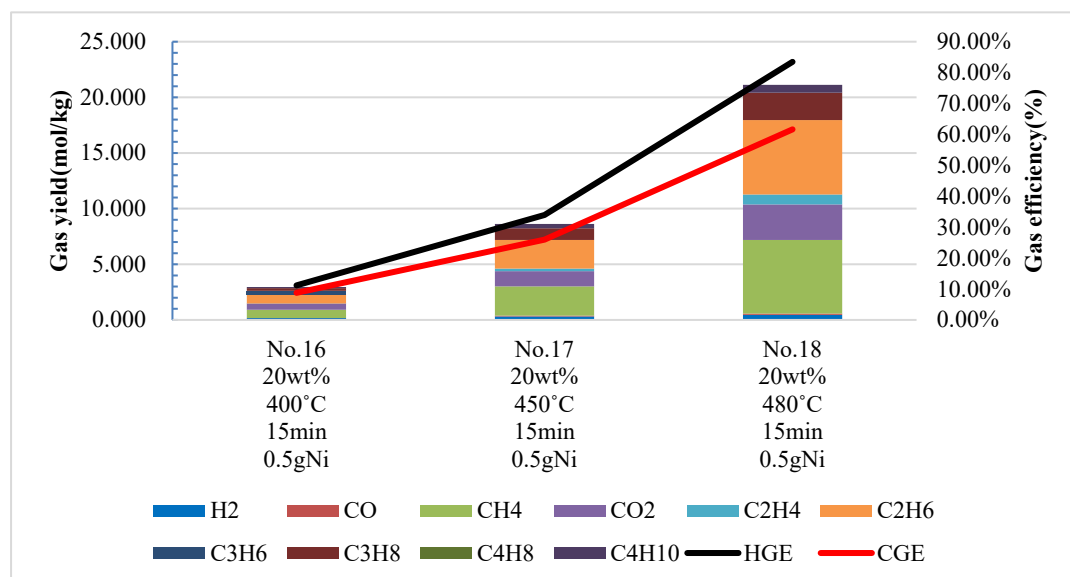


Figure 3-42 Gas yield and efficiency of SCWG at 20wt% gutter oil, 25 MPa and 15min residence time with 0.5g Ni catalysts.

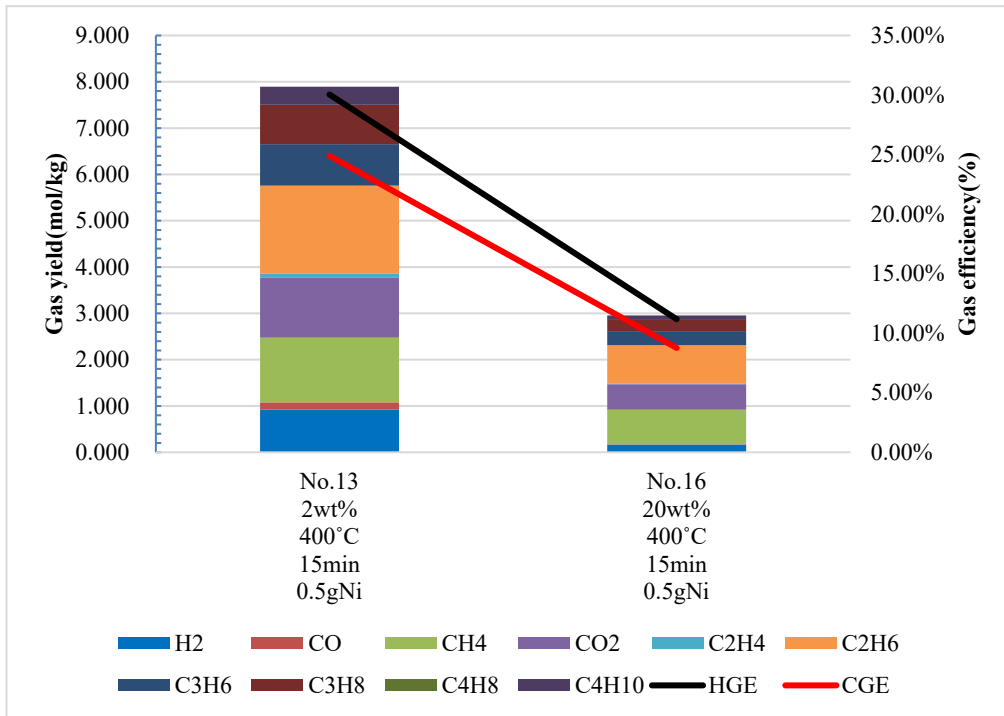


Figure 3-43 Gas yield and efficiency of SCWG at 400°C, 25 MPa and 15min residence time with 0.5g Ni catalysts.

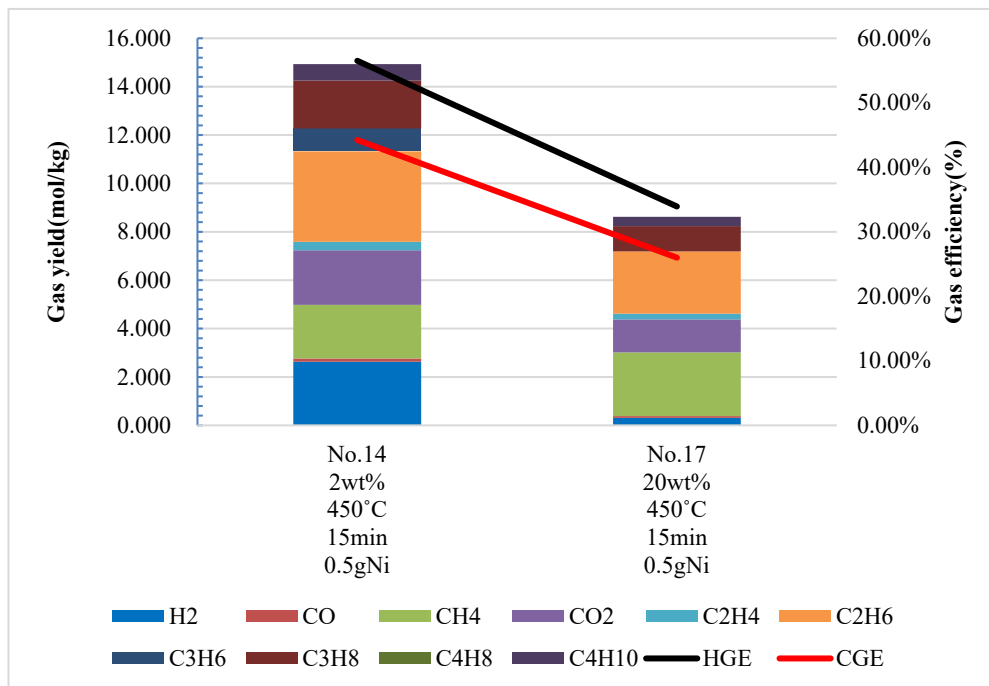


Figure 3-44 Gas yield and efficiency of SCWG at 450°C, 25 MPa and 15min residence time with 0.5g Ni catalysts.

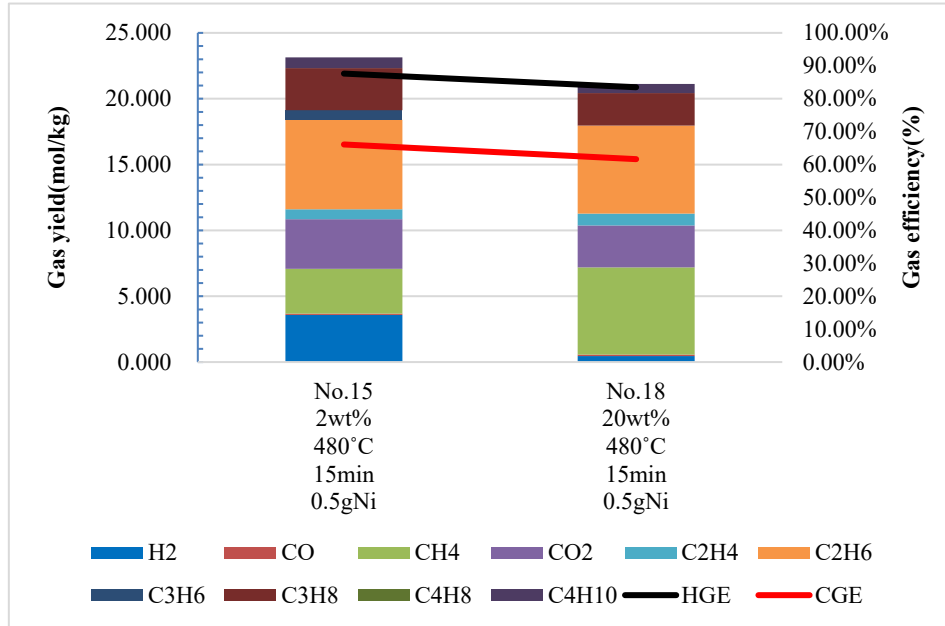


Figure 3-45 Gas yield and efficiency of SCWG at 480°C, 25 MPa and 15min residence time with 0.5g Ni catalysts.

### 3.4.2. Overall carbon balance

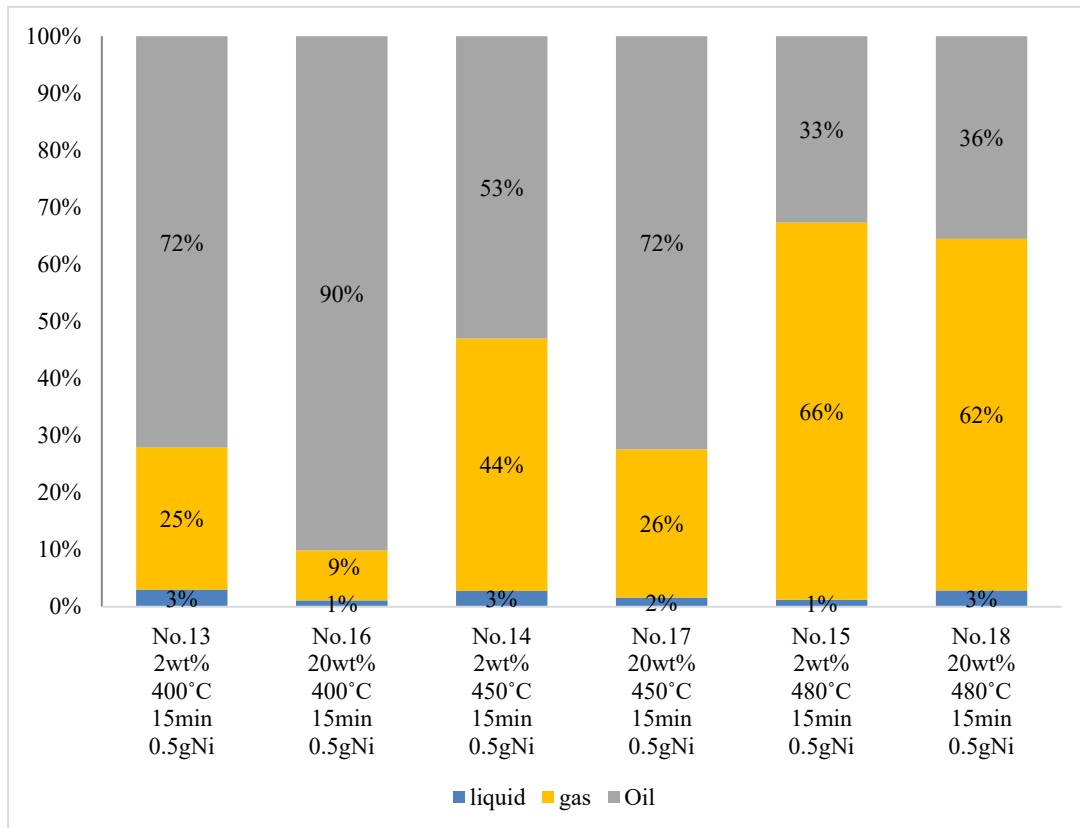


Figure 3-46 Carbon balance of SCWG with 0.5g catalysts.

### 3.4.3. Summary and discussion

The catalytic SCWG exhibited the same regular variation as the non-catalytic SCWG, where an increase in temperature and residence time resulted in an increase in gas product, but the opposite was true for an increase in SGO concentration.

Comparing the results of these experiments, it can be concluded that the use of catalysts in the SCWG process leads to an improvement in the performance parameters. From Figure 3-41 to Figure 3-42, it is indicated that the hydrogen production increased at 2wt% SGO by adding catalyst and did not get a significant enhancement at 20wt% SGO, but it can promote the carbon gasification efficiency. Therefore, high concentration of biomass feedstock was successfully gasified at high reaction temperature.

As can be seen from Figures 3-43 to 3-45, the performance is better at low concentrations relative to high concentrations of SCWG. Looking at No.16, No.17 and No.18, the C2-C4 gas products make up a large portion of the gas product distribution. This demonstrates the inability of the larger hydrocarbons to be converted into the desired product by the system, but the opposite effect is observed for the low concentration SCWG process, where C2-C4 hydrocarbons make up less than half of the overall product gas, as shown in No.13, No.14, and No.15.

In addition, the performance of the catalytic experiment is much better compared to the non-catalytic SCWG. First, the share of the C2-C4 gas product in the gas product distribution decreases with the addition of the catalyst. This indicates that the system converts larger alkanes into the desired product with the help of catalyst. Secondly, the increase in CH<sub>4</sub> gas content implies that the steam reforming reaction is fully executed. It can be concluded that the addition of catalyst at high temperatures resulted in a significant increase in the gasification yield of highly concentrated biomass. Three main reactions were identified in the SCWG process, which included steam reforming, water gas transfer, and CO and CO<sub>2</sub> methanation reactions. The larger yields of CH<sub>4</sub> and CO<sub>2</sub> and lower yields of CO with the help of catalysts indicate that the reactions are proceeding properly.

The product distribution of the catalytic SCWG is shown in Figure 3-46, with the best gas distribution reaching 66%, even at high concentration conditions, the better one is up to 62% of the gas distribution. In addition, the selectivity of the desired gas product is better in the catalytic process. In terms of economics, the incorporation of catalysts into the process leads to viable economic results, as the process is carried out in favor of the production of the desired gas product.

## Chapter 4. CHARACTERIZATION OF CATALYST

In Chapter 3, the effect of catalyst on the SCWG experiments can be clearly shown by the variation of biomass concentration. In these experiments, lower biomass concentrations performed better in terms of gas yield and efficiencies compared to experiments performed at higher biomass concentrations. Using these findings, the importance of the catalyst was determined, but catalyst deactivation has been something that occurs in hydrothermal gasification experiments, so additional experiments and analyses were added in the fourth section of the chapter to find out when catalysts lose their catalytic efficiency. The first part of this chapter presents the results of the characterization obtained for the non-volatilized catalyst. The second part presents the results of the catalyst characterization obtained after the SCWG experiments, including the analysis of the catalysts using XRD and SEM-EDX to determine the deactivation behavior of the catalysts.

### 4.1. Initial catalysts characterization

In this study, catalyst is an alloy of 67.2% Ni, 31.9% Al, and 0.9% Mo, based on manufacturer's data. SEM images were obtained to probe the catalyst's surface, and a corresponding EDX analyzed to quantify the components attached to the surface. Figure 4-1 shows the image of the fresh catalyst used before the reaction.

The SEM images of the fresh catalyst is shown in Figure 4-2. The surface of the catalyst appears to be smooth, with apparent cracks nicks in this image. The findings of the EDX study are presented in Table 4-1. It is concluded that the catalyst particles are indeed composed mainly of Ni. Meanwhile, the presence of C and O on the catalytic surface may be the result of impurities that were exposed during the analysis.



Figure 4-1 The fresh catalyst

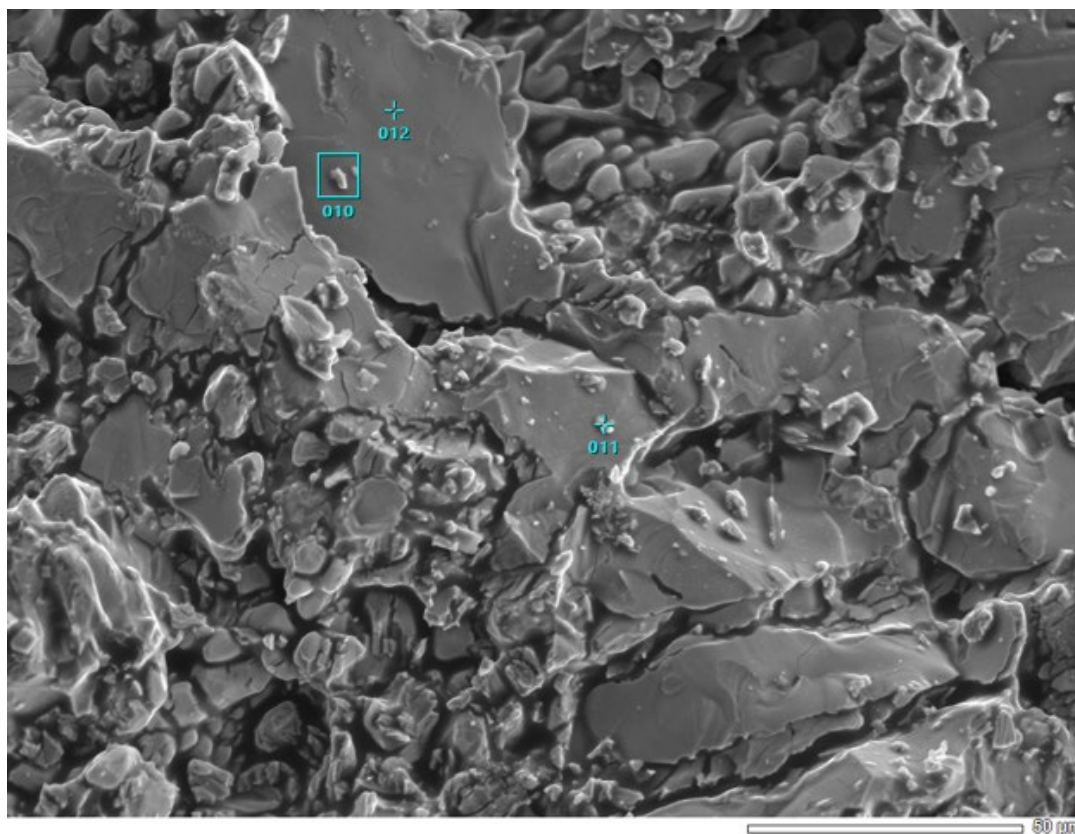


Figure 4-2 SEM image of the fresh catalyst.

Table 4-1 EDX analysis of the fresh catalyst.

Point of analysis	Weight percentage (%)					
	C	O	Al	Ca	Ni	Mo
10	27.99	19.26	5.84	0.45	42.94	3.52
11	0	0	6.87	0.42	87.08	5.63
12	22.94	19.57	6.53	0.35	47.6	3

#### 4.2. Catalyst characterization after SCWG

To probe the surface of the catalyst after hydrothermal experiments, multiple SEM images were taken and corresponding EDX analysis was also performed to quantify the compounds attached to the surface. Meanwhile, the XRD analysis also was performed in order to investigate the deactivation reason of catalysts.

#### 4.2.1. SEM-EDX Analysis

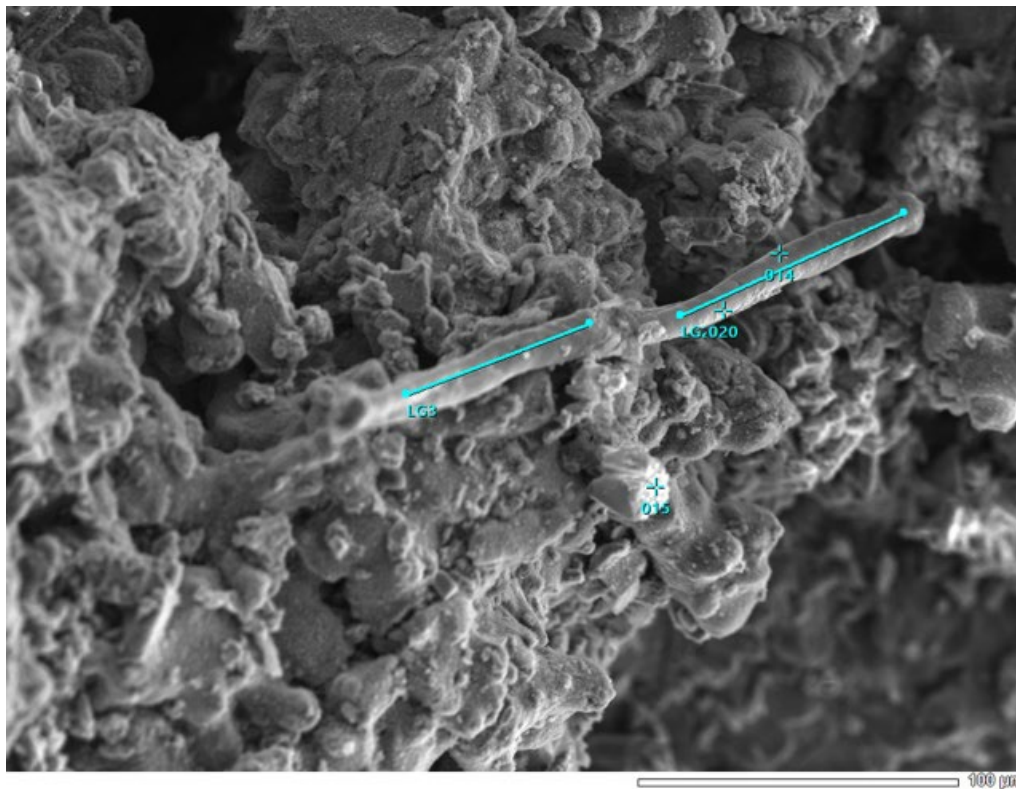


Figure 4-3 SEM image of the catalyst after SCWG (2wt%, 400°C, 15min)

Table 4-2 EDX analysis of the catalyst after SCWG

Point of analysis	Weight percentage (%)					
	C	O	Al	Ca	Ni	Cu
20	64.86	31.72	0	0	2.98	0.45

Looking at Figure 4-3, after the reaction, the surface of the catalyst lost its original flatness and smoothness, as well as the whisker carbon has appeared which is the most typical carbon deposition and occurs on the surface of the Ni catalyst.

Comparing Table 4-2 it can be seen that the content of C increased after SCWG and the content of the main components of the catalyst decreased, it can be presumed to deactivate the catalyst. The presence of Cu on the catalytic surface may be the result of impurities.

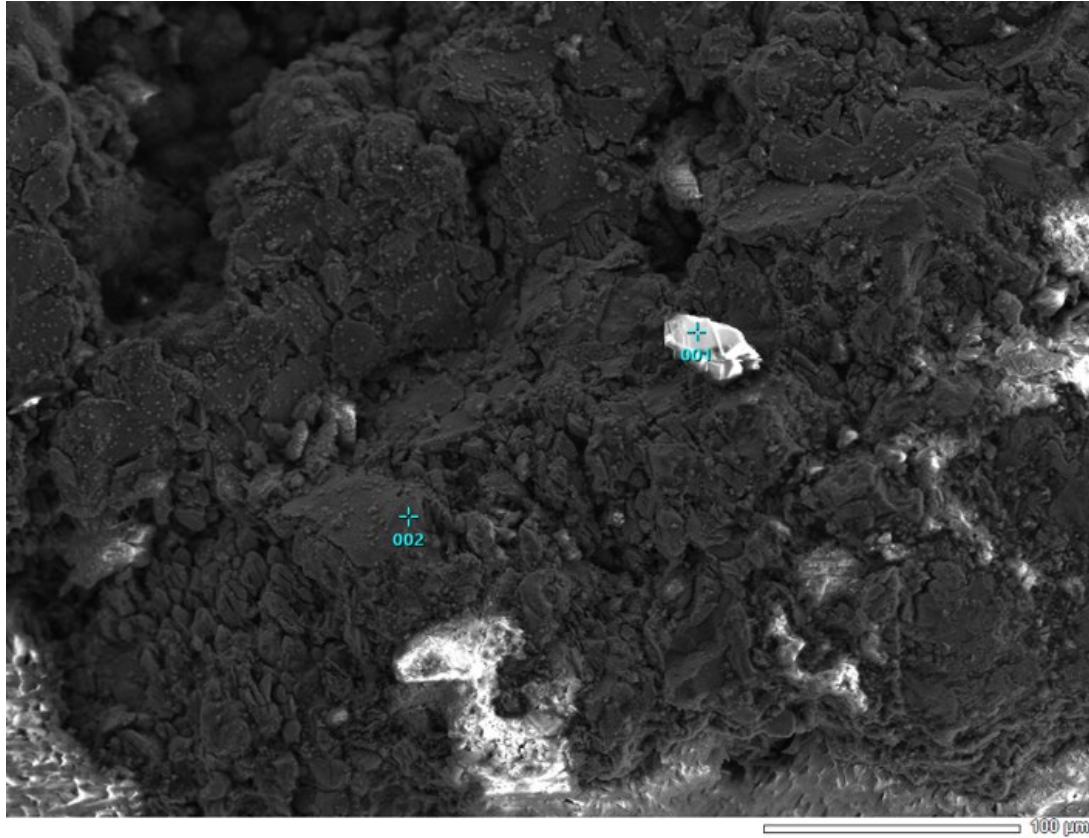


Figure 4-4 SEM image of the catalyst of No.13 (2wt%, 400°C, 15min) experiment

Table 4-3 EDX analysis of the catalyst of No.13 experiment

Point of analysis	Weight percentage (%)						
	O	Al	Si	S	K	Ca	Ni
1	45.1	10.4	28.27	0	11.43	0	4.81
2	29.91	16.64	0	0.4	0	0.4	52.65

Observing Table 4-3, it can be speculated by EDX analysis that the white part at point 1 is a staining impurity, and at point 2, the content of O increases, presumably due to the oxidation of that part of the metal element, which may produce oxidation products. Combined with the Figure 4-4, the fragmentation is severe, and the original base result is destroyed, and a large crushing appears. This implies a possible deactivation of the catalyst after its involvement in the SCWG experiments.

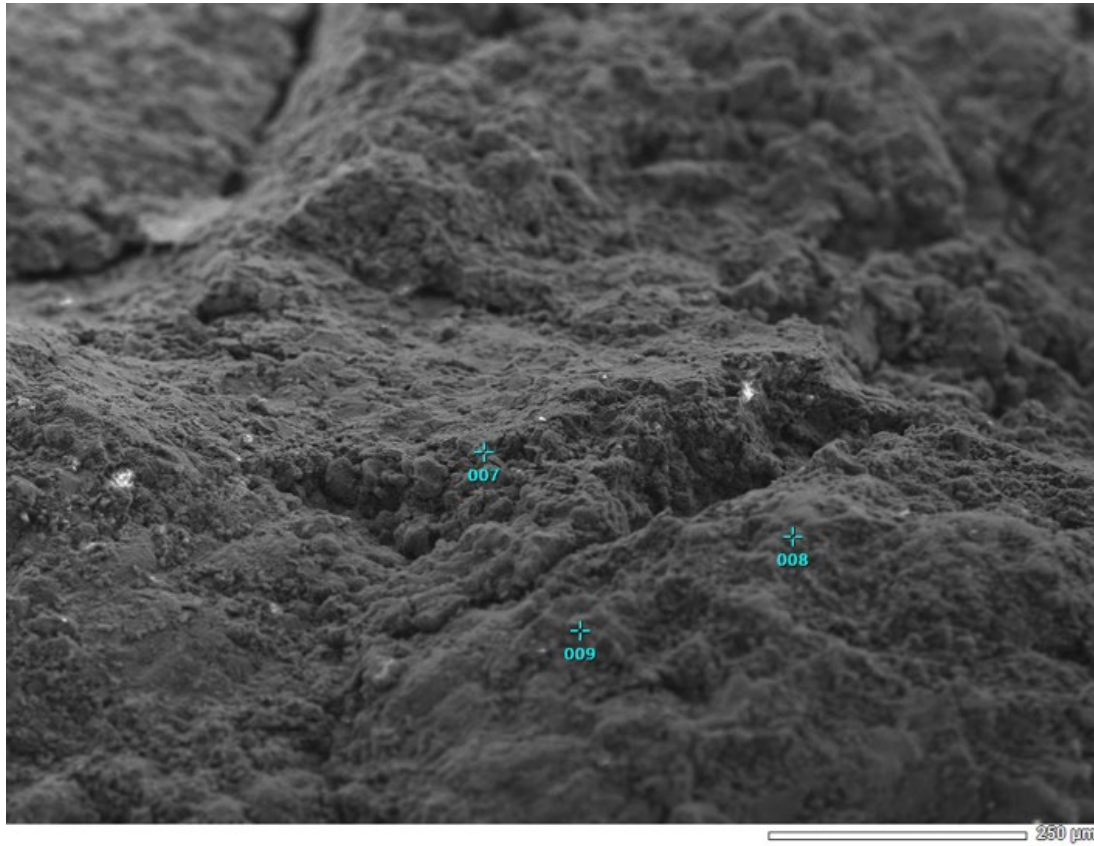


Figure 4-5 SEM image of the catalyst of No.14 (2wt%, 450°C, 15min) experiment

Table 4-4 EDX analysis of the catalyst of No.14 experiment

Point of analysis	Weight percentage (%)				
	O	Al	Ca	Ni	Mo
8	36.96	31.1	2.16	24.47	5.31
9	31.16	18.63	0.35	3.28	45.54

Figure 4-5 shown that severe breakage of the catalyst surface as the temperature rises. Table 4-4 indicates that the oxygen content increases, the nickel content decreases, which could be the occurrence of oxidation. As EDX analysis calculates the elemental composition based on the weight fraction of the detected elements, the increase in the Al and Mo quantity ratio may be due to a decrease in the Ni quantity.

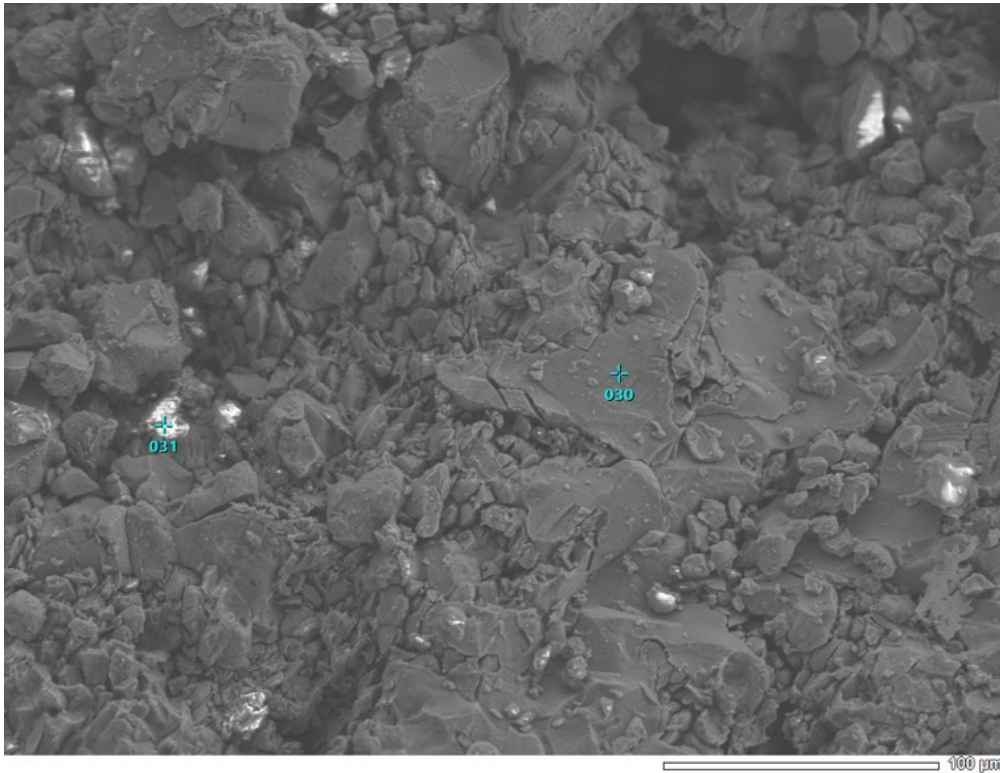


Figure 4-6 SEM image of the catalyst of No.16 (20wt%, 400°C, 15min) experiment.

Table 4-5 EDX analysis of the catalyst of No.16 experiment.

Point of analysis	Weight percentage (%)					
	O	Al	S	Ca	Ni	Mo
<b>30</b>	26.73	9.97	0.49	0	62.81	0
<b>31</b>	45.39	48.37	0.52	0.27	5.44	0

Figure 4-5 shows that the catalyst surface breaks down less severely around point of analysis 30 as the concentration increases, and the Ni content remains high on the smoother catalyst surface. As for point 31, which shows a very low nickel content and a high oxygen content, is presumed to have an increase of oxides.

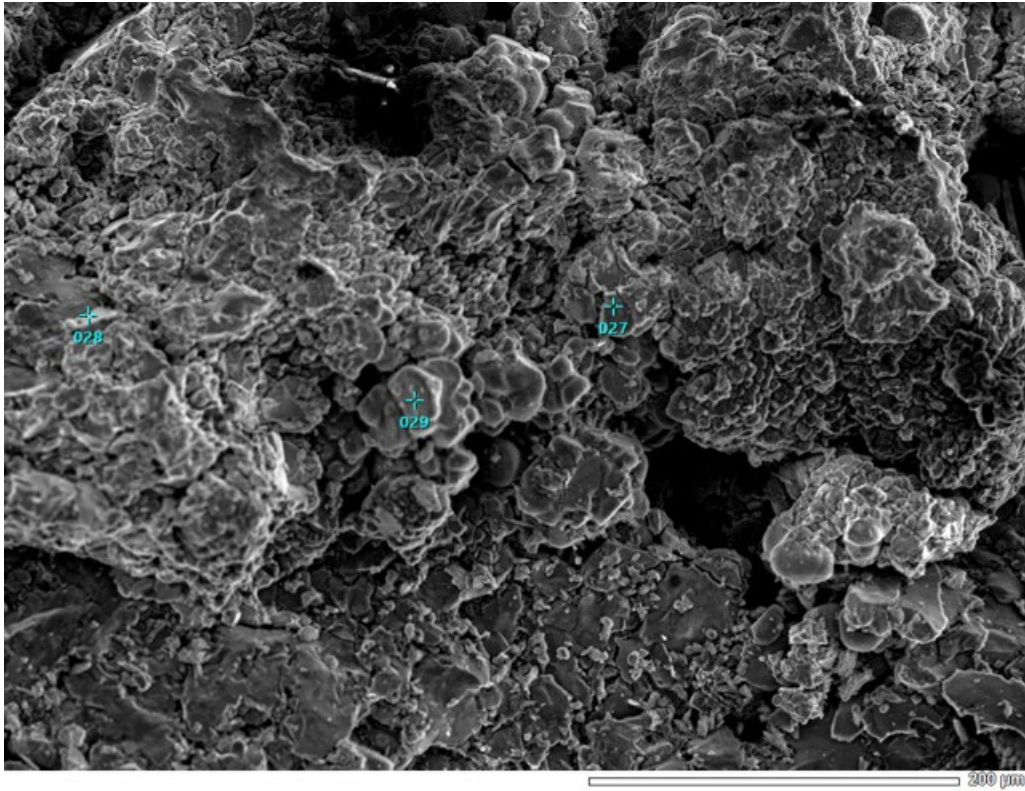


Figure 4-7 SEM image of the catalyst of No.17 (20wt%, 450°C, 15min) experiment.

Table 4-6 EDX analysis of the catalyst of No.17 experiment.

Point of analysis	Weight percentage (%)				
	O	Al	S	Ni	Mo
27	24.26	5.74	68.91	1.09	24.26
28	34.48	25.92	0.52	39.08	0
29	23.3	3.87	0	72.83	0

By observing the Figure 4-7, it is seen to indicate that the tectonic damage is not severe, and the content of nickel is higher than that of the catalyst at low concentrations. Based on this comparison, it can be assumed that the high temperature and low concentration reaction conditions are more likely to damage the catalyst surface and produce more oxides. This also means that it is easier to deactivate the catalyst at low concentration and high temperature.

#### 4.2.2. XRD Analysis

The catalyst surface was characterized by XRD analysis. The XRD analysis was selected to compare a catalyst that did not participate in the reaction with four groups of catalysts after the reaction at different concentrations and temperatures.

The appearance of oxidation peaks was observed, so it can be assumed that the oxidation of the catalyst surface led to the deactivation of the catalyst. In addition, it is evident from the results that the metal peaks were not emphasized in the unused catalyst. On the contrary, the increase of the metal peaks in the other samples indicates that the immersion of the catalyst in SCW induces the growth of nickel and aluminum.

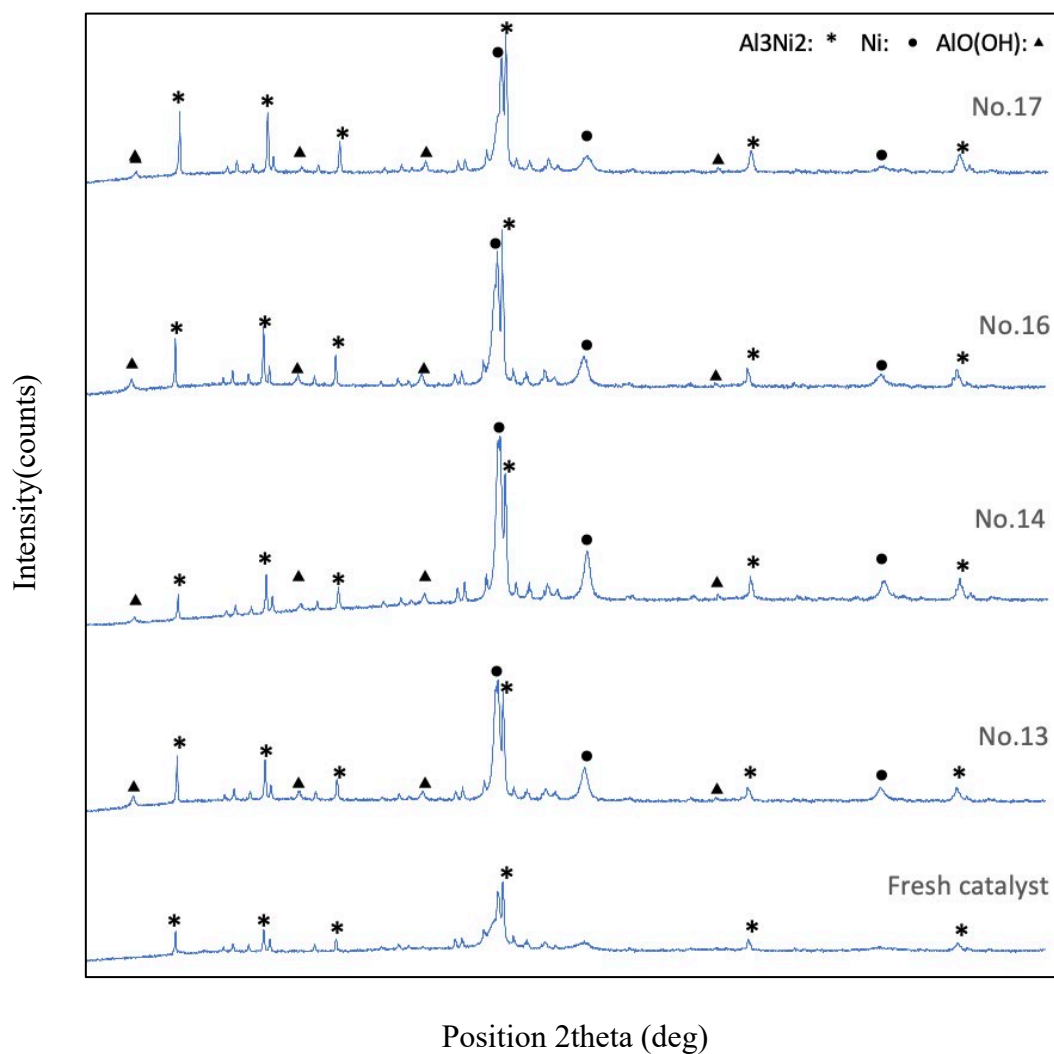


Figure 4-8 The XRD results obtained for catalytic SCWG experiments

## Chapter 5. CONCLUSIONS AND RECOMMENDATIONS

This chapter presents the main results of a supercritical water gasification study on SGO. Conclusions are drawn from these results and recommendations are made for future efforts. In the first section, the conclusions of each experimental section are discussed and answers to the research questions are given. Future recommendations on how to improve the research are given in the next section.

### 5.1. Conclusions

In this study, the decomposition of SGO in SCWG was investigated. The aim of the experiment was to investigate the results of SGO gasification in supercritical water, and the experiment also evaluated the effect of biomass concentration, using two different oil concentrations, 2wt% and 20wt%, respectively. In addition, catalytic type experiments were inferred to catalyst characterization. Also, the performance of each operating condition was evaluated in terms of gas yield and efficiency. The decomposition products determined from gas-phase and liquid-phase analyses are also presented. The results showed that the gas yield and efficiency decreased with increasing biomass concentration. This similar trend was found in other studies[42]. As the concentration of the additive increased, the yield of hydrogen decreased, while the yield of methane increased. In the present study, the yield of both hydrogen and methane decreased with increasing grease concentration, and such phenomenon was also observed in similar grease studies[43]. It can also be concluded that the system performs better at lower biomass concentrations than at higher biomass concentrations.

For the catalytic SCWG experiments, the catalyst surface was probed and analyzed using SEM, and the species attached to the surface were quantified using EDX. From the SEM images, it was found that the unused catalyst had a smooth surface with obvious cracks and fissures, and the surface of the catalyst became broken after the reaction, in addition to some impurities and oxides appeared on the catalyst surface. The results of the qualitative analysis using XRD showed oxidation peaks, confirming the speculation that the catalyst deactivation was caused by oxidation. The EDX results showed the presence of more nickel at the beginning of the reaction and its gradual loss after exposure to SCWG in oil, which indicates the loss of the active catalytic site. During the examination of the liquid products, the formation of diesel-like hydrocarbon was found. In this study, the applicability of supercritical water gasification in oil treatment was investigated. It was found that supercritical water gasification is a viable process for converting oil to desired gaseous products ( $H_2$ ) under optimal conditions in laboratory-scale catalytic experiments.

Moreover, the desired hydrocarbons can be obtained from the liquid products, and the presence of aliphatic groups (alkenes, alkanes, etc.) as the main chemical compounds and oxygenated compounds (carboxylic acids, ketones, etc.) was partially determined for diesel-like hydrocarbons. Finally, experiments with catalyst participation and possible causes of catalyst deactivation were identified, and it was concluded that

oxidation could be the cause of catalyst deactivation. The results show that the conversion of SGO to hydrogen and diesel-like hydrocarbons under supercritical water conditions is technically feasible and that the optimal gasification conditions are 480°C, 25 MPa, 2 wt% concentration of SGO.

## 5.2. Recommendations

For the improvement of this research, the following recommendations are suggested:

1. For gutter oil hydrothermal experiments, the reaction temperature should be set at 480°C or above as much as possible, because the gasification reaction at a temperature lower than 480°C is not effective and the gas products obtained are not ideal; for low concentration biomass experiments, and it is recommended to add catalysts for experiments, more hydrogen can be obtained, and for high concentration biomass experiments, the ideal hydrogen yield cannot be produced, but the conversion of carbonaceous gases. Desirable diesel-like hydrocarbons can be obtained in the liquid product. From the fuel conversion point of view, the results of high concentration SGO gasification under supercritical water conditions are good, but from the hydrogen generation point of view, high concentration experiments are not as good as low concentration, and if we insist on using high concentration as material, it is recommended to explore the use of different catalysts to study the results of gasification products. In this study, nickel alloy catalysts can only help the reactants to convert to hydrogen better at low concentration conditions. Therefore, about the catalyst for the degradation of gutter oil under supercritical water conditions is a subject worthy of further study.

2. As for the experimental operation, the batch reactor used in this experiment is very easy to leak gas and inconvenient to take samples under high temperature and high pressure conditions, and the batch reactor was determined at the beginning of the experiment because of the problem of generating solid products that would easily clog the device, but the experimental results showed that no solid products appeared, so it is recommended to try the flow-through reactor in future research. The volume of gutter oil is very large in the world, so how to deal with high concentration and large mass of gutter oil is one of the topics worthies of future research.

3. For the collection and treatment aspect of gutter oil, there is no difficulty in collection because this experiment uses simulated gutter oil, but for the real Asian underdeveloped countries, it is a problem to obtain gutter oil efficiently in the long term. In addition to policies and regulations, a set of proven collection strategies is essential, and this paper suggests referring to developed countries' programs, such as Japan, to arrange recycling companies to collect the used gutter oil in a uniform manner and on time.

## REFERENCES

- [1] U. Energy Information Administration, “IEO 2021 Narrative.” [Online]. Available: [www.eia.gov](http://www.eia.gov)
- [2] Y. Miyata *et al.*, “Fe-Assisted Hydrothermal Liquefaction of Lignocellulosic Biomass for Producing High-Grade Bio-Oil,” *ACS Sustainable Chemistry and Engineering*, vol. 5, no. 4, pp. 3562–3569, Apr. 2017, doi: 10.1021/acssuschemeng.7b00381.
- [3] Rathore NS and Panwar NL, *Renewable Energy Sources for Sustainable Development*. New India Pub Agency, 2007.
- [4] M. El-Shafie, S. Kambara, and Y. Hayakawa, “Hydrogen Production Technologies Overview,” *Journal of Power and Energy Engineering*, vol. 07, no. 01, pp. 107–154, 2019, doi: 10.4236/jpee.2019.71007.
- [5] B. C. Tashie-Lewis and S. G. Nnabuiife, “Hydrogen Production, Distribution, Storage and Power Conversion in a Hydrogen Economy - A Technology Review,” *Chemical Engineering Journal Advances*, vol. 8. Elsevier B.V., Nov. 15, 2021. doi: 10.1016/j.ceja.2021.100172.
- [6] N. L. Panwar, S. C. Kaushik, and S. Kothari, “Role of renewable energy sources in environmental protection: A review,” *Renewable and Sustainable Energy Reviews*, vol. 15, no. 3. pp. 1513–1524, Apr. 2011. doi: 10.1016/j.rser.2010.11.037.
- [7] M. Fatih Demirbas, “Technological options for producing hydrogen from renewable resources,” *Energy Sources, Part A: Recovery, Utilization and Environmental Effects*, vol. 28, no. 13, pp. 1215–1223, Sep. 2006, doi: 10.1080/009083190910488.
- [8] 尚艳娥, “我国与发达国家废弃食用油脂监管模式比较,” 国家粮油质量监督检验中心, Nov. 02, 2011.
- [9] S. K. Karmee, “Fuel not food—towards sustainable utilization of gutter oil,” *Biofuels*, vol. 8, no. 3, pp. 339–346, May 2017, doi: 10.1080/17597269.2016.1231952.
- [10] “In China, the potential for harnessing the power of waste cooking oil. ,” *Yale Environment Review*. , Apr. 30, 2017.
- [11] H. Zhang, U. Aytun Ozturk, Q. Wang, and Z. Zhao, “Biodiesel produced by waste cooking oil: Review of recycling modes in China, the US and Japan,” *Renewable and Sustainable Energy Reviews*, vol. 38, pp. 677–685, Oct. 2014, doi: 10.1016/j.rser.2014.07.042.

- [12] S. Liang, Z. Liu, M. Xu, and T. Zhang, “Waste oil derived biofuels in China bring brightness for global GHG mitigation,” *Bioresource Technology*, vol. 131, pp. 139–145, 2013, doi: 10.1016/j.biortech.2012.12.008.
- [13] LiHongen, “GUTTEROIL,BIO-DIESELANDBIO. DIESELPRODUCEDFROMGUTTEROIL,” Centria University, 2021.
- [14] Jenny. Gustavsson, Food and Agriculture Organization of the United Nations., and N. ASME/Pacific Rim Technical Conference and Exhibition on Integration and Packaging of MEMS, *Global food losses and food waste : extent, causes and prevention : study conducted for the International Congress “Save Food!” at Interpack 2011 Düsseldorf, Germany*.
- [15] D. Valenzuela Gubatanga, O. Sawai, and T. Nunoura, “Hydrogen production from supercritical water gasification of vegetable oil,” 2019.
- [16] “新华网:北科大研发成功‘地沟油’制备选矿药剂的综合利用技术-北京科技大学新闻网,” *University of Science and Technology Beijing News*, Apr. 10, 2010. <https://nnews.ustb.edu.cn/info/1087/28570.htm> (accessed Jul. 04, 2022).
- [17] “‘地沟油’生产乙醇、沼气新技术,” 中国能源网, Jun. 13, 2010.
- [18] “‘地沟油’变身新型航空油,” *Institute of coal chemistry, Chinese academy of sciences*, Sep. 02, 2013.
- [19] “‘地沟油’变身钻井润滑油,” *China Dvelopment Gateway(CnDG)*, Oct. 29, 2014.
- [20] A. A. Peterson, F. Vogel, R. P. Lachance, M. Fröling, M. J. Antal, and J. W. Tester, “Thermochemical biofuel production in hydrothermal media: A review of sub- and supercritical water technologies,” *Energy and Environmental Science*, vol. 1, no. 1. Royal Society of Chemistry, pp. 32–65, 2008. doi: 10.1039/b810100k.
- [21] M. Goto, “Chemical recycling of plastics using sub- and supercritical fluids,” *Journal of Supercritical Fluids*, vol. 47, no. 3. pp. 500–507, Jan. 2009. doi: 10.1016/j.supflu.2008.10.011.
- [22] S. S. Toor, L. Rosendahl, and A. Rudolf, “Hydrothermal liquefaction of biomass: A review of subcritical water technologies,” *Energy*, vol. 36, no. 5. Elsevier Ltd, pp. 2328–2342, 2011. doi: 10.1016/j.energy.2011.03.013.
- [23] N. Akiya and P. E. Savage, “Roles of water for chemical reactions in high-temperature water,” *Chemical Reviews*, vol. 102, no. 8, pp. 2725–2750, 2002, doi: 10.1021/cr000668w.

- [24] L. Zhan, L. Jiang, Y. Zhang, B. Gao, and Z. Xu, “Reduction, detoxification and recycling of solid waste by hydrothermal technology: A review,” *Chemical Engineering Journal*, vol. 390. Elsevier B.V., Jun. 15, 2020. doi: 10.1016/j.cej.2020.124651.
- [25] O. Yakaboylu, J. Harinck, K. G. Smit, and W. de Jong, “Supercritical water gasification of biomass: A literature and technology overview,” *Energies*, vol. 8, no. 2. MDPI AG, pp. 859–894, 2015. doi: 10.3390/en8020859.
- [26] D. Castello and L. Fiori, “Supercritical water gasification of biomass: Thermodynamic constraints,” *Bioresource Technology*, vol. 102, no. 16, pp. 7574–7582, Aug. 2011, doi: 10.1016/j.biortech.2011.05.017.
- [27] J. Xu, J. Kou, L. Guo, H. Jin, Z. Peng, and C. Ren, “Experimental study on oil-containing wastewater gasification in supercritical water in a continuous system,” *International Journal of Hydrogen Energy*, pp. 15871–15881, Jun. 2019, doi: 10.1016/j.ijhydene.2018.10.069.
- [28] Y. Liu, X. Yang, A. Adamu, and Z. Zhu, “Economic evaluation and production process simulation of biodiesel production from waste cooking oil,” *Current Research in Green and Sustainable Chemistry*, vol. 4, p. 100091, 2021, doi: 10.1016/j.crgsc.2021.100091.
- [29] H. da Silva Almeida *et al.*, “Diesel-like hydrocarbon fuels by catalytic cracking of fat, oils, and grease (FOG) from grease traps,” *Journal of the Energy Institute*, vol. 90, no. 3, pp. 337–354, Jun. 2017, doi: 10.1016/j.joei.2016.04.008.
- [30] W. Kiatkittipong, S. Phimsen, K. Kiatkittipong, S. Wongsakulphasatch, N. Laosiripojana, and S. Assabumrungrat, “Diesel-like hydrocarbon production from hydroprocessing of relevant refining palm oil,” *Fuel Processing Technology*, vol. 116, pp. 16–26, 2013, doi: 10.1016/j.fuproc.2013.04.018.
- [31] Elliott DC, “Catalytic hydrothermal gasification of biomass.,” *Biofuels Bioprod Bioref 2008*, vol. 2, no. 3, pp. 254–265, Apr. 2018.
- [32] A. Smag̃, S. Smag̃, A. Kruse, and J. Rathert, “Influence of the Heating Rate and the Type of Catalyst on the Formation of Key Intermediates and on the Generation of Gases During Hydrolysis of Glucose in Supercritical Water in a Batch Reactor,” 2004, doi: 10.1021/ie030475.
- [33] “加熱油脂劣化度判定用試験紙 Test strip for thermal degradation of frying oils.”
- [34] アドバンテック東洋株式会社, “食用油脂の「鮮度」が一目でわかる! 加熱油脂などの酸価を色で示し、劣化度を判定,” イプロス医薬食品技術, Jul. 04, 2022.

- [35] Y. Matsumura, X. Xu, and M. J. Antal, “GASIFICATION CHARACTERISTICS OF AN ACTIVATED CARBON IN SUPERCRITICAL WATER,” 1997.
- [36] X. H. Hao, L. J. Guo, X. Mao, X. M. Zhang, and X. J. Chen, “Hydrogen production from glucose used as a model compound of biomass gasified in supercritical water,” 2003. [Online]. Available: [www.elsevier.com/locate/ijhydene](http://www.elsevier.com/locate/ijhydene)
- [37] K. Koido \* 1, Y. Watanabe \* , T. N. \* 3, and K. Dowaki, “Synthesis Gas Production via Non-catalytic and Catalytic Gasification of Lignin with High-moisture Content,” 2014.
- [38] D. Castello, B. Rolli, A. Kruse, and L. Fiori, “Supercritical water gasification of biomass in a ceramic reactor: Long-time batch experiments,” *Energies (Basel)*, vol. 10, no. 11, Nov. 2017, doi: 10.3390/en10111734.
- [39] S. A. Channiwala and P. P. Parikh, “A uni@ed correlation for estimating HHV of solid, liquid and gaseous fuels q.” [Online]. Available: <http://www.fuel>
- [40] N. v Khartchenko and V. M. Kharchenko, “ADVANCED ENERGY SYSTEMS Second Edition,” 2010.
- [41] H. da Silva Almeida *et al.*, “Diesel-like hydrocarbon fuels by catalytic cracking of fat, oils, and grease (FOG) from grease traps,” *Journal of the Energy Institute*, vol. 90, no. 3, pp. 337–354, Jun. 2017, doi: 10.1016/j.joei.2016.04.008.
- [42] T. Minowa and S. Inoue, “HYDROGEN PRODUCTION PROM BIOMASS BY CATALYTIC GASIFICATION IN HOT COMPRESSED WATER,” 1999.
- [43] D. Valenzuela Gubatanga, “Supercritical Water Gasification of Vegetable Oil Using Nickel Catalyst 「ニッケル触媒を用いた植物油の超臨界水ガス化に関する研究」.”